

JPL D-9932

GALILEO HIGH GAIN ANTENNA
DEPLOYMENT ANOMALY
PIN WALKOUT ANALYSIS
FINAL REPORT

Walter Tsuha
Andrew Kissil
Paul Rapacz
James Staats
Yin Tsou
Robert Eads

July 1992

JPL

Jet Propulsion Laboratory
California Institute of Technology
Pasadena, California

TABLE OF CONTENTS

List of Figures	v
List of Tables	vii
1.0 INTRODUCTION	1
2.0 BACKGROUND	3
2.1 Antenna Description	3
2.2 Current Antenna Configuration	11
3.0 PIN WALKING MECHANISM	14
4.0 ANALYSIS APPROACH	16
4.1 Gap Element	16
4.1.1 Description	16
4.1.2 Test Problem 1	16
4.1.3 Test Problem 2	18
4.2 Antenna Models	20
4.2.1 Full Model	20
4.2.2 Four Rib Model	23
4.2.3 Single Rib Model	26
4.3 Loading History	27
4.3.1 Pin Misalignment Loads	27
4.3.2 Tower Contraction Loads	27
4.3.3 March 92 Cooling Scenario	29
5.0 RESULTS AND DISCUSSION	32
5.1 Rib Release Curves	32
5.1.1 Basic Curves	32
5.1.2 Effects of Pin Polarity	39
5.1.3 First Rib Release	42
5.1.4 Subsequent Rib Releases	46

TABLE OF CONTENTS

5.2 Cooling Turn Alternatives 56
5.2.1 130 Mil Tower Contraction 56
5.2.2 Turning at 3 AU 59
5.2.3 Deleting Turns 7, 8, 9 & 10 61

6.0 CONCLUSION 65

7.0 REFERENCES 66

8.0 APPENDICES

8.1 Warming Turn Benefits
8.2 Thermal Cycling at Fixed AU
8.3 PWS On/Off Study
8.4 Effects of Antenna Hub Offset
8.5 DDA Motor Pulse
8.6 Thermal Cycling at 3 AU
8.7 Effectiveness of Turns 7, 8, 9 & 10
8.8 Full Model - NASTRAN Data Deck
8.9 Four Rib Model - NASTRAN Data Deck
8.10 Single Rib Model - NASTRAN Data Deck

LIST OF FIGURES

1.0-1	Galileo Spacecraft	2
2.1-1	Stowed High Gain Antenna	4
2.1-2	HGA Upper Structure	5
2.1-3	Mid-Point Restraint	6
2.1-4	Mid-Point Receptacle	7
2.1-5	Tip Restraint	8
2.1-6	Mechanical Deployment System (Stowed)	9
2.1-7	Deployed High Gain Antenna	10
2.2-1	Rib Numbering Scheme	12
3.0-1	Walkout Mechanism - Pin Preload	15
3.0-2	Walkout Mechanism - Cool Down	15
3.0-3	Walkout Mechanism - Warm Up	15
4.1.2-1	Test Problem 1	17
4.1.3-1	Test Problem 2	19
4.2.1-1	Full Model	21
4.2.1-2	MDS Modelling	22
4.2.2-1	Four Rib Model	24
4.2.2-2	Pin To Receptacle Modelling	25
4.3.2-1	Feed Tower Displacement	28
4.3.3-1	March 92 Cooling Turn Schedule	30
5.1.1-1	Basic Rib Release Curves	33
5.1.1-2	Pin Force/Slippage Plot - 20 lb Preload, $\mu = 1.30$	34
5.1.1-3	Pin Force/Slippage Plot - 15 lb Preload, $\mu = 1.57$	35
5.1.1-4	Pin Force/Slippage Plot - 10 lb Preload, $\mu = 1.90$	36
5.1.1-5	Pin Forces and Slippage - Convention	37
5.1.2-1	Pin Polarity - Effects on Pin Loads	40
5.1.2-2	Pin Polarity - Effects on Rib Release	41
5.1.3-1	Rib Release Curves - All Rib and Pin Polarity Combinations	43
5.1.3-2	Rib and Pin Polarity Combinations	44
5.1.3-3	First Rib Release Curves	45
5.1.4-1	Sequential Rib Release Curves	48
5.1.4-2	Pin Slippage Plot - Ribs 9, 10 & 11, 10 lb Preload, $\mu = 1.70$	50
5.1.4-3	Pin Force/Slippage Plot - Rib 9, 10 lb Preload, $\mu = 1.70$	51
5.1.4-4	Pin Force/Slippage Plot - Rib 10, 10 lb Preload, $\mu = 1.70$	52
5.1.4-5	Pin Force/Slippage Plot - Rib 11, 10 lb Preload, $\mu = 1.70$	53

LIST OF FIGURES

5.1.4-6	Rib 1 Tip Displacements - 10 lb Preload, $\mu = 1.70$	54
5.1.4-7	Pushrod Forces - Ribs 9, 10 & 11, 10 lb Preload, $\mu = 1.70$	55
5.2.1-1	Rib Release Curves - 130 mil Tower Contraction	58
5.2.2-1	Rib Release Curves - Effects of Turning at 3 AU	60
5.2.3-1	Rib Release Curves - Effects of Deleting Turns 8, 9 & 10	63
5.2.3-2	Rib Release Curves - Effects of Deleting Turns 7, 8, 9 & 10	64

LIST OF TABLES

4.3.3-1	Loading History - March 92 Cooling Turn Scenario	31
5.1.4-1	Loading History - December 91 On-Sun Cooling Turn Scenario	47
5.2.1-1	Loading History - 130 mil Tower Contraction	57
5.2.3-1	Loading History - Modified March 92 Cooling Turn Scenario	62

6

1.0 INTRODUCTION

The Galileo spacecraft depicted in Figure 1.0-1 is designed to study three broad aspects of the Jupiter system: the planet's atmosphere, its satellites, and the surrounding magnetosphere. After being launched aboard the Space Shuttle Atlantis on October 18, 1989 and brought to Earth orbit, the spacecraft was propelled toward Venus by an Inertial Upper Stage booster to begin a complex series of gravity assist between Earth and Venus. Currently, the spacecraft is on its way back to earth for its final gravity assist and will be heading for Jupiter in December 1992. On April 11, 1991, a sequence of commands were sent to the spacecraft to unfurl its 16 foot, umbrella like, High Gain Antenna (HGA). However, telemetry data received from the spacecraft indicated an unsuccessful deployment attempt that resulted in a partially deployed antenna.

One hypothesis that has been advanced to explain the partial deployment of the HGA postulates that friction forces developed at the mid-point restraint pin to receptacle interface is the mechanism responsible for preventing some of the ribs from deploying. These friction forces are thought to arise as a result of the preloads generated when a pair of misaligned mid-point restraint pins are driven into their receptacles during stowage of the antenna, in combination with the subsequent surface abrasion that occurs between the pins and receptacle during vibration testing, ground transportation, and flight. It has been suggested, therefore, that a series of spacecraft turning maneuvers be executed to alternately heat and cool the antenna in an attempt to induce a slipping action of the pins in order to free the stuck ribs.

A study was initiated to explore the feasibility of releasing the stuck ribs by thermally loading the antenna in a cyclic fashion. In this study, an analytical investigation is conducted to determine if the pins could back themselves out from the receptacle by thermally expanding and contracting the central feed tower, and if concluded as being possible, determine whether the ribs could be released within a reasonable number of heating and cooling turns of the spacecraft. Other investigations that were conducted included studies such as: evaluating various heating/cooling strategies to optimize rib release, examining various pin misalignment sources to determine its effect on rib release, determining the effectiveness of the cooling turns in consideration of deleting some of them, and investigating the consequences of driving the dual drive actuator beyond its present state. The findings of the present study and a detailed description of the analytical models, analysis approach, assumptions and limitation of the analysis are presented in this report.

Galileo SPACECRAFT CONFIGURATION

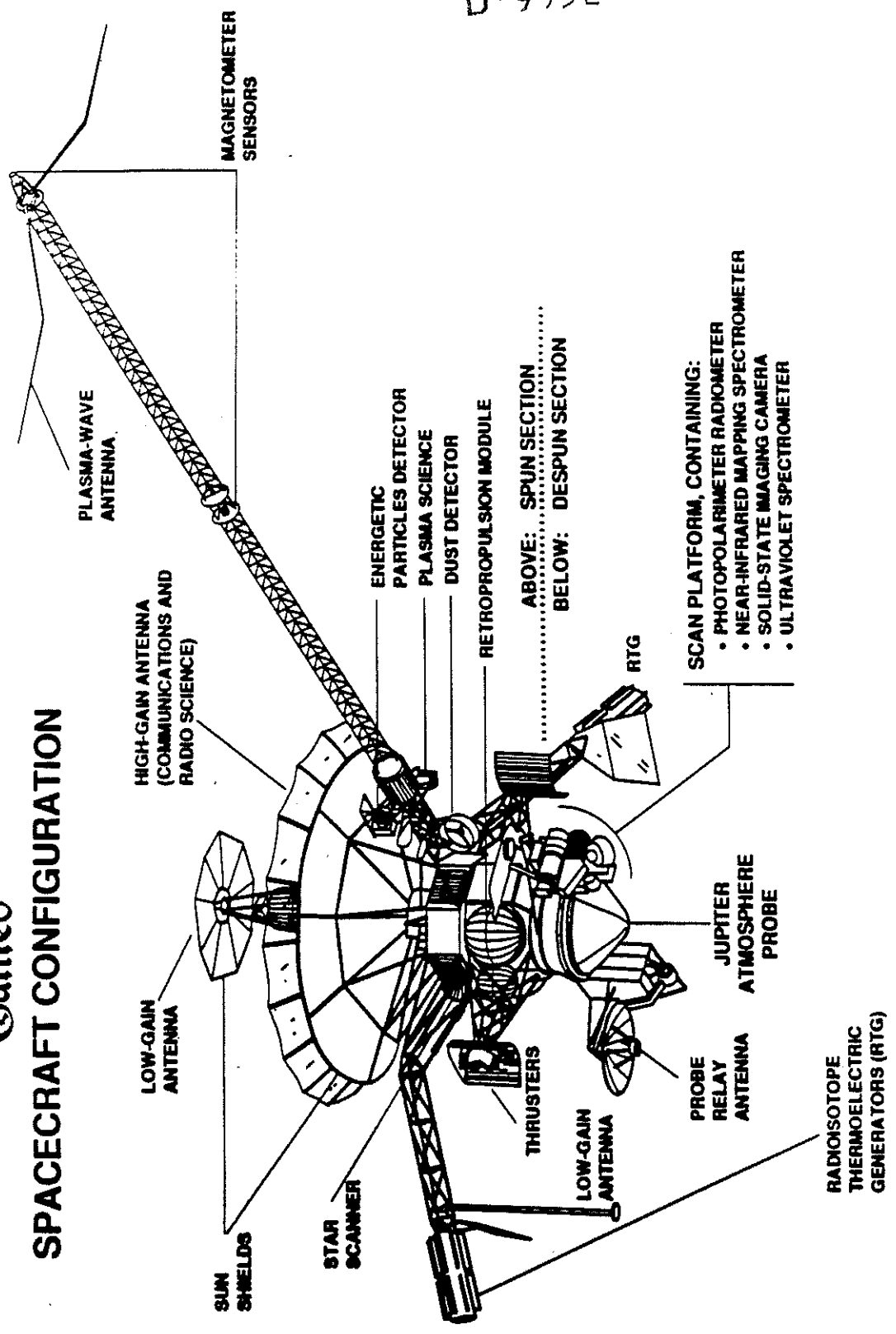


Figure 1.0-1: Galileo Spacecraft

2.0 BACKGROUND

2.1 ANTENNA DESCRIPTION

The Galileo HGA in its stowed configuration is shown in Figure 2.1-1. The antenna has an overall height of 106.5", a maximum girth diameter of 47.6", and a weight of 86.3 lbs. The antenna interfaces the spacecraft at the base of the Hub assembly at three equally spaced points that lie on an 18.0" diameter circumference (Ref. 1).

Eighteen graphite epoxy ribs, space equally apart, are mounted on top of the Hub assembly by clevises that allow each rib to pivot about the tangential axis for deployment. In the stowed configuration, the two titanium mid-point restraint pins that are fitted to each rib, approximately two-thirds up from the base of the rib (see Figure 2.1-2), seat themselves into a receptacle when preloaded by the spoke assembly shown in Figure 2.1-3. The receptacle, which mounts to the upper structure of the radome assembly, consists of an aluminum bracket to which an Inconel groove and cone insert attaches to, see Figure 2.1-4. Each rib, therefore, is restrained at the pin tip location against translations, and rotations about the radial and vertical axes. In addition, the tip restraint shown in Figure 2.1-5 restrains each rib tip against excessive tangential motions.

The central feed tower, whose major structural components consist of the beryllium struts, honeycomb radome and beryllium upper structure, forms the core structure for the feed system. In addition to housing the feed system and its related components, it provides the supporting structure for the Plasma Wave Subsystem (PWS), Low Gain Antenna-1 (LGA-1), Central Release Mechanism (CRM), Mid-Point Restraints, and Tip Restraints.

During deployment, the Dual Drive Actuator (DDA) rotates a ballscrew, which in turn elevates the carrier shown in Figure 2.1-6. As the carrier rises, a pushrod transforms the vertical motion of the carrier into a rotational motion of each rib about its pivot axis. Under nominal operating conditions, the carrier rises until it engages a switch at the top of the ballscrew at which point the deployment is terminated, and the antenna has the configuration shown in Figure 2.1-7.

D-9932

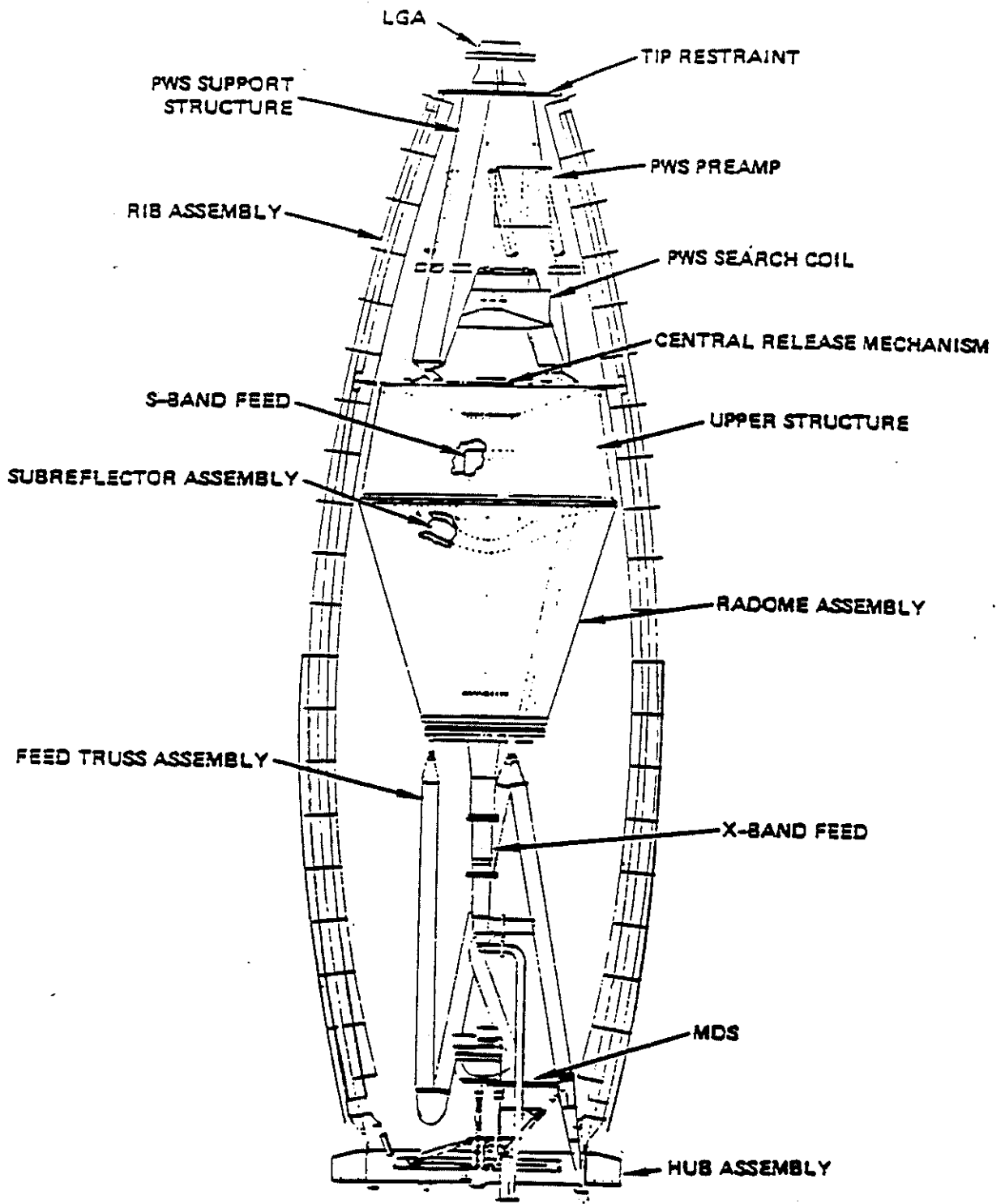


Figure 2.1-1: Stowed High Gain Antenna

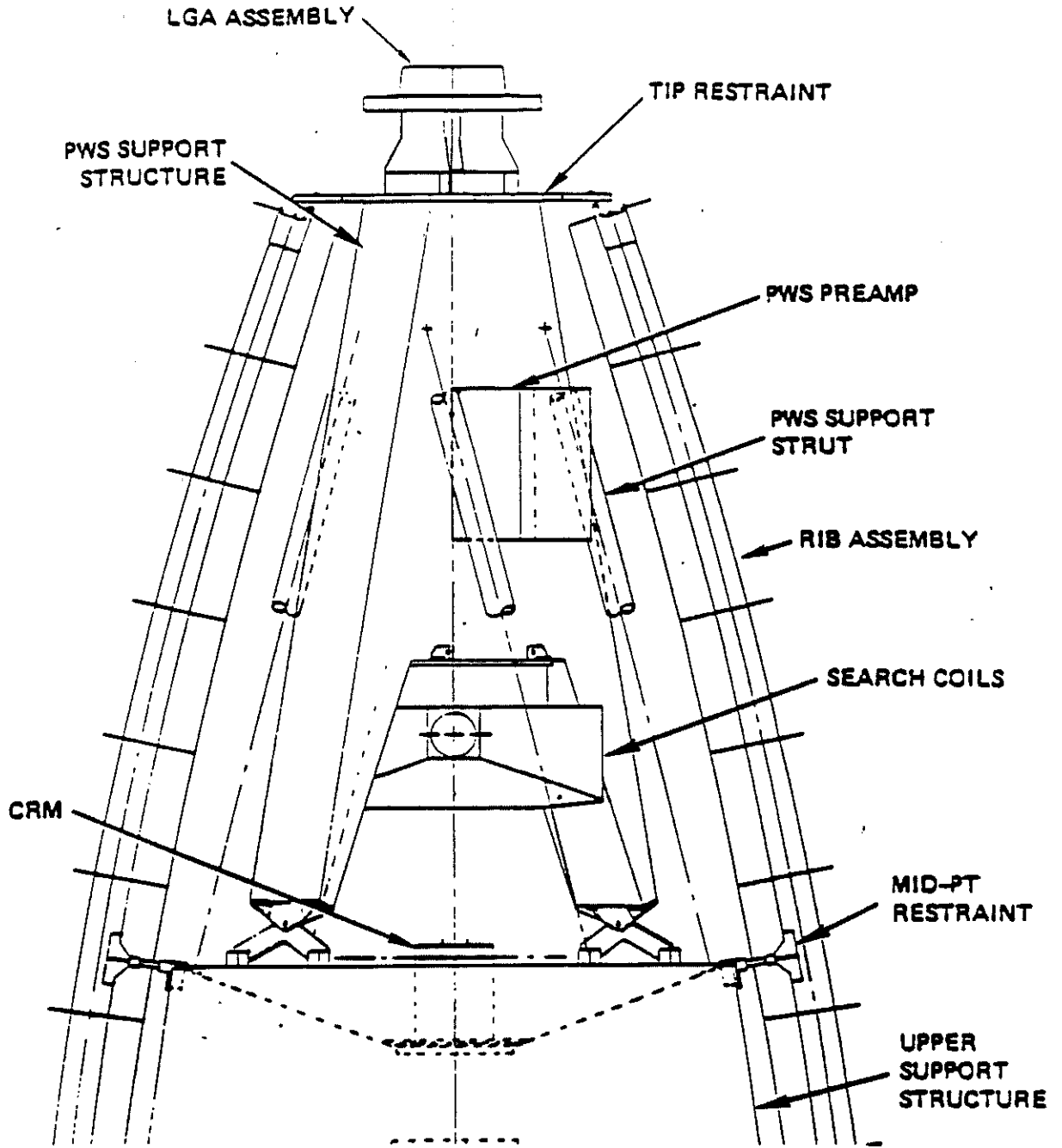


Figure 2.1-2: HGA Upper Structure

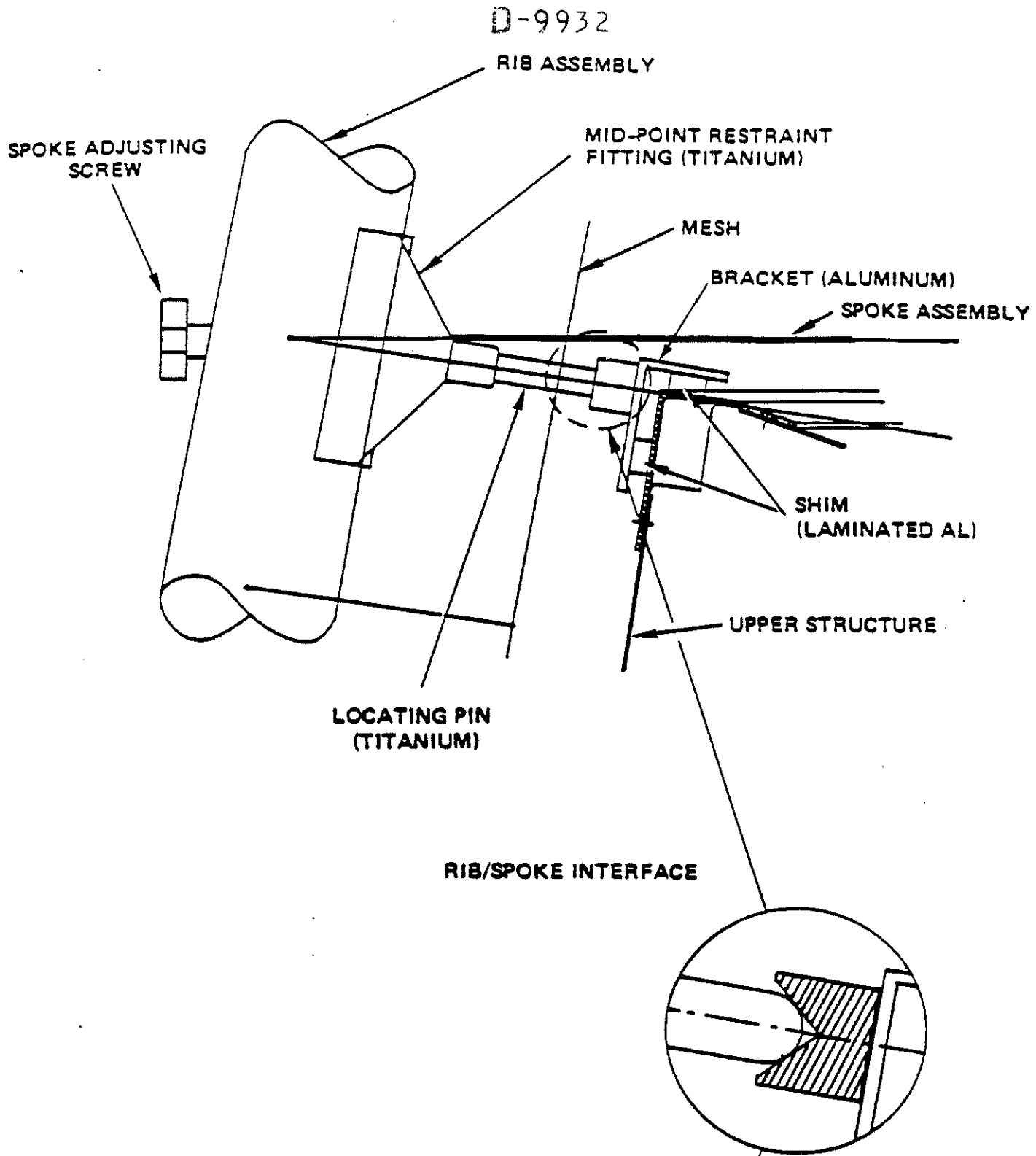
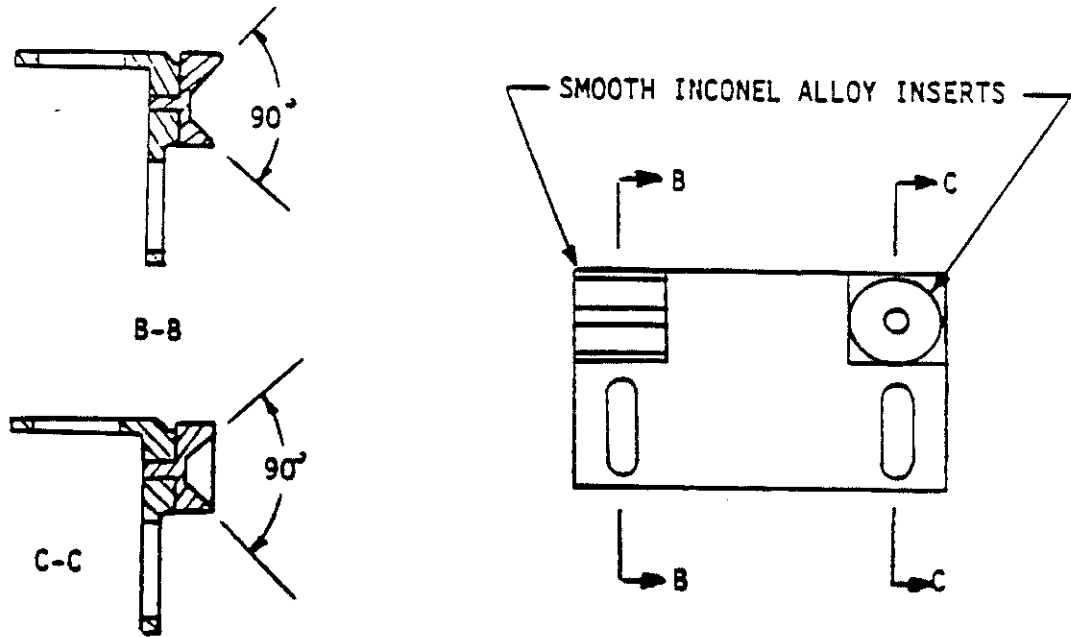


Figure 2.1-3: Mid-Point Restraint

D-9932



THREE-PIECE BRACKET DESIGN WITH ONE CONE, ONE V-GROOVE

Figure 2.1-4: Mid-Point Receptacle

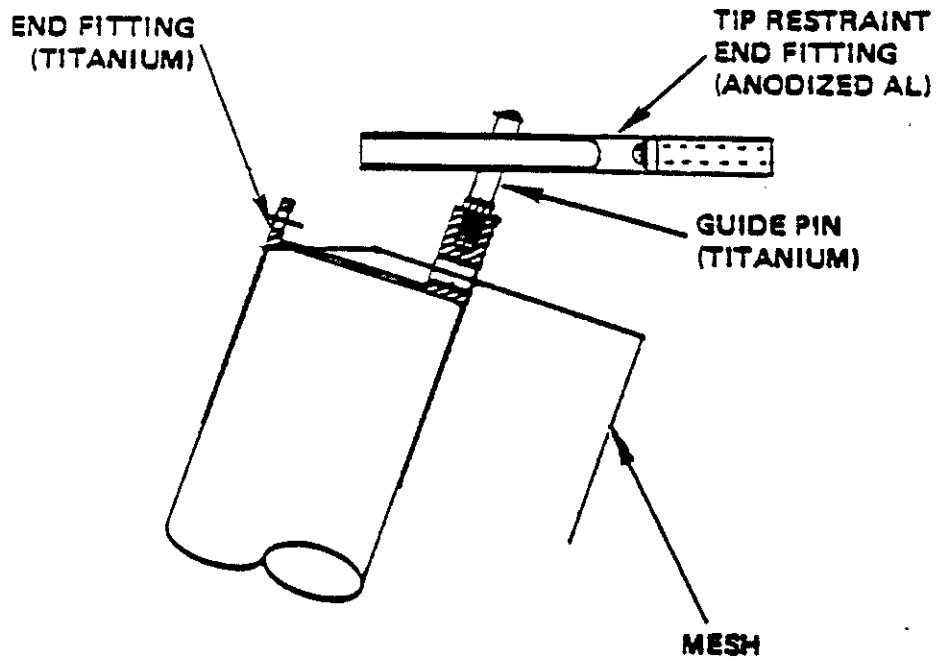


Figure 2.1-5: Tip Restraint

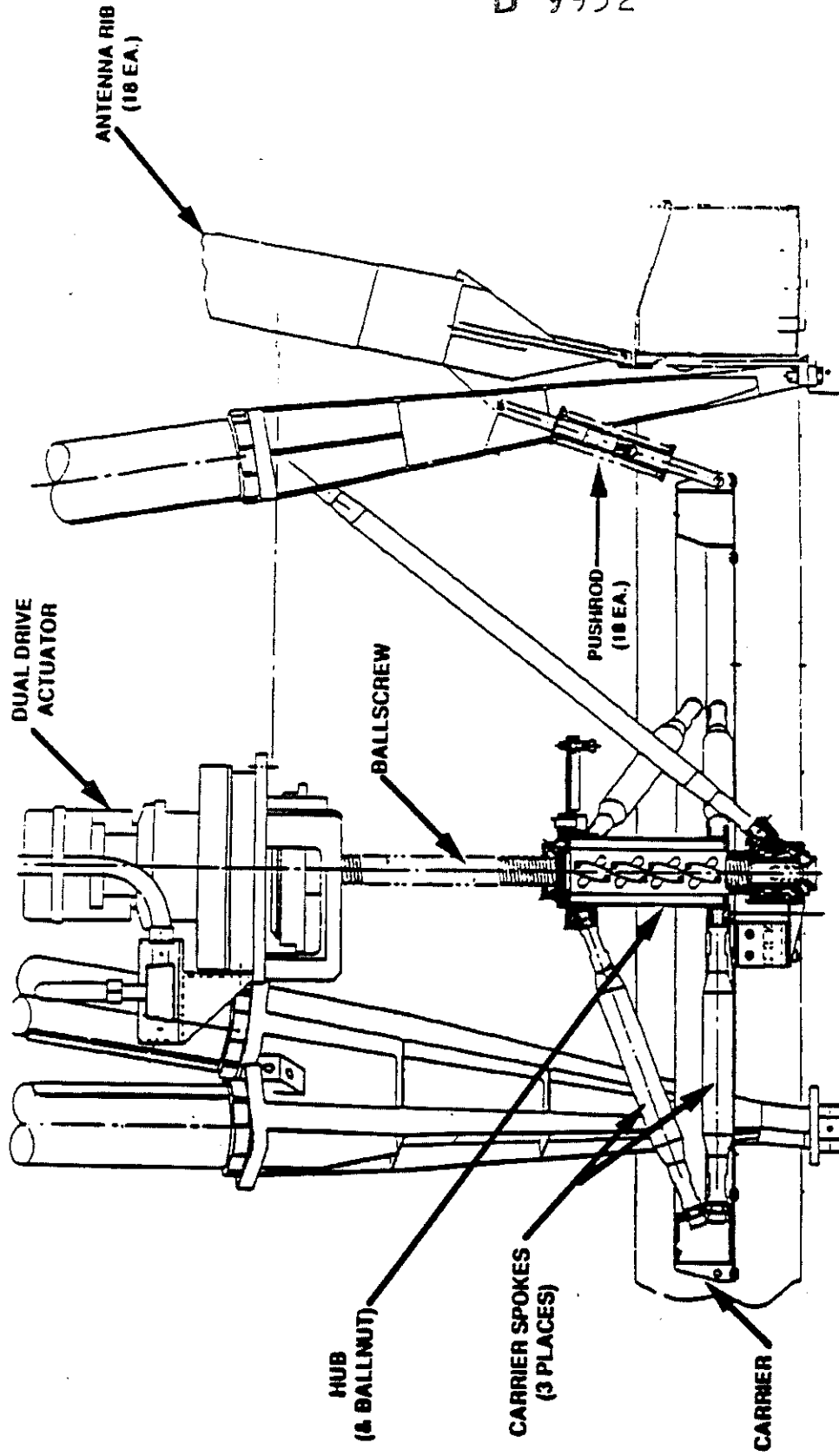


Figure 2.1-6: Mechanical Deployment System (Stowed)

D-9932

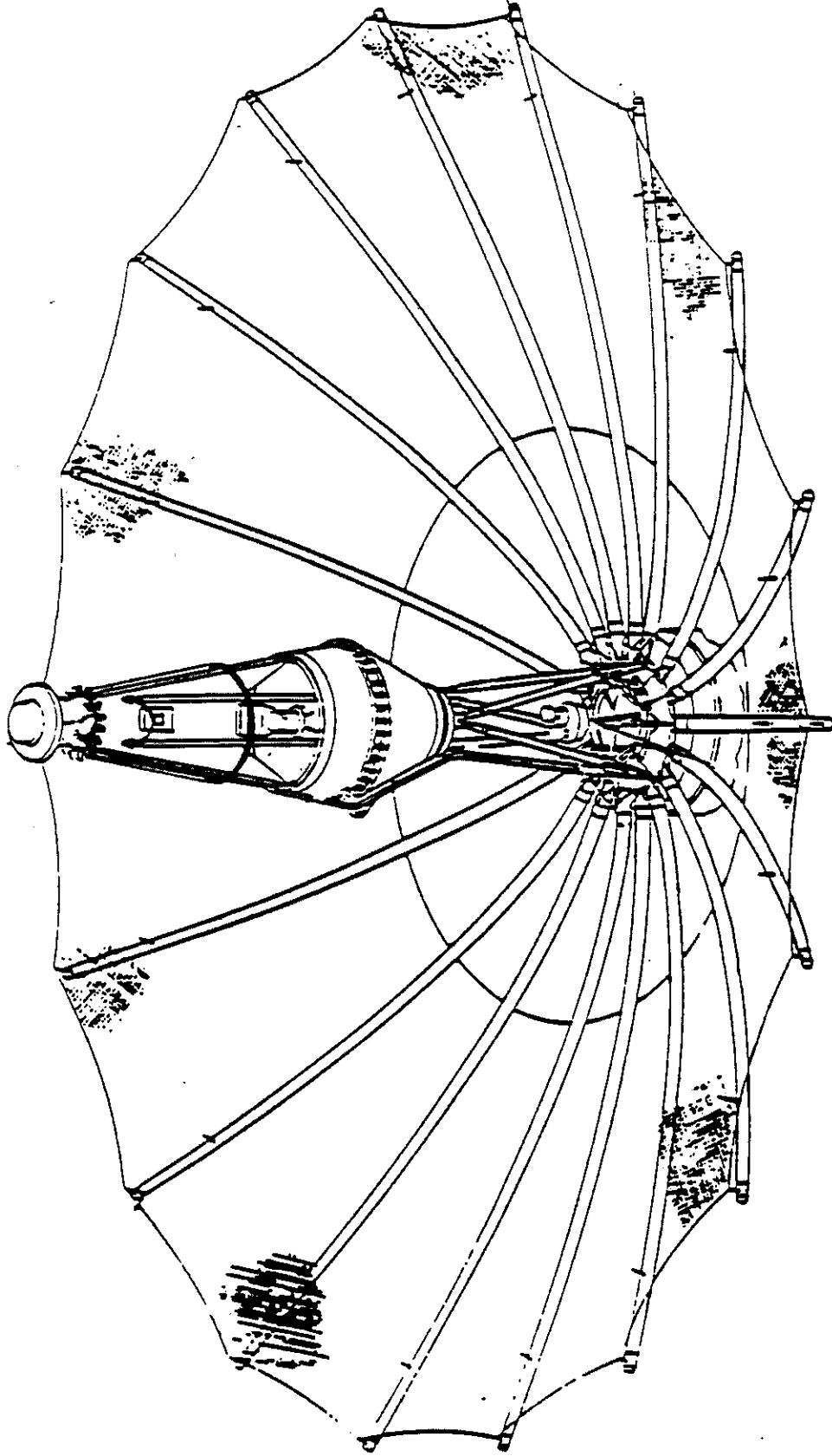


Figure 2.1-7: Deployed High Gain Antenna

2.2 CURRENT ANTENNA CONFIGURATION

Based on analysis and evaluation of the spin sensor and sun gate obscuration data, evidence was presented that showed the antenna to be unsymmetrically deployed with rib number two (see Figure 2.2-1 for rib numbering scheme) being deployed 35 degrees (Ref 2). Furthermore, spacecraft wobble data and additional analysis, showed that rib number one is furthest out and that several ribs are probably stuck in (or near) their stowed position, centered about rib ten (Ref 3).

Ground tests performed on the flight spare antenna (SN01) with one to four ribs restrained showed that DDA stall torque (58 in-lb), ballscrew stall position (5.0 turns), and maximum rib deployment angle (35-36 degrees) were best matched with three ribs restrained (Refs. 4 - 6). Studies performed by P. Rapacz, however, showed that gravity would have an effect on the stiffness and load distribution of the antenna (Ref. 7) which questioned the applicability of using the ground test data to predict the state of the antenna for the flight condition, where gravity is zero. To address this issue, Rapacz analytically simulated the ground test, with gravity removed, and found that uncertainties in ballscrew stall position (5.0 +/-0.5 turns) combined with the limited amount of flight data made it uncertain whether three or four ribs are stuck (Ref. 8). Currently, the best estimate for the number of stuck ribs is three, and they are believed to be centered near the x-axis of the antenna (ribs numbers 9, 10 & 11).

There are several mechanisms which could prevent the ribs from deploying. Examples are:

- 1.) Spoke hangup: from sources such as cocking of the CRM release cap, misrigged spokes, cold welding, or spoke snag with the CRM or its neighboring parts.
- 2.) Stuck rib tip: due to cold welding, tip shade snag, or inadequate clearance between the rib tip and fork that results when the feed tower contracts.
- 4.) Stuck mid-point restraint pins: due to cold welding.
- 5.) Entanglement, bonding or fusing of the mesh.
- 6.) Mechanical or structural failure of the MDS.
- 7.) "Pin friction theory."

Failure modes 1 thru 6 were investigated with varying levels of testing and analyses, and are presently concluded as having a low probability of occurrence (Refs. 1,2,4,5 & 6).

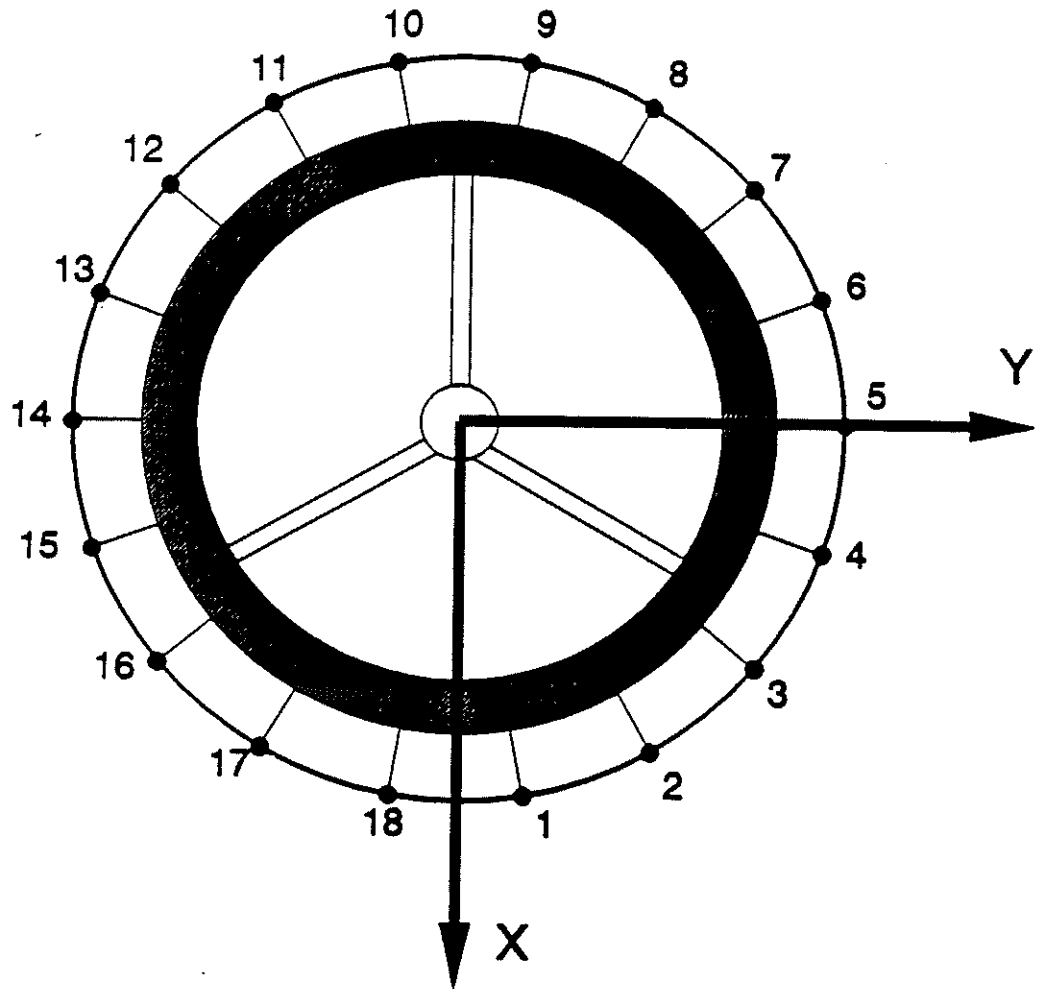


Figure 2.2-1: Rib Numbering Scheme

In failure scenario 7, the ribs are assumed to be held in their stowed position by friction forces developed at the mid-point restraint pin to receptacle interface. These forces are thought to arise as a result of the loads generated when a pair of misaligned mid-point restraint pins are preloaded by the spoke assembly during stowage of the antenna, in combination with the subsequent surface abrasion that occurs during vibration testing, ground transportation, and flight. To date, this failure scenario is considered a most likely candidate, because of the circumstantial evidence in favor of it.

Circumstantial evidences in favor of the pin friction theory:

- 1.) The stuck ribs are most likely centered about the x-axis (Ref. 5).
- 2.) A single x-axis sine test was performed on the flight antenna that exercised the x-axis mid-point restraint pins to their design limit loads (Ref. 5).
- 3.) Aggravating the situation, the flight antenna underwent four (one-way) cross-country truck transports while being cantilevered in the horizontal position with its x-axis normal to the ground. This produces bending motions of the tower that causes relative motions between the pin tips and receptacles for ribs centered about the x-axis (Ref. 5)
- 4.) Inspection of the flight spare antenna (SN01) showed evidence of galling and material transfer between the pins and seats of the receptacle (Ref. 9); therefore, it is reasonable to assume that similar degradation exists for the flight antenna.
- 5.) For the pin and receptacle material combination, a static coefficient of friction of 1.24 (nominal and in vacuum) was projected by test performed by JPL and LeRC. They also stated that higher values could be expected for lighter loads (Ref. 6).
- 6.) Tolerance studies showed that pin misalignments on the order of 5 to 10 mils could be expected, and as a result, 5 to 10 lb of preload can be generated. (Ref. 5).

3.0 PIN WALKING MECHANISM

In an attempt to free the stuck ribs, a series of spacecraft warming and cooling turns have been executed to produce a cyclic expansion and contraction of the central tower (relative to the thermally stable ribs) with the hope of causing the pins to back themselves out, or "walkout," from the receptacles. A qualitative description of the pin walkout mechanism is presented below.

When a pair of misaligned mid-point restraint pins are forced into their receptacle, one of the pins will be in contact with the upper surface of the receptacle while the other will be in contact with the lower surface, see Figure 3.0-1. As the tower contracts, the vertical motion of the receptacle causes the pin forces on the lower surface to decrease, while those on the upper surface increase, see Figure 3.0-2. Since the pin end opposite the receptacle attaches to the rib, which is relatively soft in rotation but stiff vertically, the downward movement of the receptacle causes the pins to rotate counter clockwise, about the pin contact point with the upper surface, which produces an incremental slip for the lower pin. When the tower expands, the reverse occurs. This time, the upper pin slips as its force decreases and the pins rotates clockwise about the pin contact point with the lower surface, see Figure 3.0-3. Each time a cooling and heating cycle is encountered, an incremental slip is produced for both the lower and upper pins. By repeating this process, it is hoped that sufficient slippage can be accumulated to eventually release the stuck ribs.

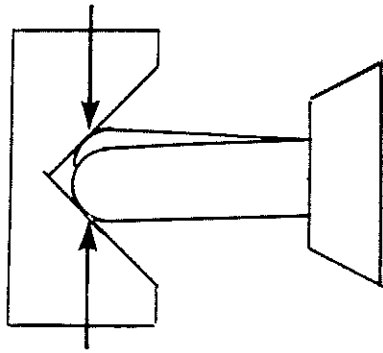


Figure 3.0-1: Walkout Mechanism - Pin Preload

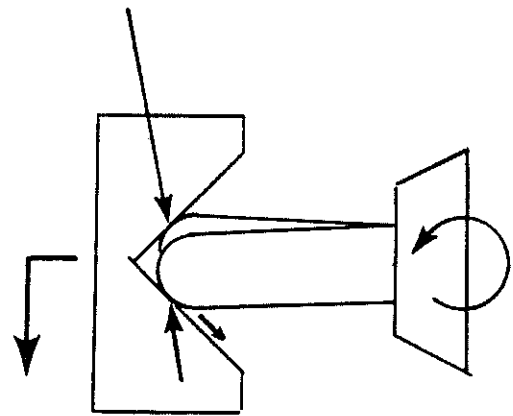


Figure 3.0-2: Walkout Mechanism - Cool Down

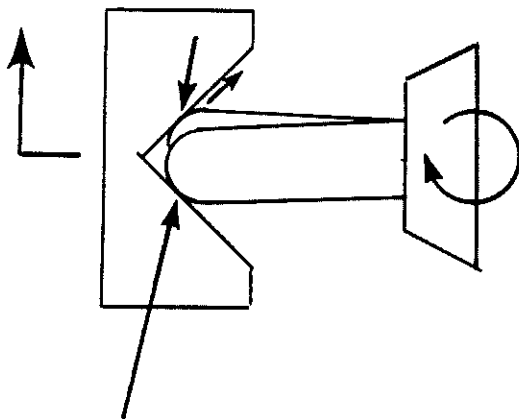


Figure 3.0-3: Walkout Mechanism - Warm Up

4.0 ANALYSIS APPROACH

4.1 GAP ELEMENT

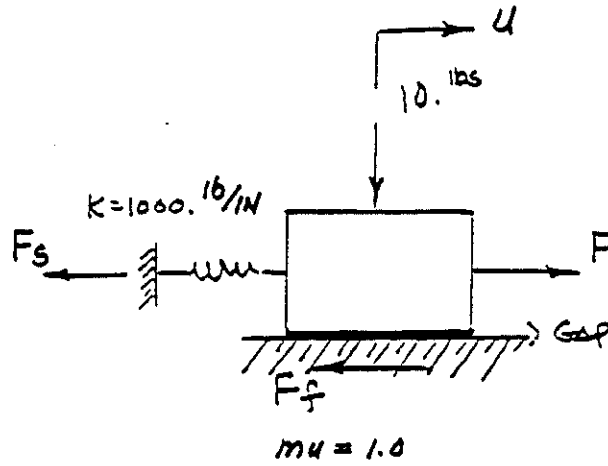
4.1.1 Description

MSC/NASTRAN gap elements were utilized to model the non-linear, stick/slip, friction behavior of the mid-point restraint pins in their receptacle. The gap element is designed to model the interface contact problem, and has options for including friction, preloads, and initial gap openings. The element connects the translational degree-of-freedom (dofs) of two grid points in space and cannot transmit any moments across the element. Depending on the state of the element (i.e., gap closed or open), it transmits a compressive force (normal to the contact surface) or no force at all. If the gap is closed and friction is present, a friction force is developed across the element that acts in the plane of the contact surface and in a direction opposite to the applied shear load. The maximum friction force developed is equal to the product of the instantaneous normal force and friction coefficient. In accordance with the Coulomb friction model, slip occurs when the applied shear force exceeds the available friction force.

4.1.2 Test Problem 1

Since the gap element is not routinely used for most structural analysis problems, a test problem was devised to verify the correctness of the element, at least for a simple problem. The problem consisted of a massless block resting on a rough horizontal surface whose friction coefficient is assumed to be one. A 1000 lb/in linear spring was attached to the block as shown in Figure 4.1.2-1. To develop a compressive force between the block and horizontal surface, a 10 lb vertical force was applied. A lateral force (F), was then applied to the block and gradually increased from 0 to 20 lbs. The resulting spring force (F_s), friction force (F_f), and displacement (u) are plotted against the applied force (F), and is shown in Figure 4.1.2-1. The results are as expected and confirms the gap element and the non-linear solution sequence to be working properly.

D-9932



TEST PROBLEM 1
REACTION FORCE VS APPLIED FORCE

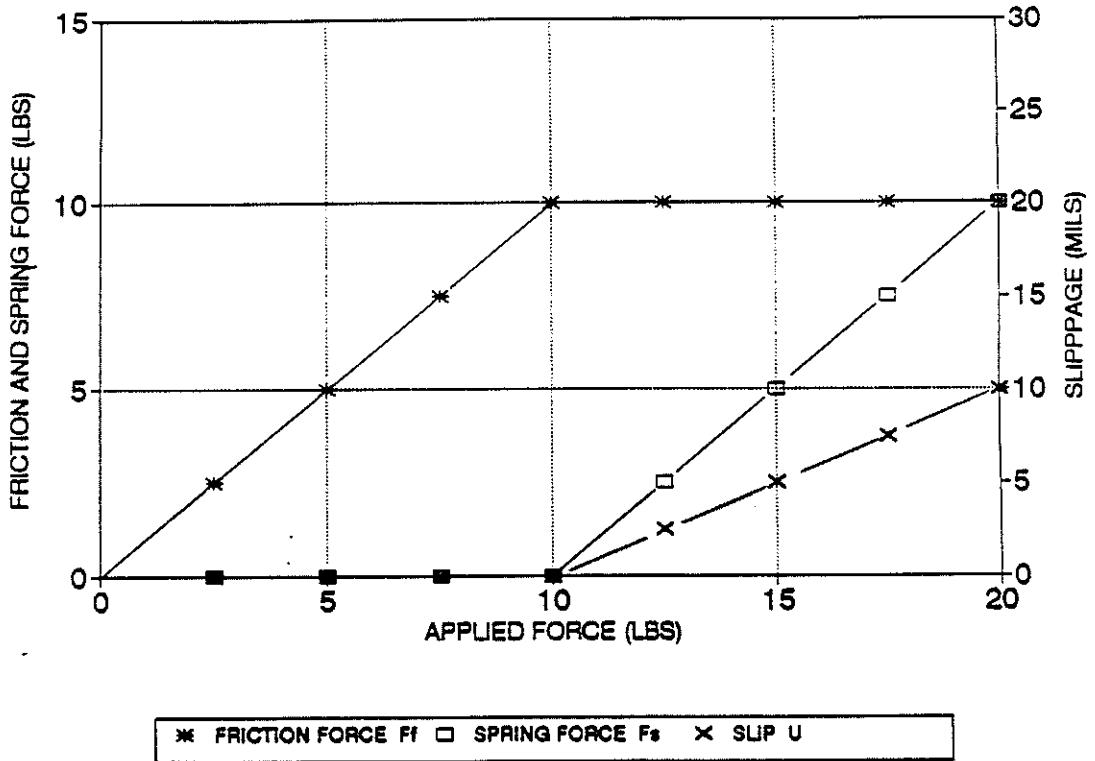
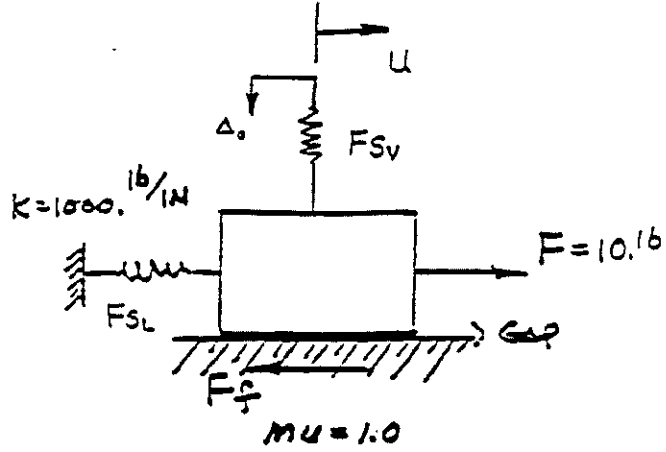


Figure 4.1.2-1: Test Problem 1

4.1.3 Test Problem 2

To gain further confidence, a second problem was examined. A vertical spring was added to the problem described earlier and was then compressed to develop an initial preload of 20 lb, see Figure 4.1.3-1. This time, the lateral force (F) was held constant at 10 lb, while the vertical spring was allowed to gradually expand and relieve its preload. The friction force (F_f), lateral spring force (F_s), and displacement (u), are plotted against the compressive force of the vertical spring. Again, the expected results were obtained.

D-9932



TEST PROBLEM 2
REACTION FORCE VS VERT. SPRING FORCE

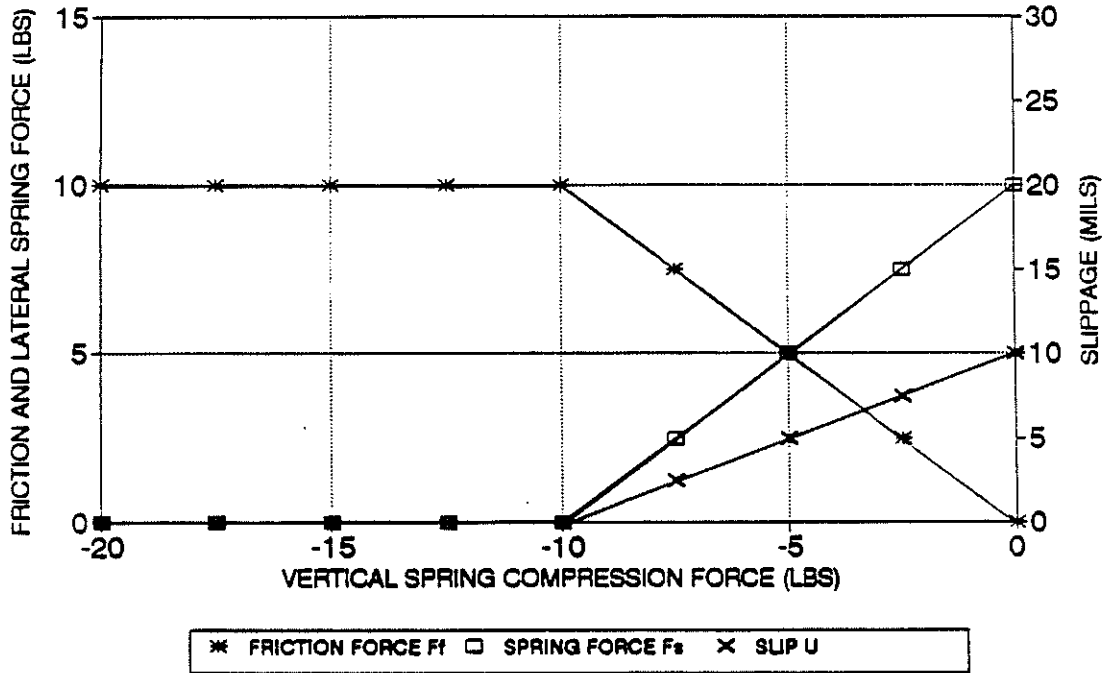


Figure 4.1.3-1: Test Problem 2

4.2 ANALYTICAL MODELS

4.2.1 Full Model

Development of the non-linear finite-element model of the antenna was accomplished through a serial effort, which started with C. Satter, followed by A. Kissil, and ended with P. Rapacz. Satter developed a linear model of the antenna for the purpose of conducting modal analyses for the cruise configured spacecraft. Kissil later converted the linear model into a large displacement, non-linear, model and used it to conduct preliminary investigations into the deployment anomaly (Ref. 10). Rapacz then added material nonlinearity to the model to capture the nonlinear load-deflection characteristics of the pushrod and ballnut. He also refined/improved the model in many areas and updated the model based on available ground test data (Ref. 11).

A plot of the model is shown in Figure 4.2.1-1. All 18 ribs (their pushrod and mid-point restraint pins), the mechanical deployment system (which consists of the carrier, ballscrew, DDA, ballscrew tripod supports and motor mounts), and the antenna hub, are represented in the model. Modelling of the mechanical deployment system is illustrated in Figure 4.2.1-2. Antenna deployment is accomplished by moving the lower end of the ballscrew, vertically, at a rate of 0.125" per ballscrew turn. The central tower was omitted, since its effect on the remaining structure is considered negligible. Being a fairly accurate representation of the hardware and having full deployment capability, the model was exercised heavily in conducting numerous deployment studies and was used to obtain displacement boundary conditions for a single rib model (to be described later). A more complete and detailed description of the model is available in Ref. 11.

D-9932

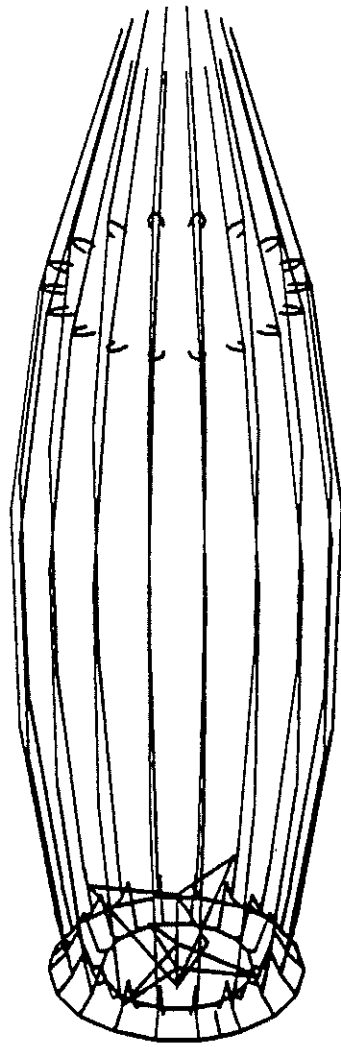


Figure 4.2.1-1: Full Model

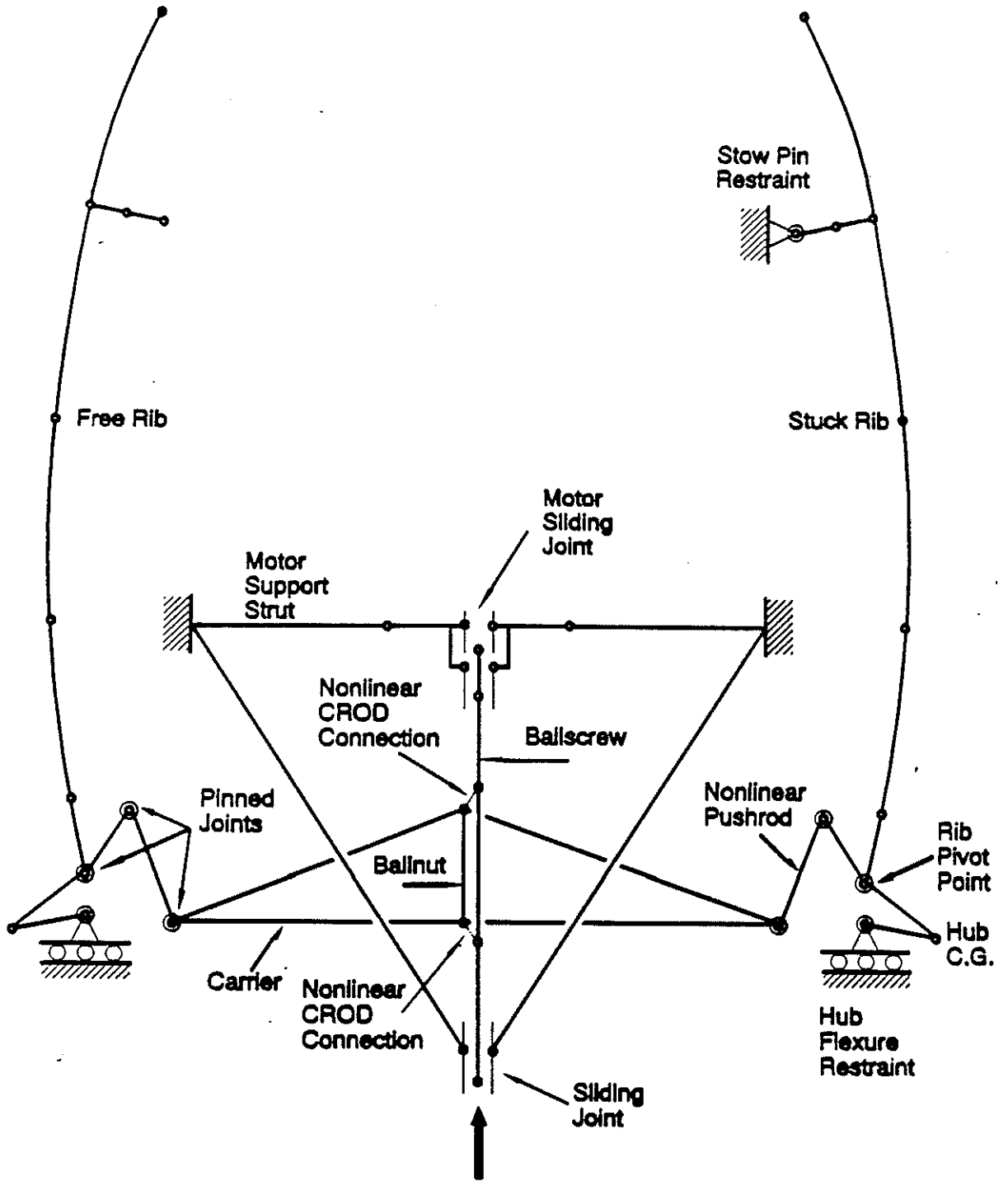


Figure 4.2.1-2: MDS Modelling

4.2.2 Four Rib Model

In an effort to reduce solution time and cost, for the computation intensive pin walkout analysis, Rapacz removed all unnecessary ribs and their associated pushrods from the full model (Ref. 12). Only four ribs were retained, the three that are assumed to be stuck (nos. 9, 10, & 11), and one free rib (no. 1) directly opposite the stuck ribs, see Figure 4.2.2-1. The free rib was retained for convenience in displaying rib deployment for the rib that is furthest out.

Gap elements, with friction, were added to the reduced model to represent the contact interface between the mid-point restraint pin and receptacle. Each pin utilizes two gap elements, one representing the contact interface of the pin with the upper surface (of the groove or cone), while the second represents the contact interface of the pin with the lower surface (of the groove or cone), see Figure 4.2.2-2. Each gap element is oriented to reflect the inclination of the contact surface it represents. Since each rib has two pins, and three ribs are assumed to be stuck, a total of twelve gap elements are used in the model.

In the pin friction theory, the pins are assumed to have an initial misalignment that results from design tolerances. This is modelled by displacing the pins opposite to one another in the vertical plane, and in a direction perpendicular to the pin axis. Its worth mentioning, that this also represents the case in which both pins are aligned, but the receptacle is rotated. The forms of misalignment considered here, however, only represent two of the many possible cases, and the actual misalignment could be different.

D-9932

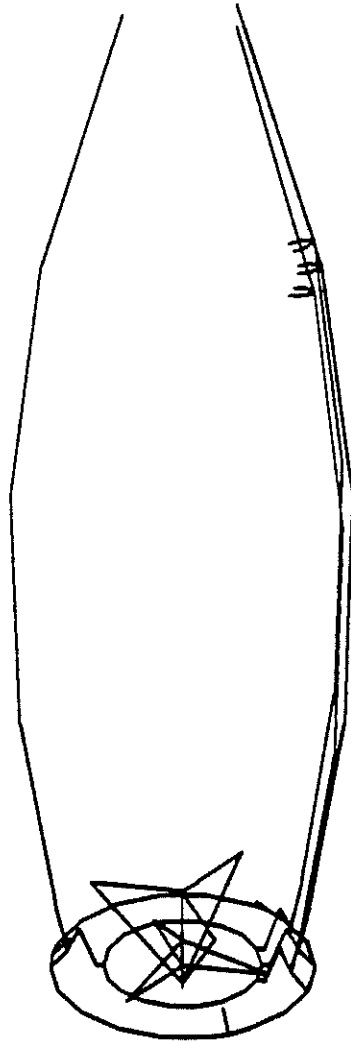


Figure 4.2.2-1: Four Rib Model

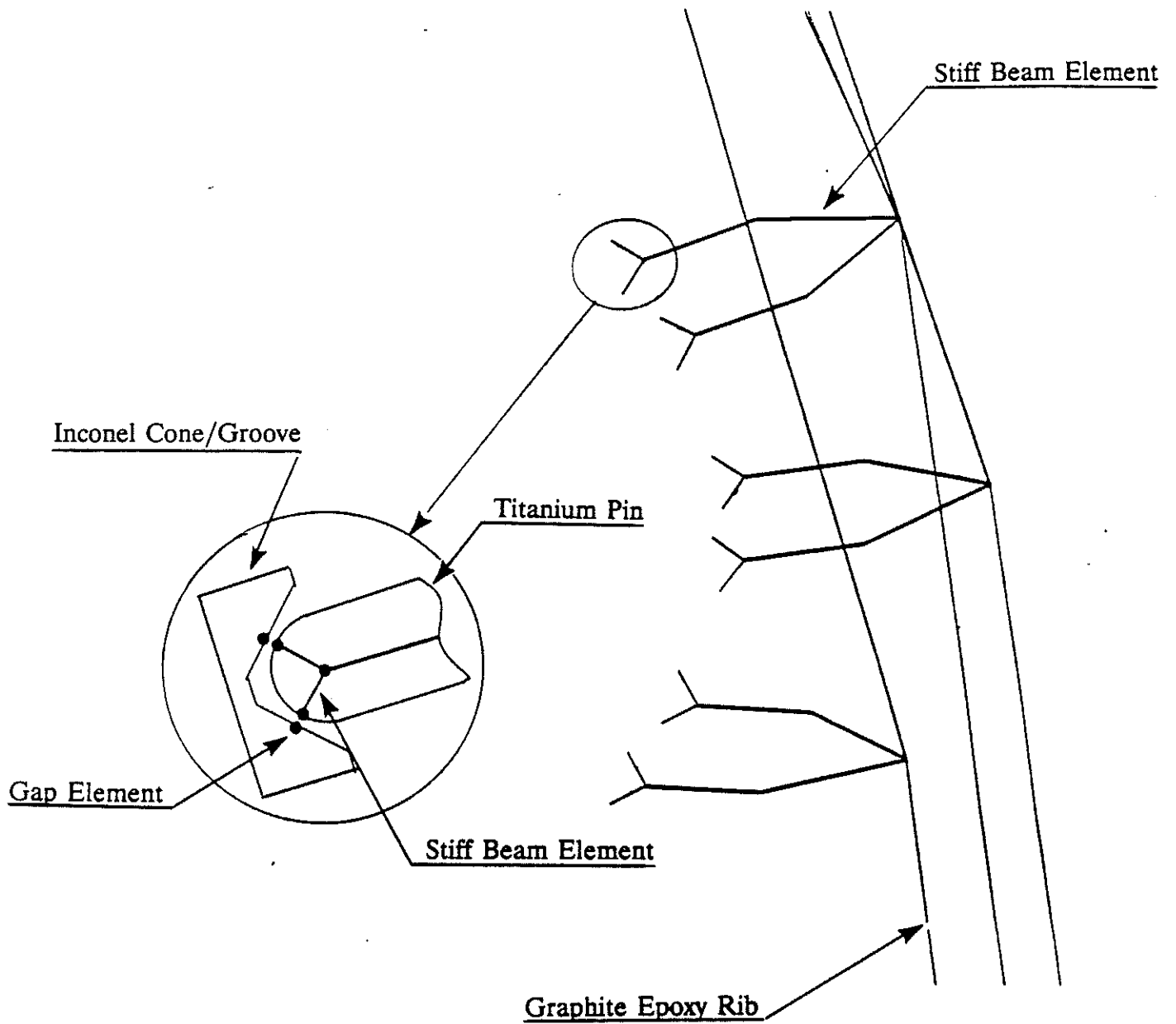


Figure 4.2.2-2: Pin To Receptacle Modelling

4.2.3 Single Rib Model

The localized nature of the nonlinearities, namely the stick/slip friction joints, and problem tractability motivated the use of a single rib model for the initial proof-of-concept studies. The analytical complexity of solving the pin walkout problem in combination with the nonroutine nature of the analysis also favor this approach. In view of this, a model consisting of a single graphite epoxy rib together with its titanium fittings and mid-point restraint pins was extracted from the four rib model. The resulting simplified model permitted cost effective solutions to be obtained while maintaining accuracies consistent with the objectives of the present study. Although, the model was originally intended for the initial proof-of-concept investigations, it was later used for many other investigations due to its accuracy and quick turn around times (as compared to the four rib model).

In using the single rib model, displacement boundary conditions were specified for the rib pivot point. This was necessary to account for the rib base distortions that are introduced by the surrounding, but missing structure. These displacements are functions of carrier and feed tower position, and were obtained from the full model (with three ribs restrained and ballscrew stalled at 5.1 turns) for a few selected antenna states and linearly interpolating for the specific loading states of interest.

4.3 LOADING HISTORY

4.3.1 Pin Misalignment Loads

Pin misalignment loads are produced by an enforced displacement process that eliminates the misalignment between the pair of mid-point restraint pins. This procedure introduces a pair of pin tip forces that are perpendicular to the pin axis, lie in the vertical plane, and are equal and opposite to each other. The amount of preload, of course, depends on the amount of misalignment assumed.

4.3.2 Tower Contraction

As the antenna is cooled or heated, the tower contracts or expands, relative to the rib. The amount of relative motion, being dependent on the temperature distribution of the antenna, varies with the spacecraft's attitude and heliocentric distance. The vertical component of tower displacement (relative to the rib) has been estimated by the Thermal group and is presented in Figure 4.3.2-1, as a function of heliocentric distance and spacecraft attitude (Ref. 13). Room temperature is used as the reference state for zero tower displacement.

In Figure 4.3.2-1, tower displacements are provided for three spacecraft attitudes. Nominally, the spacecraft is in a sun-pointed attitude (antenna pointed toward the sun) and the tower has the displacement values given by the "Sun-Pointed" curve. When the antenna is cooled, the spacecraft is turned 165 degrees away from the sun, and the displacement state of the tower is given by the "165 degree Off-Sun" curve. Finally, the "45 degree Off-Sun" curve provides the tower displacements when a warming turn is performed and the spacecraft is brought to a 45 degree off-sun attitude.

Before using these values, however, adjustments must be made to account for the moisture release from the composite members. The relative contraction that occurs between the ribs and tower, because of the moisture release from the graphite epoxy ribs and honeycomb radome (which puts the ribs in tension), has been estimated by Harris Corporation to be 9 mils. This

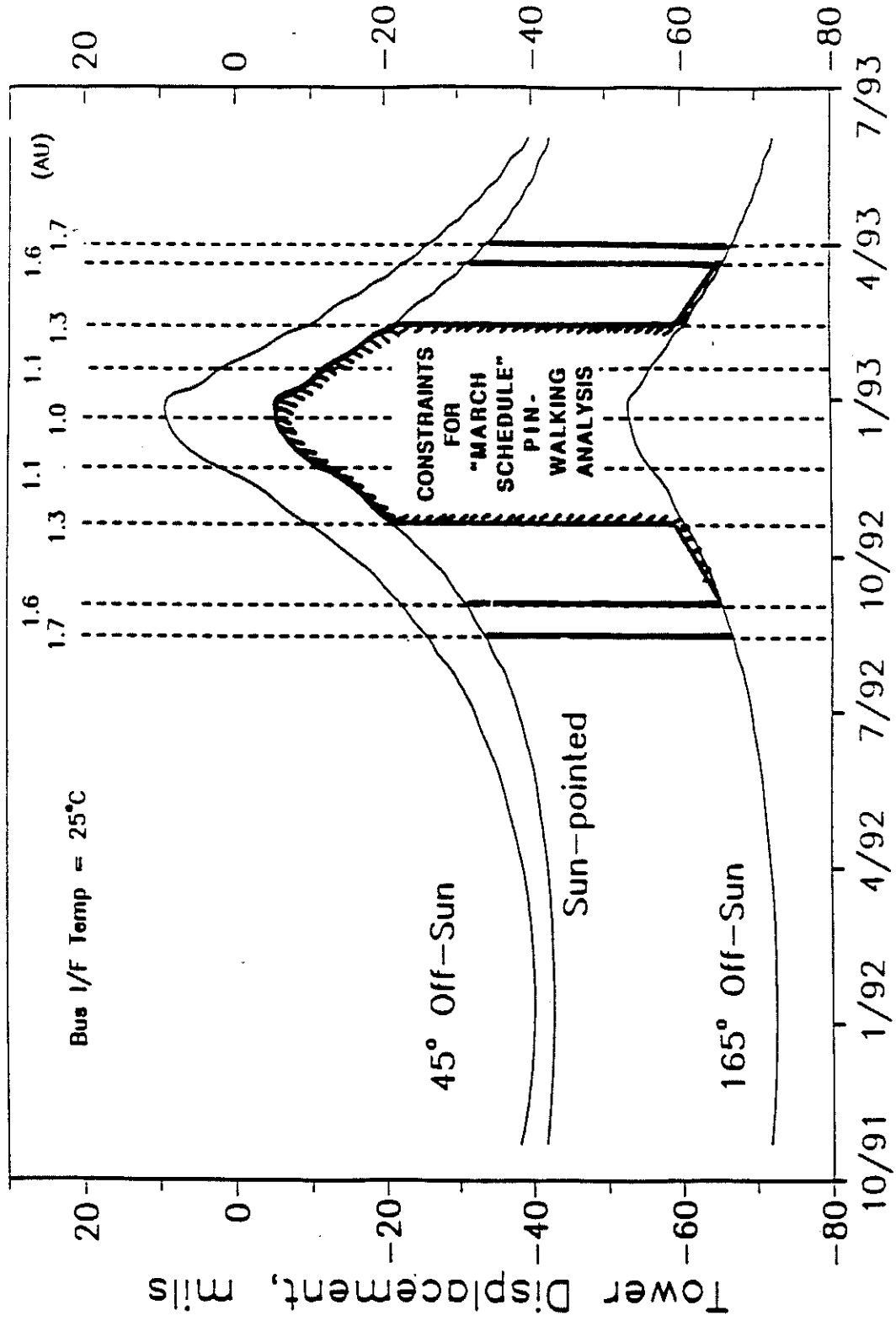


Figure 4.3.2-1: Feed Tower Displacement

34

introduces an equivalent static expansion of the tower which must be subtracted from the displacement values shown in Figure 4.3.2-1. For a given heliocentric distance and spacecraft attitude, the relative motion that occurs between the tower and ribs, is simulated by displacing the pin tips vertically by an amount 9 mils less than that specified in Figure 4.3.2-1.

4.3.3 March 92 Cooling Turn Scenario

Taking into consideration the pre-planned spacecraft activities and findings from an earlier, but preliminary investigation of the pin walkout problem (Appendix 8.1 & 8.2), the Galileo Flight Operations Team developed a schedule for performing the spacecraft warming and cooling turns that attempts to maximize the chances of releasing the ribs. This schedule is shown graphically in Figure 4.3.3-1 for turns executed this year, which are for turns 4 thru 12. The complete turning schedule and corresponding tower contraction estimates are shown in Table 4.3.3-1.

In Appendix 8.1, the benefit of performing warming turns, in addition to the cooling turns, is examined. The additional tower expansion provided by the warming turn was found to provide quicker rib release when compared to cases where no warming turns were performed. Table 4.3.3-1 reflects this finding by including a warming turn, prior to each cooling turn, starting with turn 4 (warming turn 1 was performed before any pin walkout studies were conducted).

A study which investigates the benefit of performing warming and cooling turns at a fixed heliocentric distance is described in Appendix 8.2. The study found that cooling turns performed at distances less than 1.3 AU was ineffective due to the constraints placed on the spacecraft by the thermal limitations of various hardware. This is reflected in the March 92 Cooling Turn Scenario which does not have any cooling turns for spacecraft distances less than 1.3 AU.

In addition to defining the cooling turn scenario, Table 4.3.3-1 defines the loading history for the antenna. The first two columns on the left shows the correspondence between the NASTRAN load case (subcase) number and the event it represents. The events represented include: pin preloading (subcase 1), antenna deployment attempt (subcase 3), warming/cooling turns 1 - 12 (subcases 5 - 31), and Earth-2 encounter (subcase 25).

PRELIMINARY HGA ACTIVITIES SCHEDULE

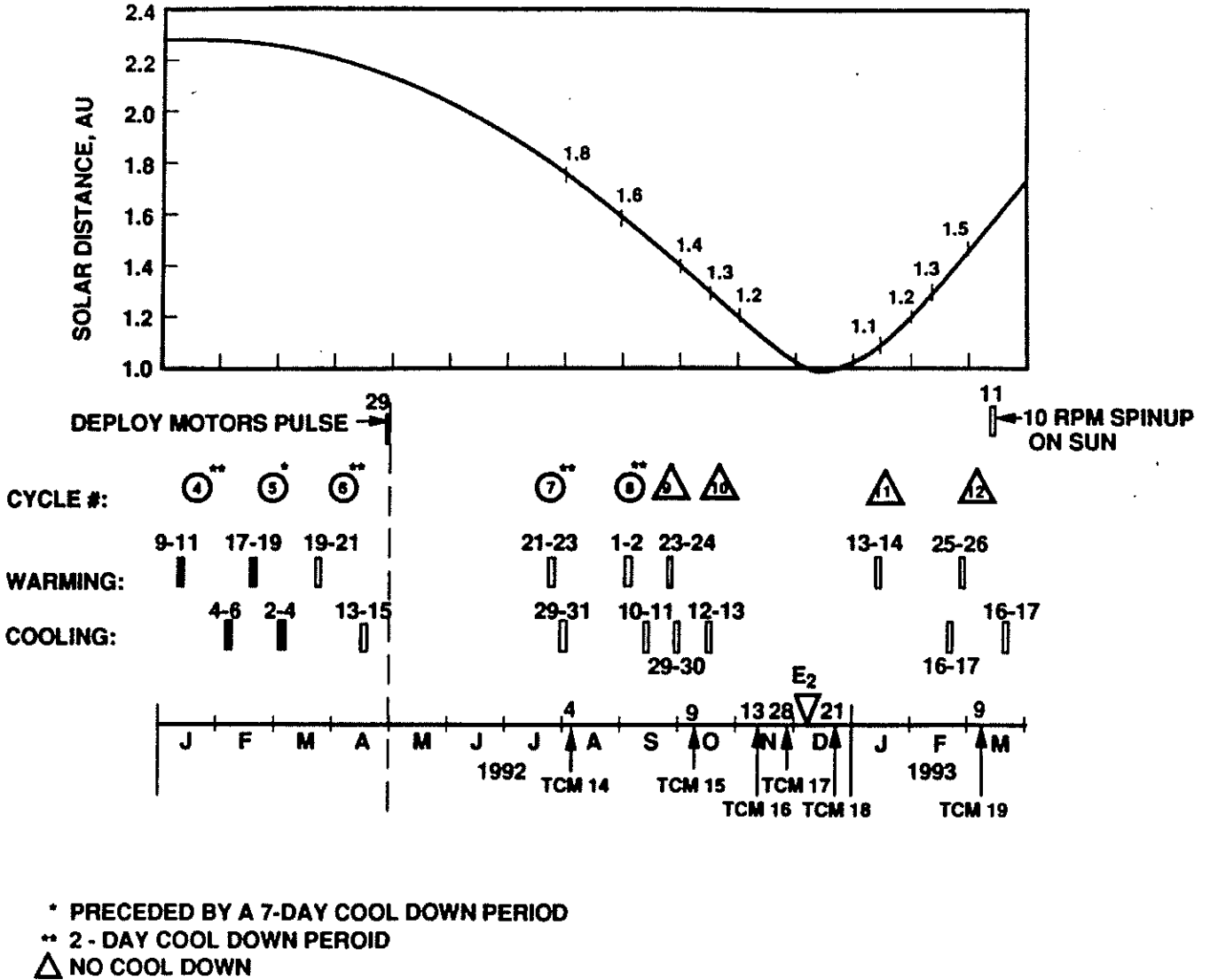


Figure 4.3.3-1: March 92 Cooling Turn Schedule

Table 4.3.3-1: Loading History - March 92 Cooling Turn Scenario

NASTRAN Subcase	EVENT	Heliocentric Distance (AU)	Tower Displacement (mils)	Tower Displacement + 9 mil Rib Contraction (mils)
1	Pin Preload	1.00	0.0	N/A
2	Pre-Deploy	1.32	-21.4	-12.4
3	Deploy Attempt	1.32	-21.4	-12.4
4	Pre-Warming Turn 1	1.57	-30.4	-21.4
5	Warming Turn 1	1.57	-21.4	-12.4
6	Cooling Turn 1	1.84	-67.9	-58.9
7	Post Cooling Turn 1	1.84	-36.1	-27.1
8	Cooling Turn 2	1.98	-70.0	-61.0
9	Post-Cooling Turn 2	1.98	-39.1	-30.1
10	Cooling Turn 3	2.25	-72.3	-63.3
11	Warming Turn 4	2.27	-40.1	-31.1
12	Cooling Turn 4	2.26	-71.7	-62.7
13	Warming Turn 5	2.25	-39.7	-30.7
14	Cooling Turn 5	2.24	-71.6	-62.6
15	Warming Turn 6	2.21	-38.9	-29.9
16	Cooling Turn 6	2.16	-71.2	-62.2
17	Warming Turn 7	1.81	-29.1	-20.1
18	Cooling Turn 7	1.77	-68.5	-59.5
19	Warming Turn 8	1.58	-21.7	-12.7
20	Cooling Turn 8	1.53	-64.4	-55.4
21	Warming Turn 9	1.45	-16.6	-7.6
22	Cooling Turn 9	1.41	-62.6	-53.6
23	Pre-Cooling Turn 10	1.33	-22.4	-13.4
24	Cooling Turn 10	1.33	-60.7	-51.7
25	Earth Encounter	1.00	-5.4	3.6
26	Pre-Warming Turn 11	1.07	-9.8	-0.8
27	Warming Turn 11	1.07	3.8	12.8
28	Cooling Turn 11	1.32	-60.7	-51.7
29	Warming Turn 12	1.40	-14.7	-5.7
30	Cooling Turn 12	1.57	-65.1	-56.1
31	Post-Cooling Turn 12	1.57	-30.4	-21.4

5.0 RESULTS AND DISCUSSION

5.1 RIB RELEASE CURVES

5.1.1 Basic Curves

Figure 5.1.1-1 summarizes the results from an extensive nonlinear analyses effort. The curves provide, for an assumed pin preload and friction coefficient, the number of spacecraft cooling turns that are required to release one of the three stuck ribs. Each point on the curve represents a nonlinear analysis that was performed using the single rib model and the loading history defined in Table 4.3.3-1. Associated with each curve, is a single rib model with its pins misaligned by an amount that gives the desired preload. Displacement boundary conditions for rib 11, obtained from the full model with three stuck ribs and ballscrew stalled at 5.1 turns, was applied to the single rib model. Moisture dryout from the composite members was accounted for by using the reduced tower contractions shown in Table 4.3.3-1. Each curve is produced by varying the friction coefficient (assumed to be the same for both pins), performing a nonlinear analysis for each friction value, and noting the cooling turn at which rib release occurs.

To gain some insight into the pin walking phenomenon, plots detailing the pin forces and slippage, as a function of the loading state, were generated for representative cases. They are shown in Figures 5.1.1-2 through 5.1.1-4. In these plots, the forces and slippage associated with the upper pin are shown in the upper half of the plot, while the same quantities for the lower pin are shown in the lower half of the plot. Figure 5.1.1-5 defines the normal and shear force, and slip convention used. The mapping between the NASTRAN load case numbers, shown on the abscissa, and loading event is provided by the loading history given in Table 4.3.3-1.

The amount of information provided by these plots can be overwhelming at first sight, and therefore, some of the more important features of the curves will be highlighted using Figure 5.1.1-2. First, in subcase 1, the pins are preloaded to 20 lbs, and the normal and shear forces are approximately equal, indicating a preload that is perpendicular to the pin axis (since, the angle between the pin axis and contact surface is 45 degrees). The amount of preload can be verified by summing (vectorially) the two force

COOLING TURNS REQUIRED FOR RIB RELEASE
Basic Rib Release Curves

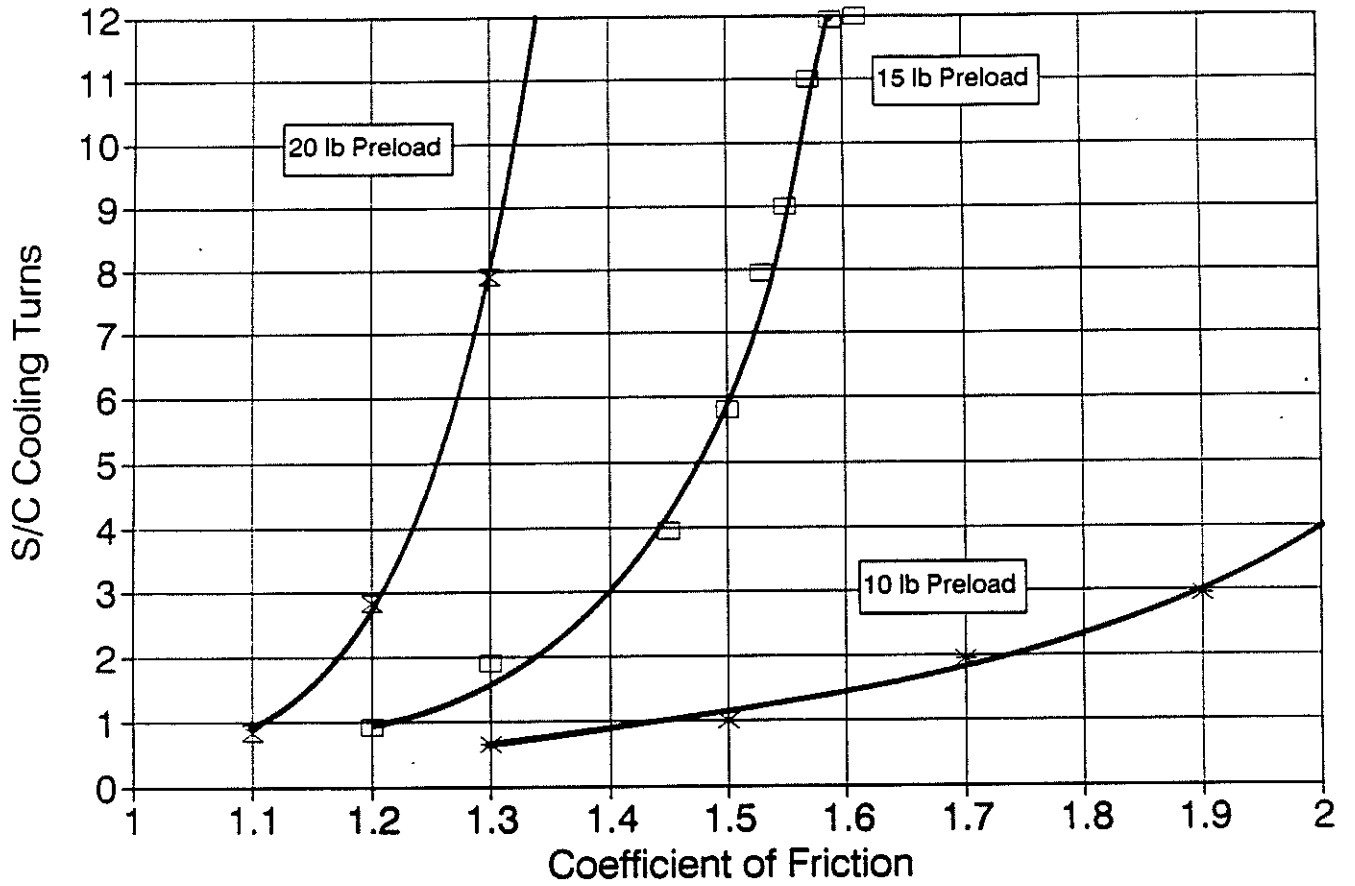


Figure 5.1.1-1: Basic Rib Release Curves

PIN FORCES AND SLIPPAGE

Mar 92 Scenario, 20 lb Preload, $\mu=1.30$

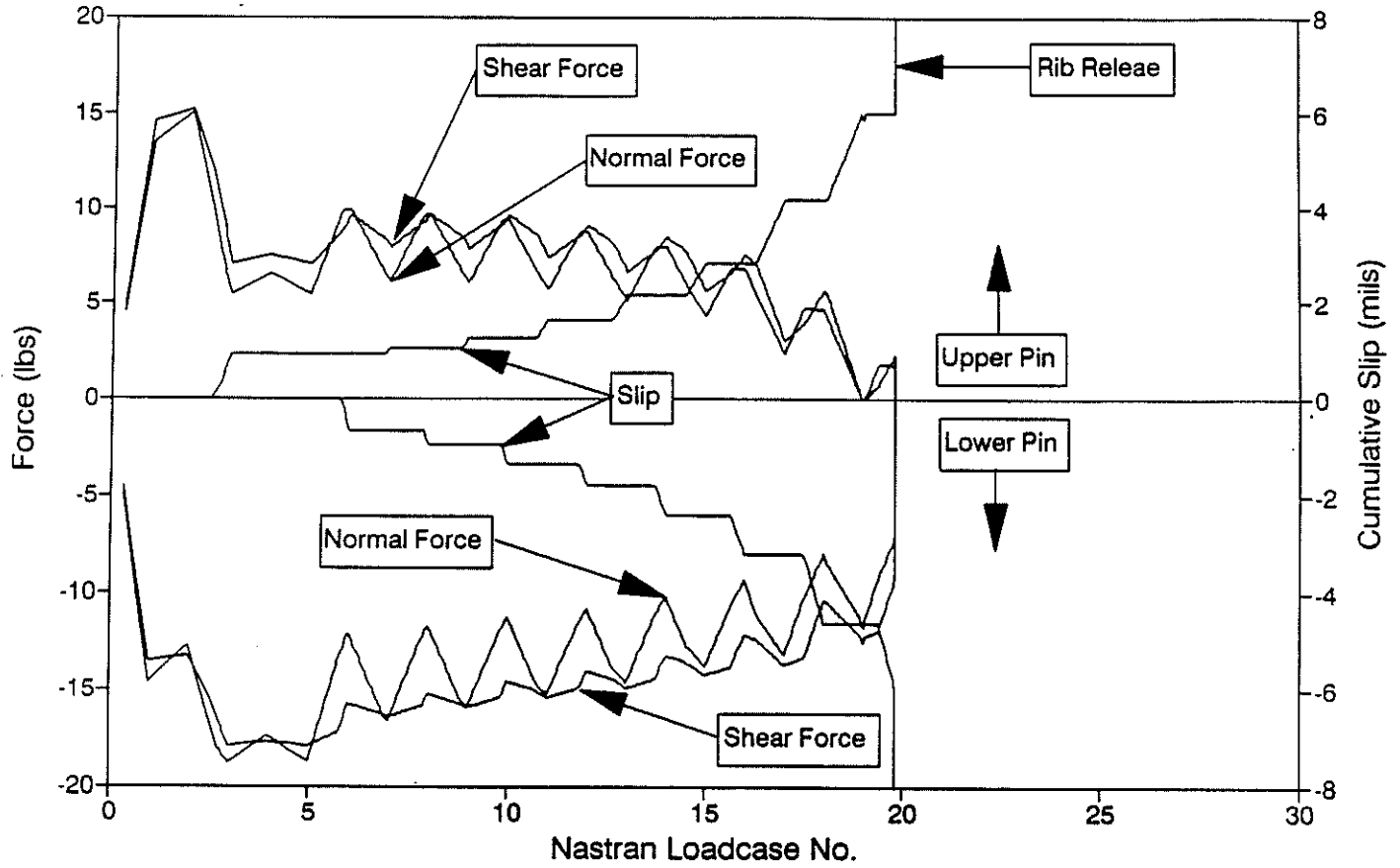


Figure 5.1.1-2: Pin Force/Slippage Plot - 20 lb Preload, $\mu = 1.30$

PIN FORCES AND SLIPPAGE

Mar 92 Scenario, 15 lb Preload, $\mu=1.57$

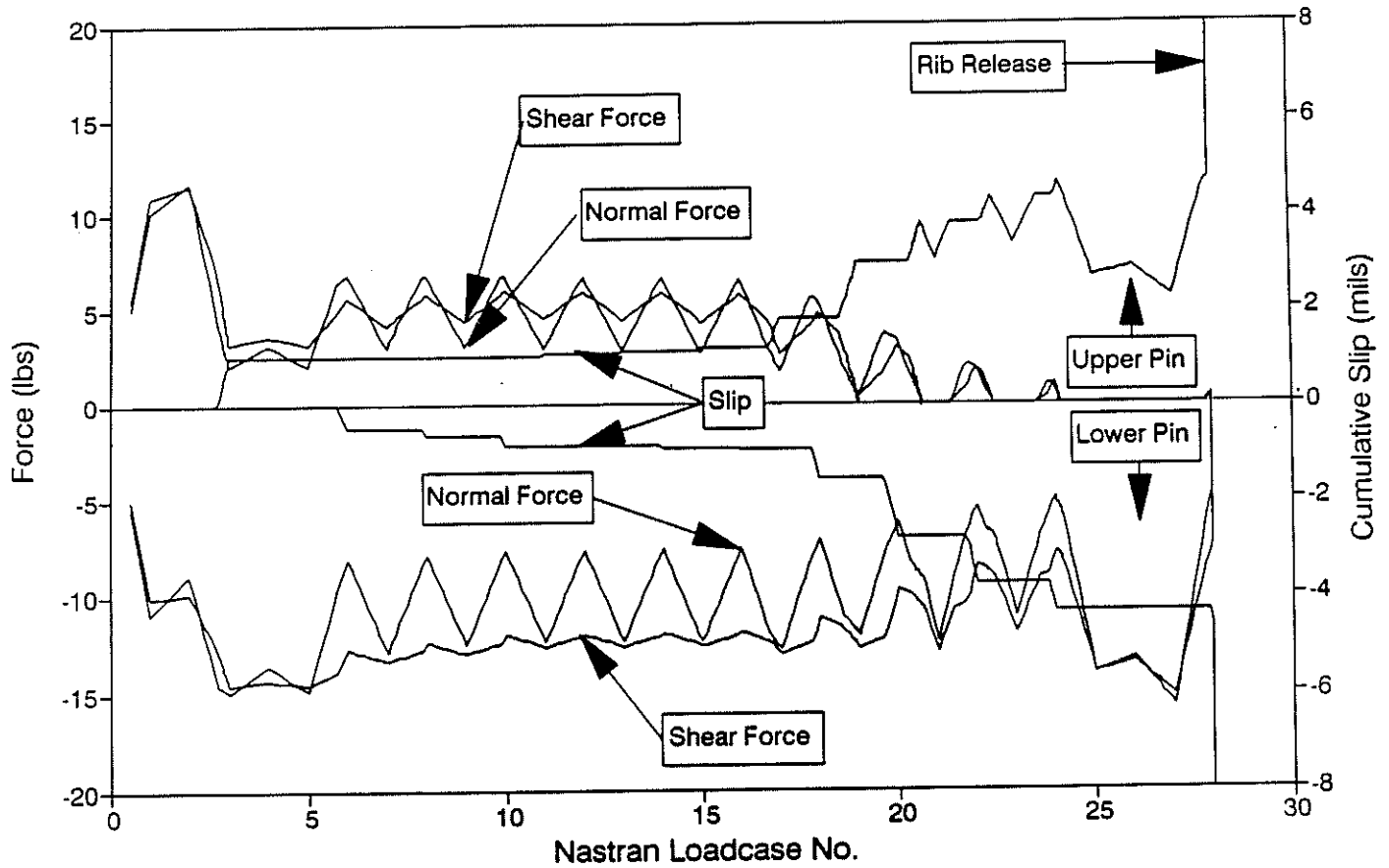


Figure 5.1.1-3: Pin Force/Slippage Plot - 15 lb Preload, $\mu = 1.57$

PIN FORCES AND SLIPPAGE

Mar 92 Scenario, 10 lb Preload, $\mu = 1.90$

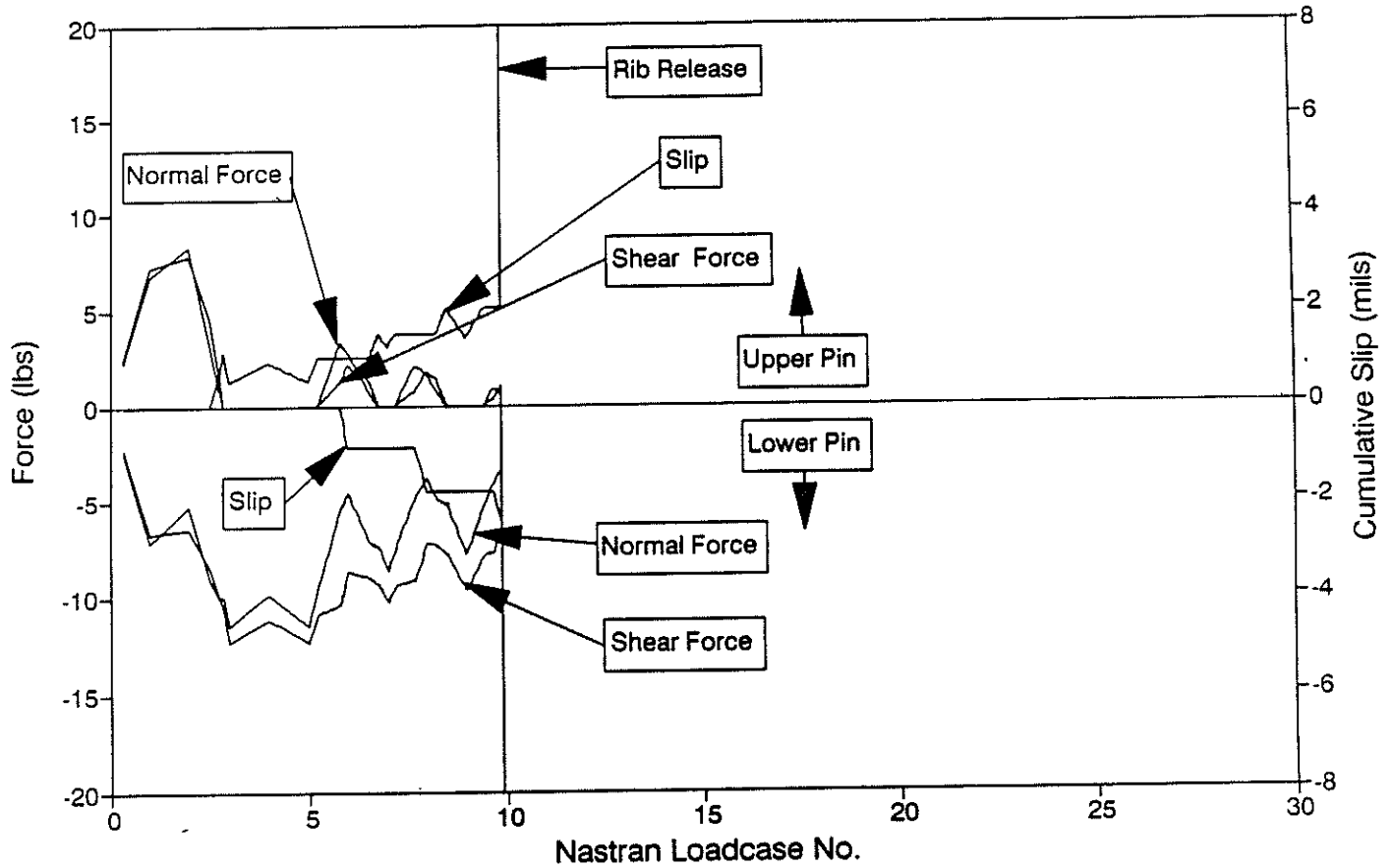


Figure 5.1.1-4: Pin Force/Slippage Plot - 10 lb Preload, $\mu = 1.90$

Cone/Groove

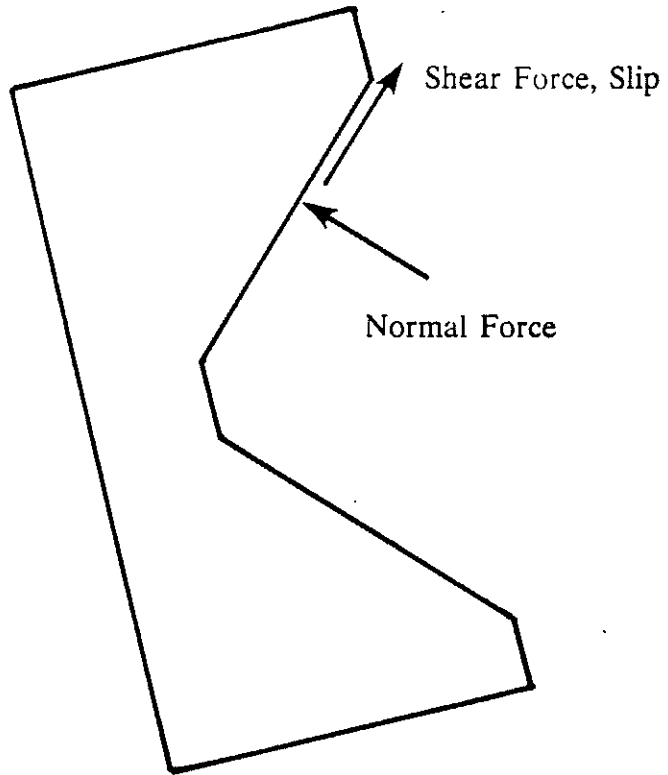


Figure 5.1.1-5: Pin Forces and Slippage - Convention

components, it should be equal to the value shown in the plot title. After preloading the pins, the analysis simulates the thermal state of the antenna at 1.32 AU by contracting the tower 12.4 mils. This causes the forces for the lower pin to decrease and those for the upper pin to increase. In subcase 3, an attempt is made to deploy the antenna which causes the pin forces for the lower pin to increase, while the upper pin forces decrease. During this time, slip is initiated at the upper pin. Following the deployment attempt, the antenna is brought to the thermal state corresponding to 1.57 AU by contracting the tower to 21.4 mils. This reduces the load in the lower pin and produces an opposite load change for the upper pin. Warming turn 1 (subcase 5), expands the tower by 9 mils causing the lower pin forces to increase while those for the upper pin decrease. Starting with subcase 6, the spacecraft cooling and warming turns are performed. Each cooling turn results in a peak for both the normal and shear force curves, while the warming turns produces a valley in these curves. Lower pin slippage is initiated at cooling turn 1 (subcase 6). Subsequent warming, causes the lower pin to stick while the upper pin slips. Cooling the antenna once again, causes the upper pin to stick and the lower pin to slip. Repeating this process 6 more times, finally causes the rib to release during cooling turn 8.

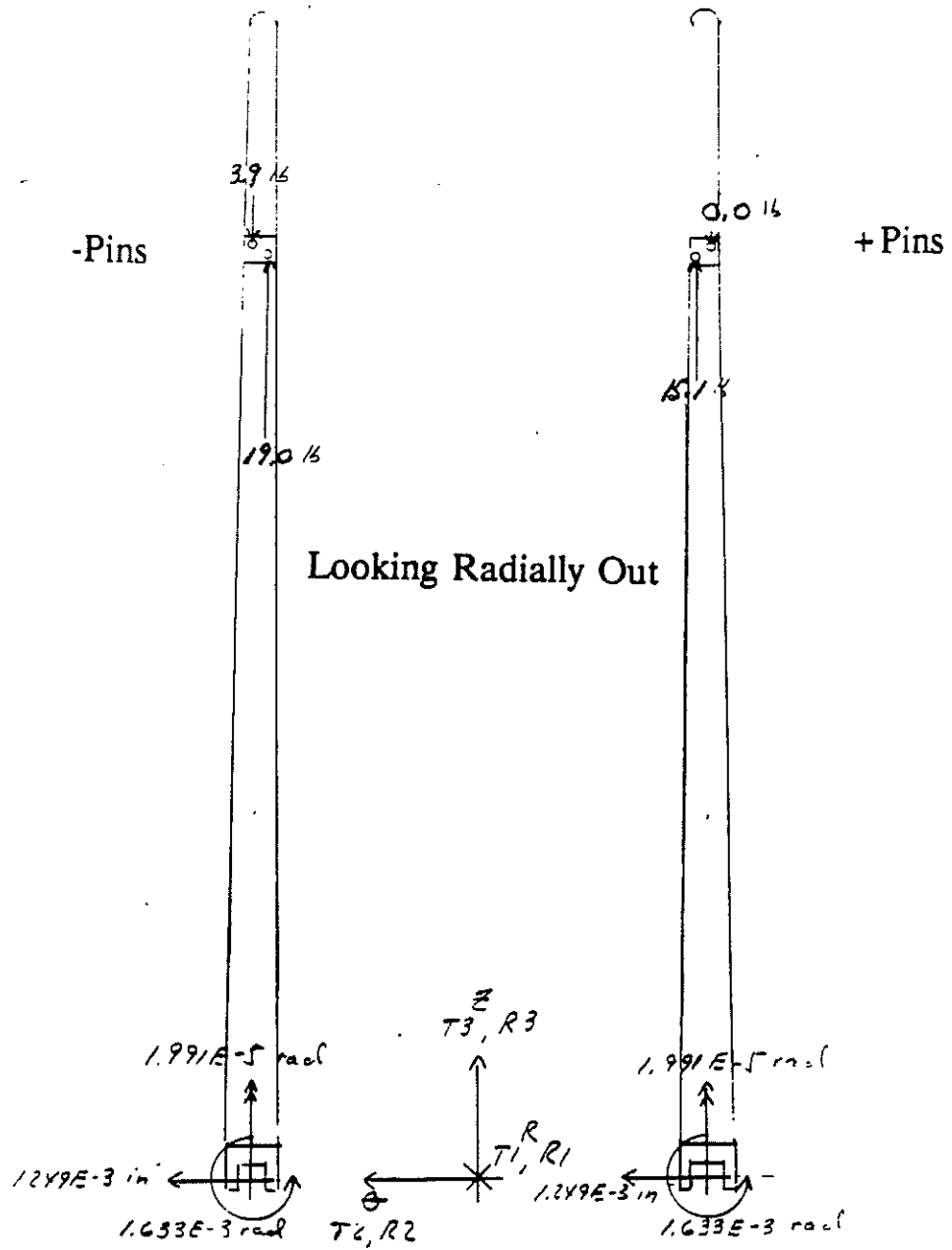
During the warming and cooling turns, the rate of change in normal force is found to be greater than the rate of change in shear force. The rapid rise and fall of normal force combined with the relatively small change in shear force is what drives pin walkout. During cool down, the normal force rapidly rises for the upper pin causing it to anchor itself on its contact surface, while the rapid loss in normal force and resulting pin rotation causes the lower pin to slip. During warm-up, just the opposite occurs; this time the rapid rise in normal force cause the lower pin to anchor itself, while the upper pin slips.

5.1.2 Effects of Pin Polarity

Although the single rib model has a longitudinal plane of symmetry (i.e., about the r-z plane), Hub distortions occurring at the base of the rib introduces nonsymmetry into the problem. The nonsymmetric displacement terms, especially the radial rotation, that are applied to the base of the single rib model causes the pin loads to be dependent on the direction of pin misalignment. More specifically, in Figure 5.1.2-1, the rib on the left has its left pin up and right pin down. When this rib is stowed, a counter clockwise moment is produced by the preloads. On the other hand, when the pins are oppositely misaligned, like those shown for the rib on the right, a clockwise moment is developed by the preloads. At deployment, the radial rotation developed at the base of the rib causes the pin loads to be larger for the rib on the left than for the one on the right.

This load difference causes the rib with less pin loads to release quicker than the other. Figure 5.1.2-2 illustrates this by presenting the rib release characteristics for the two possible pin misalignment configurations. The curves identified as "+Pins" are the same as those shown in Figure 5.1.1-1, and were produced using the single rib model with its pins oriented as shown by the rib on the right in Figure 5.1.2-1. The "-Pins" curves were generated using the same model but with its pins in the reverse orientation. These results show that pin polarity plays a significant role in rib release.

D-9932
PIN FORCES
AT END OF DEPLOYMENT ATTEMPT



Non-Symmetric Displacement BCs

Figure 5.1.2-1: Pin Polarity - Effects on Pin Loads

COOLING TURNS REQUIRED FOR RIB RELEASE Effects of Pin Polarity

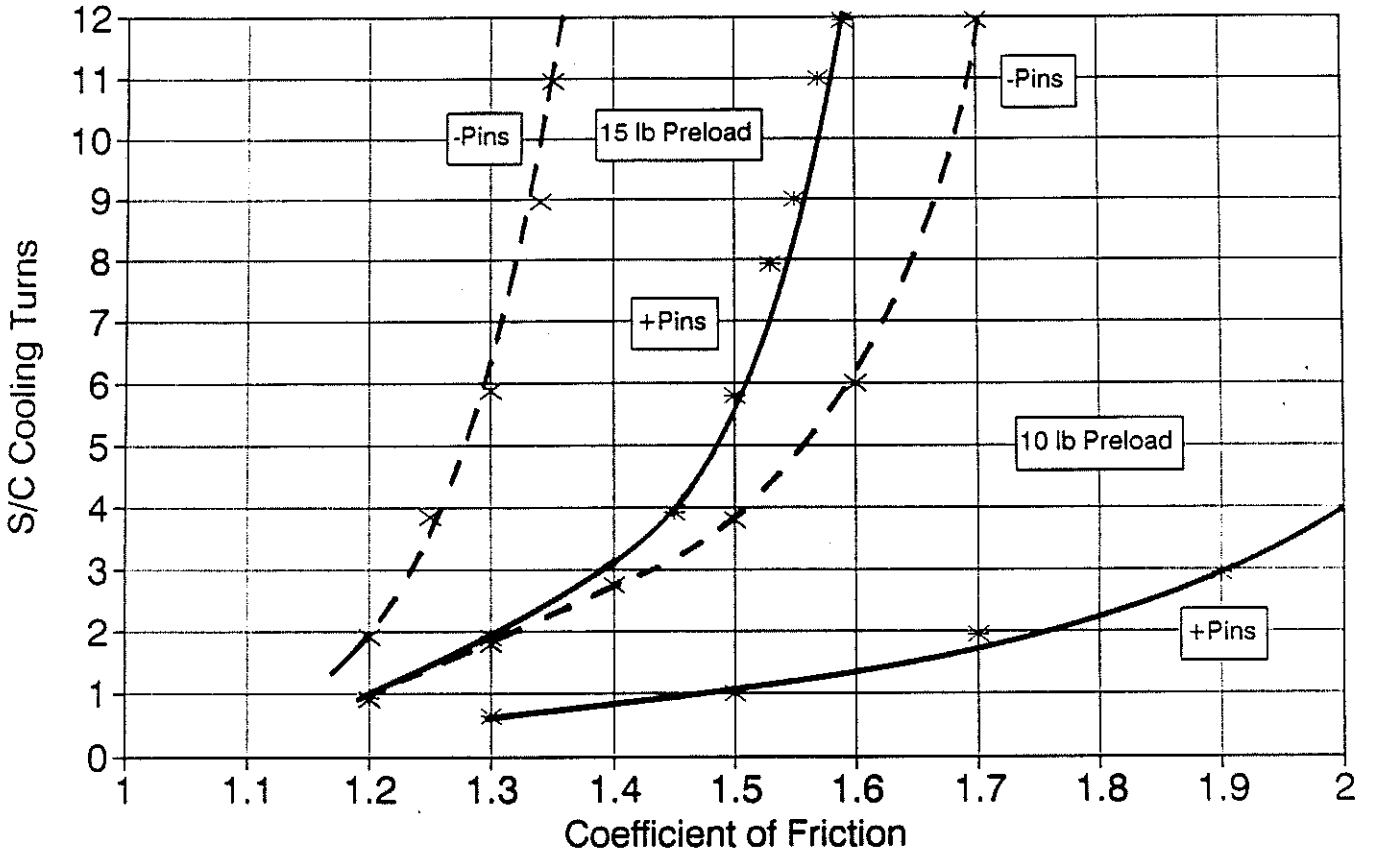


Figure 5.1.2-2: Pin Polarity - Effects on Rib Release

5.1.3 First Rib Release

Analyses performed so far, reflect the fact that three ribs are stuck, but it does not provide answers to questions regarding the release sequence of the ribs. In this section, an analysis is described that attempts to determine which of the three ribs releases first.

Presented in Figure 5.1.3-1, are the rib release characteristics for the each of the three stuck ribs with their pins oriented in one of the two possible pin configurations. For clarity, only the 10 lb curves are shown; similar results are obtained for the 15 lb preload. These results were obtained by applying the various rib displacement boundary conditions to the single rib model. For each rib, two pin polarities are possible, and therefore, a total of six curves are presented.

To answer the first rib releases question, pin polarity combinations for the three stuck ribs must first be determined. Since each rib has two possible pin configurations, and there are three stuck ribs, a total of eight rib and pin polarity combinations are possible. These are shown in Figure 5.1.3-2. Using this Figure and the results presented in Figure 5.1.3-1, one can determine which of the three ribs releases first for each of the possible combinations. This has been done and the results are shown in the Figure. From these results, the upper two curves for each preload are found not to be possible candidates for first rib release. These curves have therefore been removed and the resulting plot is shown in Figure 5.1.3-3.

This Figure bounds the first rib release problem. The lower curve (solid line) represents the rib and pin combination that is easiest to release first, while the upper curve (dashed line) represents the rib and pin combination that is the most difficult to release first.

COOLING TURNS REQUIRED FOR RIB RELEASE
Effects of Rib and Pin Combinations

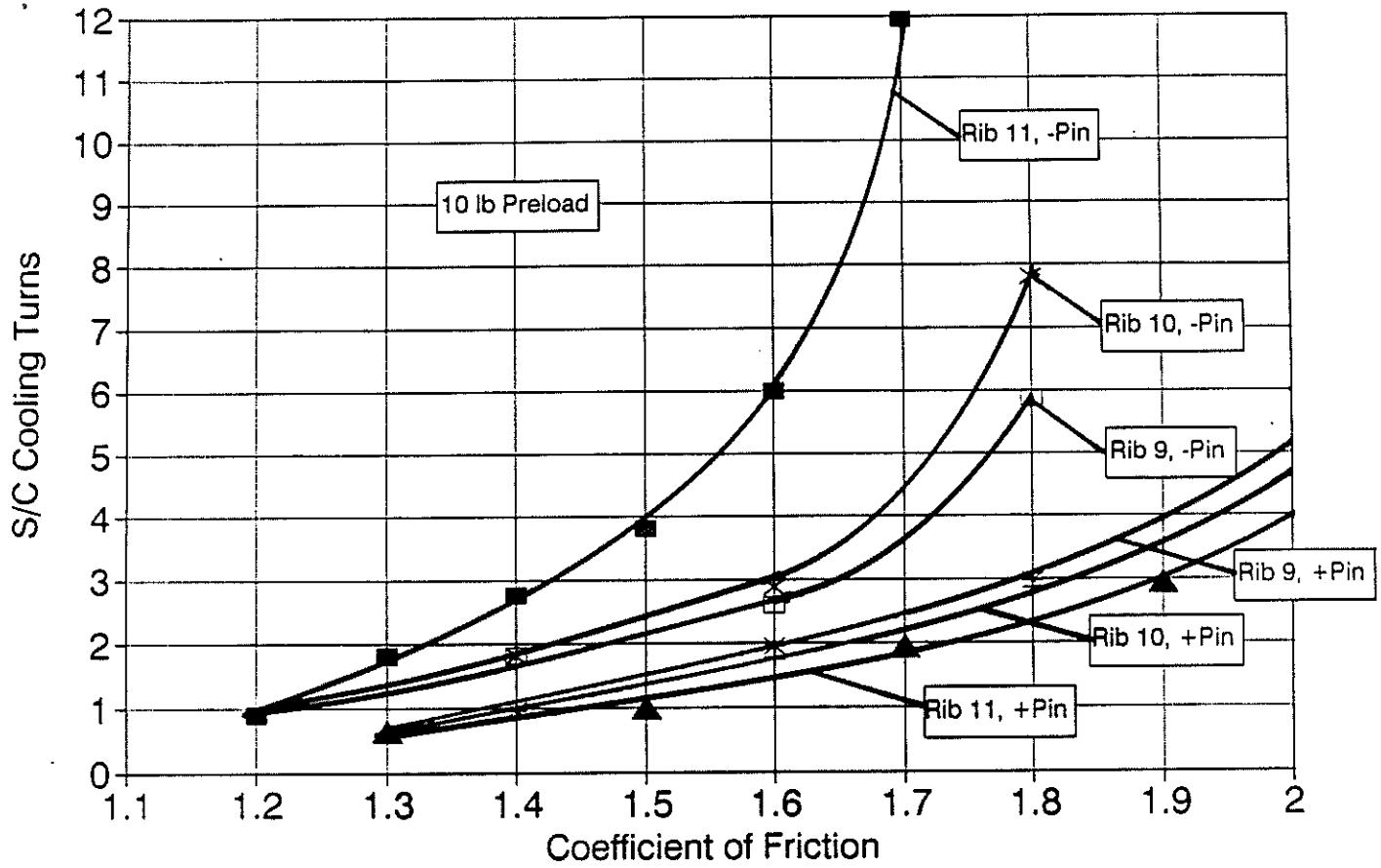
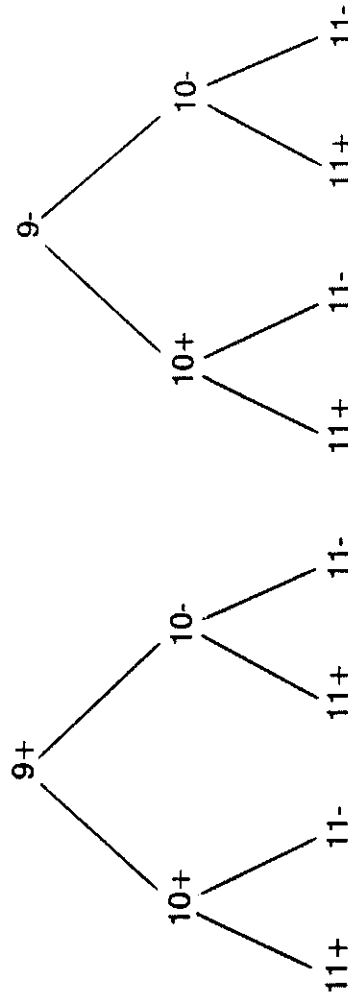


Figure 5.1.3-1: Rib Release Curves - All Rib and Pin Polarity Combinations

First Rib Release For All Combinations of Rib BCs and Pin Polarities



1st Rib Release	11+	10+	11+	11+	9+	10+	11+	11+	9-
-----------------	-----	-----	-----	-----	----	-----	-----	-----	----

Nomenclature: 9+ = Rib 9 BCs, + Pins

Figure 5.1.3-2: Rib and Pin Polarity Combinations

COOLING TURNS REQUIRED FOR RIB RELEASE First Rib Release Curves

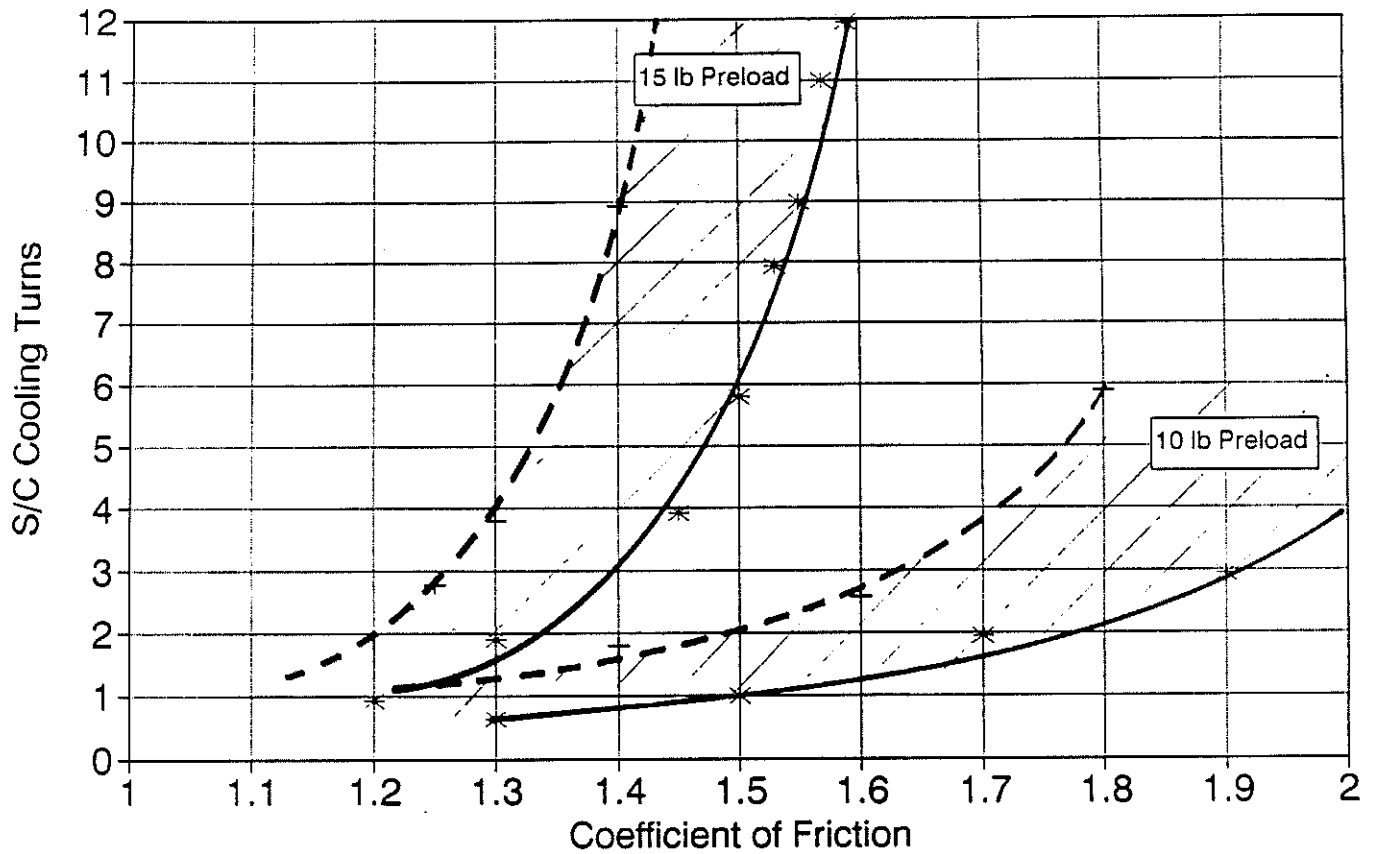


Figure 5.1.3-3: First Rib Release Curves

5.1.4 Subsequent Rib Releases

Having released the first rib, can the second and third ribs be released? This section answers this question for a special case in which the pin characteristics (preload, polarity and friction) are assumed to be same for all three ribs.

Using the four rib model and the loading history shown in Table 5.1.4-1, pin walkout analyses were performed to investigate the problem of releasing all three ribs. In this analysis, all ribs had their pins oriented in the "+Pin" configuration and friction was assumed to be the same for all pins. The analysis is initiated by preloading the pins to cause them to stick to their receptacles (assumes friction coefficients greater than one). Following this, the antenna is brought to the thermal state corresponding to 1.32 AU by displacing its pin tips 20.3 mils vertically down. (Note: the 9 mil rib contraction that results from moisture dryout was not included in this analysis, since its effect was not known at the time this analysis was performed.) Once brought to the thermal state corresponding to 1.32 AU, the lower end of the ballscrew was displaced 0.6375" vertically upwards (5.1 ballscrew turns) to bring the antenna into its unsymmetrically deployed state. Thermal cycling was then performed according to the loading history shown in Table 5.1.4-1, until all ribs were released or all cooling turns were performed.

The loading history shown in Table 5.1.4-1 is not the March 92 scenario, but is an earlier version that was used for preliminary investigations into the pin walkout problem. Due to the high cost and long run times (approximately 4k and 5 days for one preload and one friction value), this analysis was never updated. With the exception of the results documented in some of the Appendices, this is the only section of the report that uses this loading history.

The results from this analysis effort are summarized in Figure 5.1.4-1. Two preloads were investigated. For a preload of 15 lbs, three curves are shown (dashes indicates extrapolation). The lowest curve represents first rib release, the next higher one, second rib release, and finally, the top curve last rib release. For a preload of 10 lb, only two curves are shown; the lowest is first rib release and the higher one second rib release. Last rib release never occurred for a preload of 10 lb and the friction values assumed (1.5, 1.7 & 1.9); the reason for this is explained later in this section.

Table 5.1.4-1: Loading History - December 91 On-Sun Cooling Turn Scenario

ANALYSIS SUBCASE	EVENT	SOLAR AU	TOWER DISPLACEMENT (MILS)
1	PRELOAD PIN (20, 15 or 10 LB.)		
2	PRE-DEPLOYMENT	1.32	-20.3
3	DEPLOYMENT	1.32	-20.3
4	SUN POINTED	1.58	-29.7
5	WARMING TURN #1	1.58	-20.1
6	RETURN TO SUN	1.58	-29.7
7	COOLING TURN #1 (TAIL TO SUN)	1.84	-68.1
8	RETURN TO SUN	1.84	-35.8
9	COOLING TURN #2 (TAIL TO SUN)	1.98	-70.3
10	RETURN TO SUN	1.98	-40.0
	28° OFF-SUN	2.08	-40.7
	RETURN TO SUN	2.24	-45.0
11	COOLING TURN #3 (TAIL TO SUN)	2.25	-71.7
12	RETURN TO SUN	2.25	-42.2
13	COOLING TURN #4 (TAIL TO SUN)	2.27	-71.8
14	RETURN TO SUN	2.27	-42.4
15	COOLING TURN #5 (TAIL TO SUN)	2.22	-71.6
16	RETURN TO SUN	2.22	-42.0
17	COOLING TURN #6 (TAIL TO SUN)	2.15	-71.2
18	RETURN TO SUN	2.15	-41.1
19	COOLING TURN #7 (TAIL TO SUN)	2.0	-70.4
20	RETURN TO SUN	2.0	-39.1
21	COOLING TURN #8 (TAIL TO SUN)	1.75	-68.6
22	RETURN TO SUN	1.75	-34.4
23	COOLING TURN #9 (TAIL TO SUN)	1.55	-66.8
	RETURN TO SUN	1.55	-29.4
24	EARTH ENCOUNTER	1.00	-4.7
25	COOLING TURN #10 (TAIL TO SUN)	1.60	-67.3
26	RETURN TO SUN	1.60	-30.8
27	COOLING TURN #11 (TAIL TO SUN)	1.90	-69.8
28	RETURN TO SUN	1.90	-37.5

COOLING TURNS REQUIRED FOR RIB RELEASE Sequential Rib Release Curves

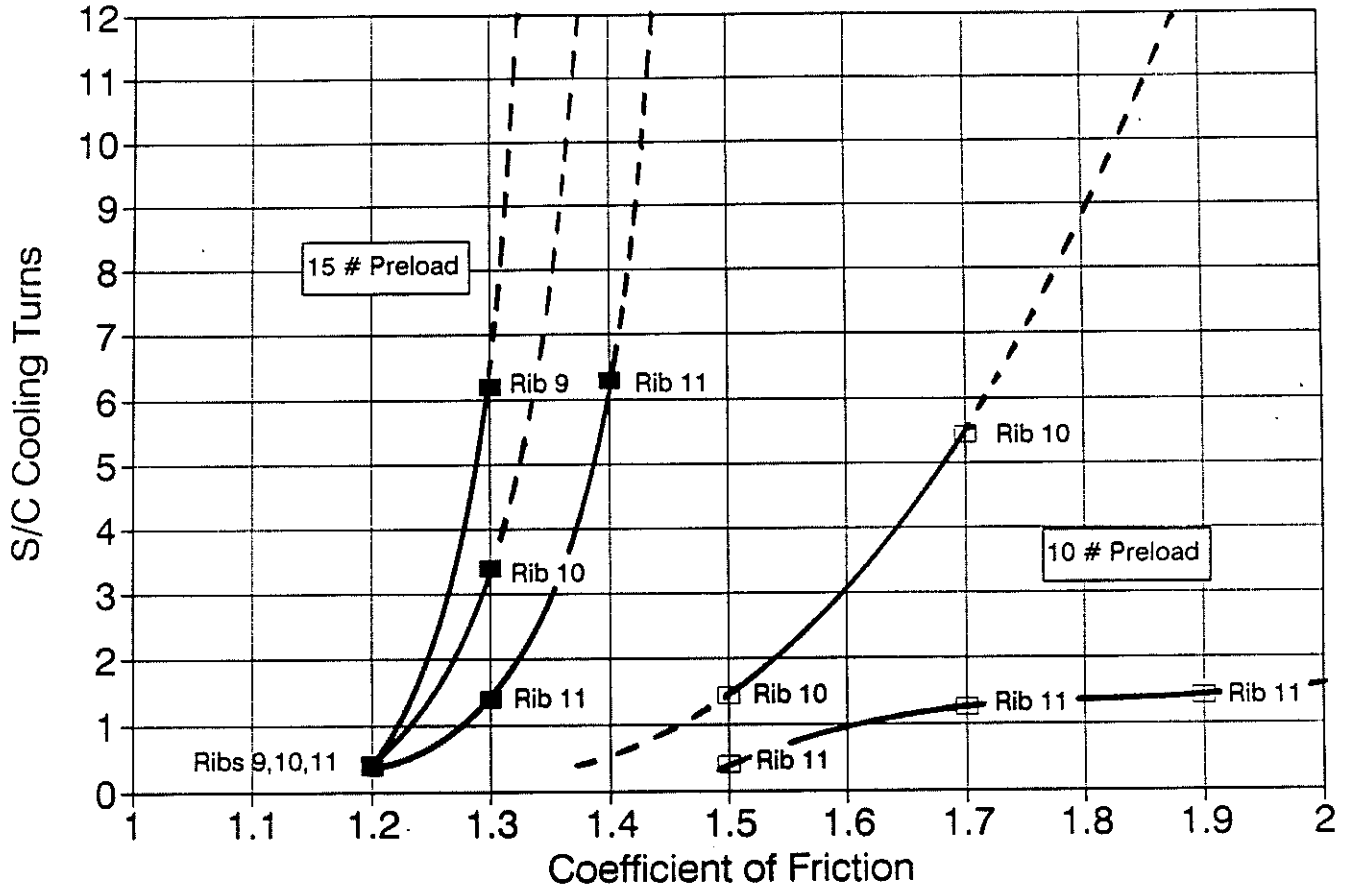


Figure 5.1.4-1: Sequential Rib Release Curves

The relative positions of the curves, show that rib release becomes more difficult as more ribs are released. This is seen by the second rib release curve being above and to the left of the first rib release curve. Likewise, the last rib release curve is above all other curves and is furthest to the left. This occurs because of the load increase that results, for the lower pins, when a rib is released. More on this is discussed below.

Plots detailing the state of the antenna as the loading history progresses are presented in Figures 5.1.4-2 through 5.1.4-7 for specific variables of interest. Pin slippage for all three stuck ribs are shown in Figure 5.1.4-2. The format for this plot and the three plots that follow is the same as those presented earlier; namely, the variable of interest for the upper pin are shown in the upper half of the plot, while the same variable for the lower pin are shown in the lower half. The vertical lines that appear in the pin slippage plot indicate rib release and it shows that rib 11 releases first, followed by rib 10, and no release is indicated for rib 9. Pin force/slippage plots for ribs 9, 10 & 11 are shown in Figures 5.1.4-3 through 5.1.4-5. In Figure 5.1.4-3, the notch that appears in the force curves during cooling turn 2 occurs because of the load redistribution that takes place when rib 11 releases. This produces a small load increase for the lower pin and a small load reduction for the upper pin. During the sixth cooling turn, rib 10 releases which produces a large increase in load for the lower pin. At the same time, the upper pin disengages from the upper surface and comes into contact with the lower surface. Since, this pin disengagement occurs during the cooling process and the pin never regains contact with the upper surface (for the tower contractions considered in this analysis), pin walkout is terminated from this point on, and rib 9 never releases. Figure 5.1.4-6 shows the tip displacements for the free rib (rib 1) as a function of the loading state. The discontinuities that appear are associated with rib releases and it shows the free rib to be moving up and in towards the feed tower, as ribs are released. Pushrod forces for ribs 9, 10 & 11 are shown in Figure 5.1.4-7. When rib release occurs (noted by the discontinuities), pushrod loads for the stuck ribs increases, while the pushrod load for the released rib goes to zero.

PIN SLIPPAGE (ON-SUN) Three Rib Model, 10 lb Preload, $\mu=1.70$

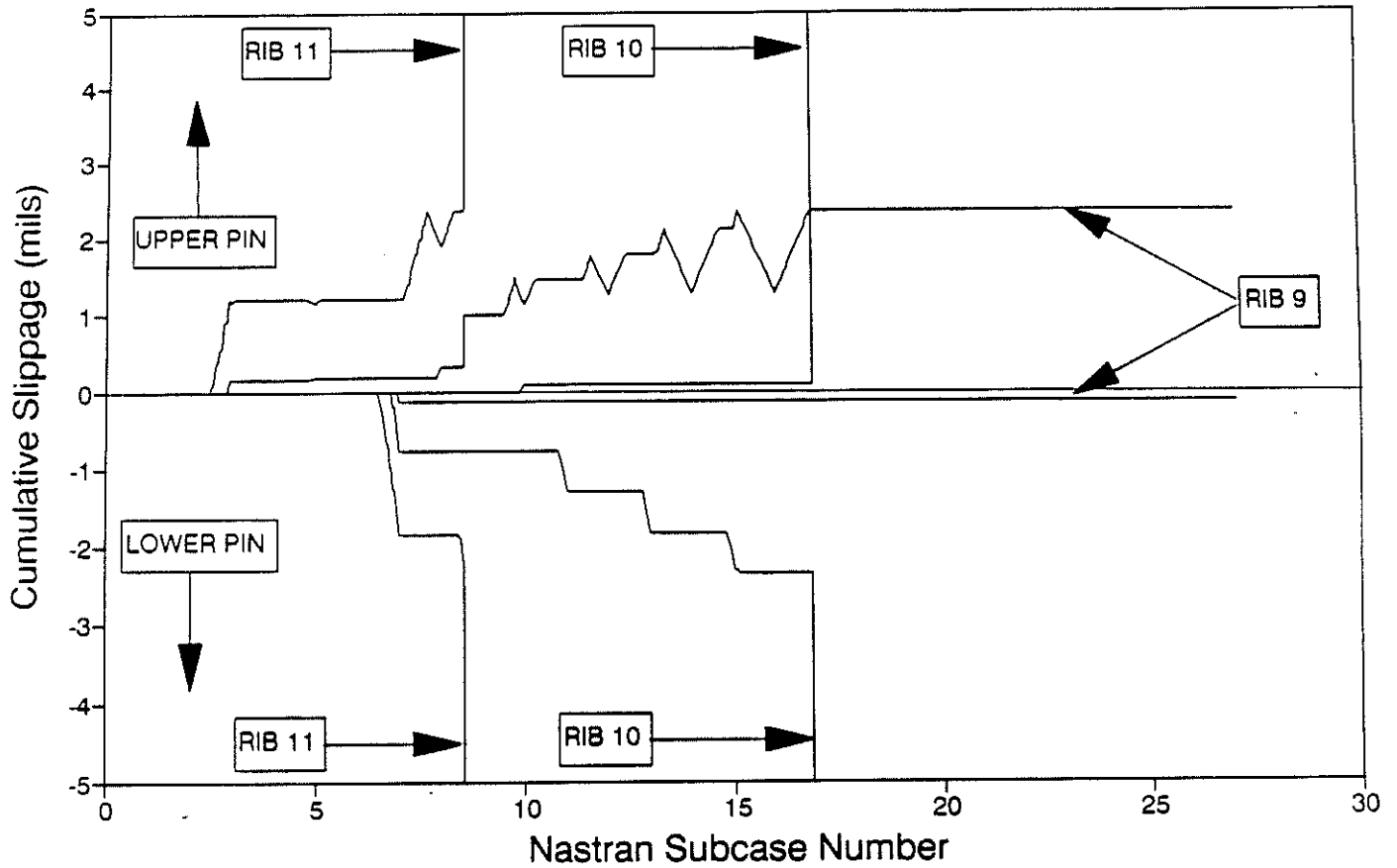


Figure 5.1.4-2: Pin Slippage Plot - Ribs 9, 10 & 11, 10 lb Preload, $\mu = 1.70$

RIB 9 PIN FORCES AND SLIPPAGE (ON-SUN) Three Rib Model, 10 lb Preload, $\mu=1.70$

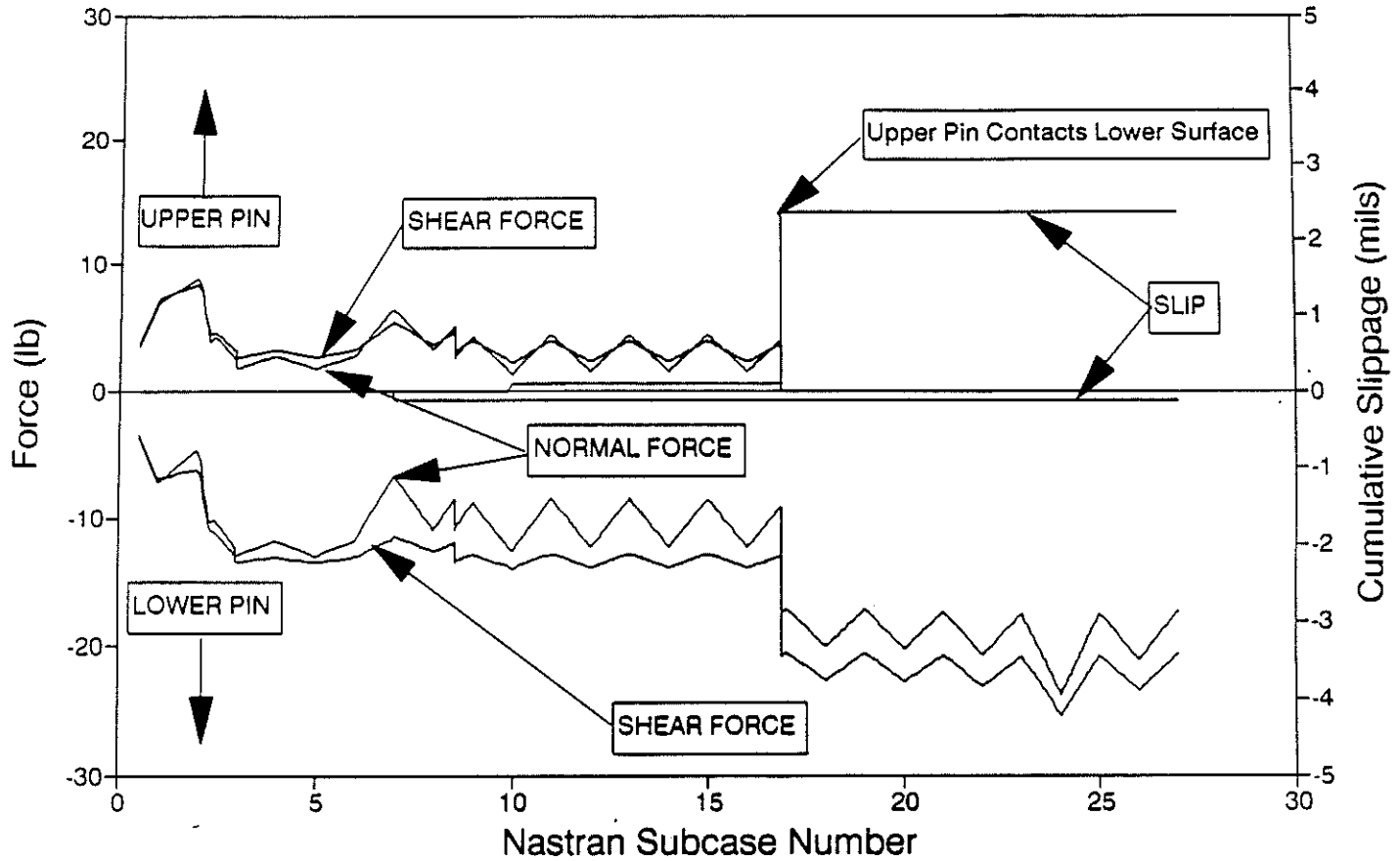


Figure 5.1.4-3: Pin Force/Slippage Plot - Rib 9, 10 lb Preload, $\mu = 1.70$

RIB 10 PIN FORCES AND SLIPPAGE (ON-SUN)

Three Rib Model, 10 lb Preload, $\mu = 1.70$

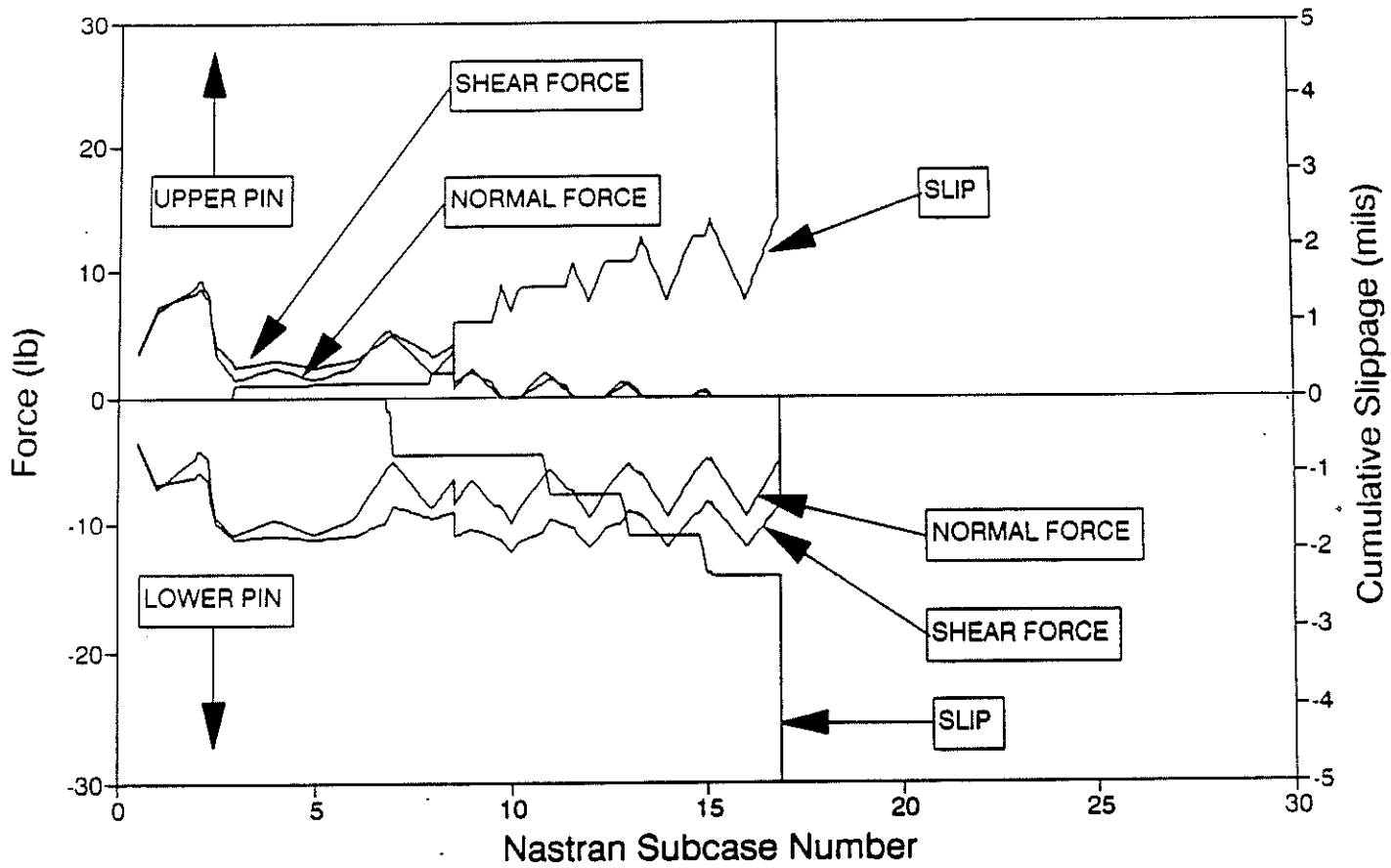


Figure 5.1.4-4: Pin Force/Slippage Plot - Rib 10, 10 lb Preload, $\mu = 1.70$

RIB 11 PIN FORCES AND SLIPPAGE (ON-SUN) Three Rib Model, 10 lb Preload, $\mu=1.70$

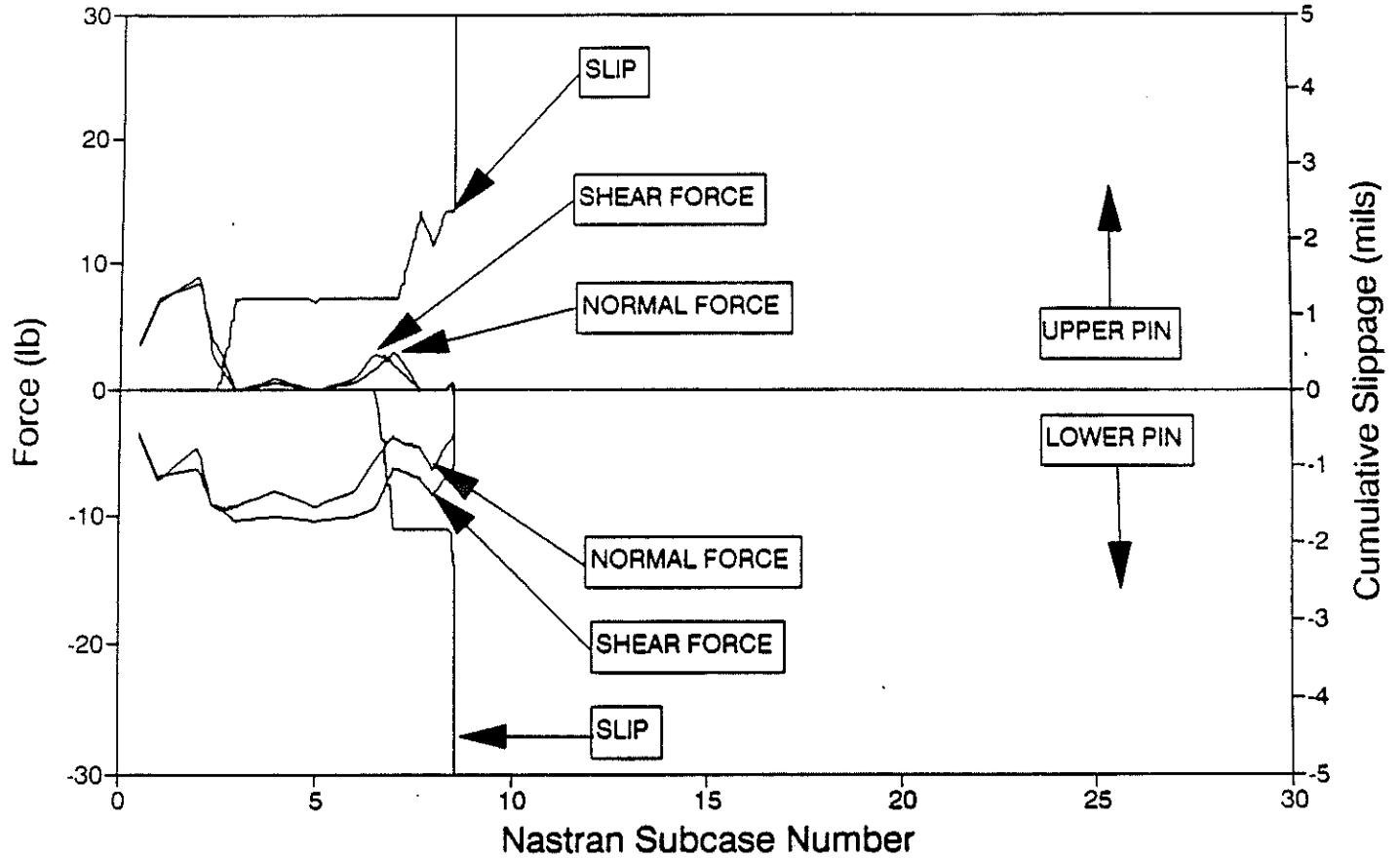


Figure 5.1.4-5: Pin Force/Slippage Plot - Rib 11, 10 lb Preload, $\mu = 1.70$

RIB 1 TIP DISPLACEMENT

Three Rib Model, 10 lb Preload, $\mu=1.70$

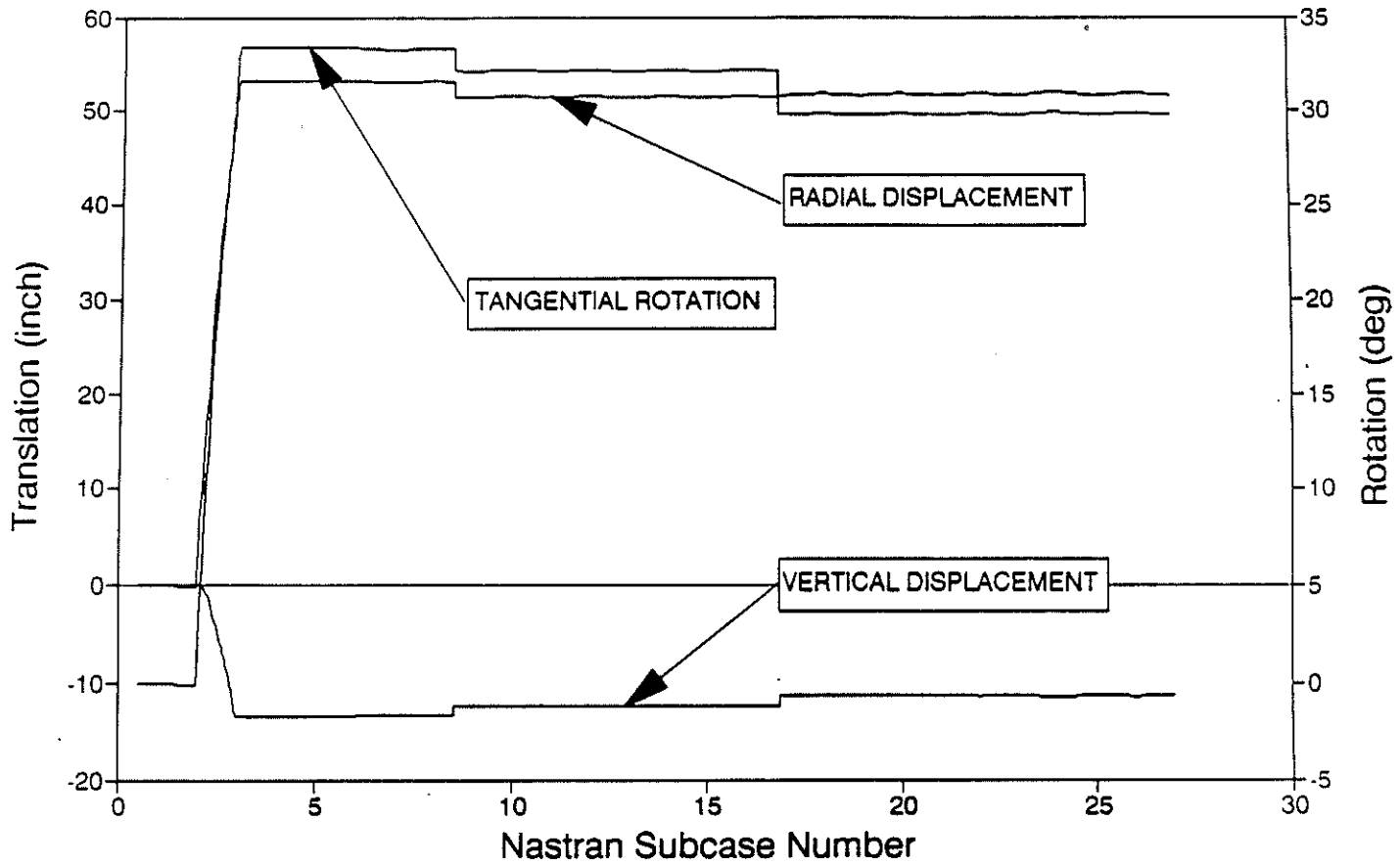


Figure 5.1.4-6: Rib 1 Tip Displacements - 10 lb Preload, $\mu = 1.70$

STUCK RIB PUSHROD FORCES

Three Rib Model, 10 lb Preload, $\mu = 1.70$

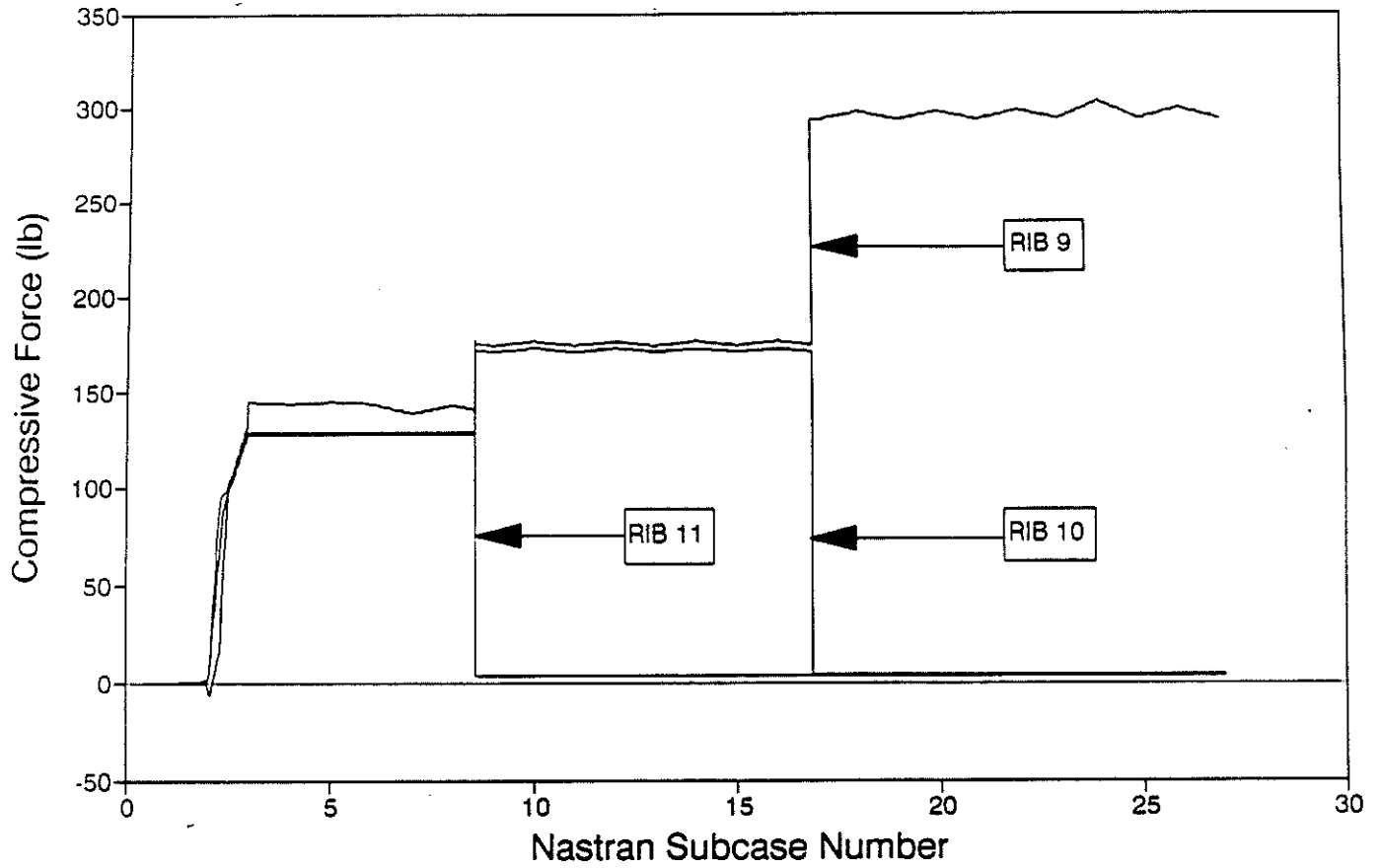


Figure 5.1.4-7: Pushrod Forces - Ribs 9, 10 & 11, 10 lb Preload, $\mu = 1.70$

61

5.2 COOLING TURN ALTERNATIVES

With six cooling turns completed and having no indications of rib release, the possible preload and friction combinations that still allows all ribs to release has been reduced considerably. For the ribs to presently be stuck, preloads greater than 10 lbs are required; otherwise, friction coefficients greater than 1.8 are necessary (Figure 5.1.3-3, first rib release curves). However, as preload increases, the effectiveness of the cooling turns are reduced, and diminishes as more turns are performed (i.e., the rib release curve becomes steeper with increasing preload and as more turns are performed). Moreover, the sequential rib release curves (Figure 5.1.4-1) showed that, if rib release had not occurred by the sixth turn for a preload of 15 lb, then release of the first rib during a subsequent turn would make it impossible for the remaining ribs to release by turn 12. Although no data is available for the 20 lb preload case, the same conclusion can be drawn, since its curves are steeper than the 15 lb preload curves. Therefore, to have any chance of releasing all the ribs, preloads less than 15 lb but greater than 10 lb are required, and friction coefficients greater than 1.35 (first rib release curves, Figure 5.1.3-3) are necessary. In view of the current situation, a number of alternatives for releasing the ribs were investigated and are described in the remainder of this section.

5.2.1 130 Mil Tower Contraction

A study was conducted to investigate the feasibility of releasing the stuck ribs by contracting the tower 130 mils. In this analysis, the antenna is brought to the state in which six cooling turns have been executed with no rib release. A warming turn is then performed, and is followed by a fictitious cooling turn capable of producing 130 mils of tower contraction, see Table 5.2.1-1. For a given preload and friction coefficient, the tower contraction that causes rib release during the final cooling turn (no. 7) was determined and has been plotted as shown in Figure 5.2.1-1.

As one would expect, the curves show that as friction increases, so does the tower contraction required to cause rib release. In fact, for low preloads (e.g. 10 lb) the benefit can be significant if substantial tower contractions can be achieved (e.g. greater than 100 mils). However, current best estimates for the maximum tower contraction is 85 mils at 5 AU. For this tower contraction, no significant benefits are seen from these results.

Table 5.2.1-1: Loading History - 130 mil Tower Contraction

NASTRAN SUBCASE NO.	COOLING TURN CYCLE NO.	EVENT	HELIOCENTRIC DISTANCE (AU)	TOWER CONTRACTION (MILS)
1	N/A	Pin Preload	1.00	0.0
2	N/A	Pre-Deploy	1.32	21.4
3	0.000	Deploy Attempt	1.32	21.4
4	0.333	Pre-Warming Turn 1	1.57	30.4
5	0.667	Warming Turn 1	1.57	21.4
6	1.000	Cooling Turn 1	1.84	67.9
7	1.500	Post Cooling Turn 1	1.84	36.1
8	2.000	Cooling Turn 2	1.98	70.0
9	2.500	Post-Cooling Turn 2	1.98	39.1
10	3.000	Cooling Turn 3	2.25	72.3
11	3.500	Warming Turn 4	2.27	40.1
12	4.000	Cooling Turn 4	2.26	71.7
13	4.500	Warming Turn 5	2.25	39.7
14	5.000	Cooling turn 5	2.24	71.6
15	5.500	Warming Turn 6	2.21	38.9
16	6.000	Cooling Turn 6	2.16	71.2
17	6.500	Warming Turn 7	1.81	29.1
18	7.000	Cooling Turn 7	N/A	130.0

TOWER CONTRACTION REQ'D-1st RIB RELEASE
 MARCH 92 SCENARIO/130 MILS FOR TURN 7

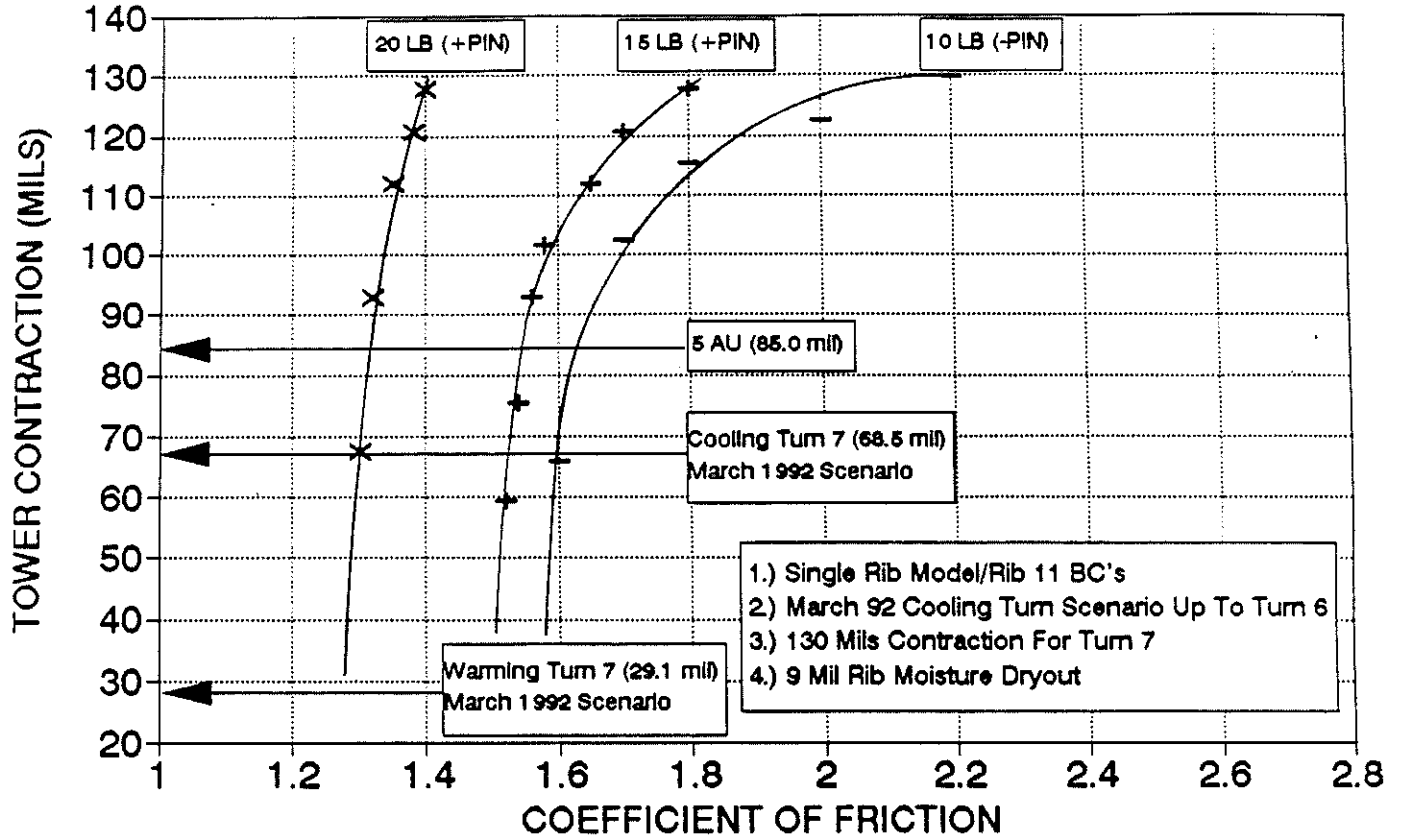


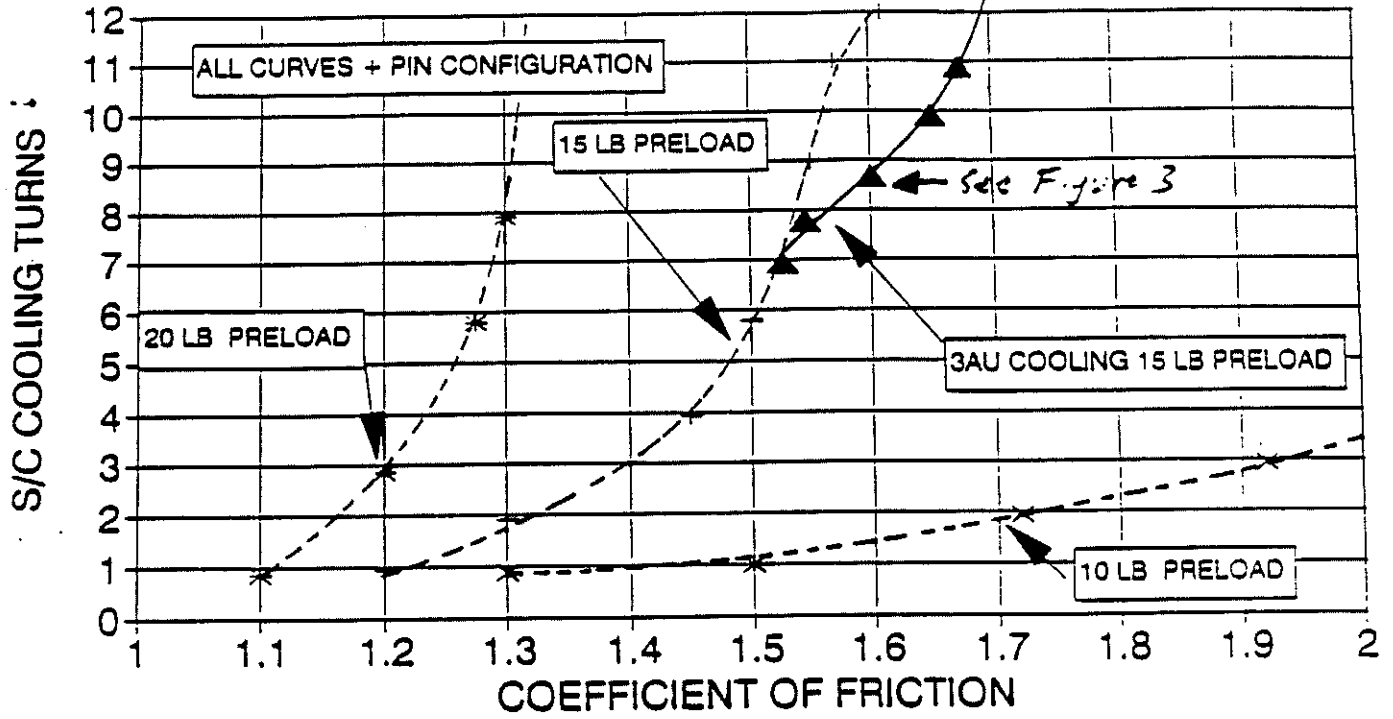
Figure 5.2.1-1: Rib Release Curves - 130 mil Tower Contraction

64

5.2.2 Turning at 3 AU

An investigation was conducted to determine the benefits of performing cooling turns 7 through 12 at 3 AU. In this study, the spacecraft undergoes the first six cooling turns as described by the March 92 scenario. Warming turn 7 is then performed at 1.07 AU and is followed by six cooling and warming turns that are performed at 3 AU. Results from this analysis are summarized in Figure 5.2.2-1; only the 15 lb preload case was investigated. The results show that performing the remaining turns at 3 AU is more beneficial than performing them in accordance with the March 92 scenario. For further details, refer to the memo provided in Appendix 8.6.

COOLING TURNS REQUIRED FOR RIB RELEASE
 3/92 Truncated & Baseline Cooling Turns



—*— 10# BASELINE + 15# BASELINE * 20# BASELINE ▲ 15# @ 3AU

Figure 5.2.2-1: Rib Release Curves - Effects of Turning at 3 AU

666

5.2.3 Deleting Turns 7, 8, 9, and 10

Because of the risk and resource requirements associated with cooling turns 7 through 10, its effectiveness in promoting pin walkout was examined. Excessive heating of the normally shaded spacecraft components presents a damage risk when cooling turns are performed at heliocentric distances less than 1.7 AU. In view of this and the resource requirements (e.g., propellant) to perform these turns, an analysis was performed to determine the effectiveness of cooling turns 7 through 10 for the modified March 92 scenario shown in Table 5.2.3-1.

The modified scenario is different from the March 92 scenario in only two areas. A cooling turn 6a has been added between turns 6 & 7, and the combination of turns 11 & 12 has been replaced by a new turn 10a.

For a preload of 10 lbs and pins in the "-Pin" configuration, deleting turns 8 thru 10 produces a 0.05 loss in friction coefficient, see Figure 5.2.3-1. Similarly, Figure 5.2.3-2 shows that eliminating turns 7 thru 10 results in a 0.07 loss in friction coefficient. Based on these results, a decision was made during the Review Board meeting on May 7 to eliminate turns 8 thru 10. Furthermore, a recommendation to delete turn 7 was made, if no rib release occurred after performing turn 6a (Ref. 14). For more details refer to the memo in Appendix 8.7.

Table 5.2.3-1: Loading History - Modified March 92 Cooling Turn Scenario

UNMODIFIED			MODIFIED			HELIOCENTRIC DISTANCE (AU)	NO DRYOUT TOWER CONTRACTION (mils)	WITH 9 MIL DRYOUT TOWER CONTRACTION (mils)
NASTRAN SUBCASE NO.	COOLING TURN CYCLE NO.	EVENT	NASTRAN SUBCASE NO.	COOLING TURN CYCLE NO.	EVENT			
1	N/A	Pin Preload	1	N/A	Pin Preload	1.00	0.0	0.0
2	N/A	Pre-Deploy	2	N/A	Pre-Deploy	1.32	-21.4	-12.4
3	0.000	Deploy Attempt	3	0.000	Deploy Attempt	1.32	-21.4	-12.4
4	0.333	Pre-Warming Turn 1	4	0.333	Pre-Warming Turn 1	1.57	-30.4	-21.4
5	0.667	Warming Turn 1	5	0.667	Warming Turn 1	1.57	-21.4	-12.4
6	1.000	Cooling Turn 1	6	1.000	Cooling Turn 1	1.84	-67.9	-58.9
7	1.500	Post Cooling Turn 1	7	1.500	Post Cooling Turn 1	1.84	-36.1	-27.1
8	2.000	Cooling Turn 2	8	2.000	Cooling Turn 2	1.98	-70.0	-61.0
9	2.500	Post-Cooling Turn 2	9	2.500	Post-Cooling Turn 2	1.98	-39.1	-30.1
10	3.000	Cooling Turn 3	10	3.000	Cooling Turn 3	2.25	-72.3	-63.3
11	3.500	Warming Turn 4	11	3.500	Warming Turn 4	2.27	-40.1	-31.1
12	4.000	Cooling Turn 4	12	4.000	Cooling Turn 4	2.26	-71.7	-62.7
13	4.500	Warming Turn 5	13	4.500	Warming Turn 5	2.25	-39.7	-30.7
14	5.000	Cooling Turn 5	14	5.000	Cooling Turn 5	2.24	-71.6	-62.6
15	5.500	Warming Turn 6	15	5.500	Warming Turn 6	2.21	-38.9	-29.9
16	6.000	Cooling Turn 6	16	6.000	Cooling Turn 6	2.16	-71.2	-62.2
17	6.500	Warming Turn 7	17	6.500	Warming Turn 6a	1.90	-31.7	-22.7
18	7.000	Cooling Turn 7	18	7.000	Cooling Turn 6a	1.90	-69.2	-60.2
19	7.500	Warming Turn 8	19*	7.500	Warming Turn 7	1.81	-29.1	-20.1
20	8.000	Cooling Turn 8	20*	8.000	Cooling Turn 7	1.77	-68.5	-59.5
21	8.500	Warming Turn 9	21*#	8.500	Warming Turn 8	1.58	-21.7	-12.7
22	9.000	Cooling Turn 9	22*#	9.000	Cooling Turn 8	1.53	-64.4	-55.4
23	9.500	Warming Turn 10	23*#	9.500	Warming Turn 9	1.45	-16.6	-7.6
24	10.000	Pre-Cooling Turn 10	24*#	10.000	Cooling Turn 9	1.41	-62.6	-53.6
25	10.250	Earth Encounter	25*#	10.500	Pre-Cooling Turn 10	1.33	-22.4	-13.4
26	10.500	Pre-Warming Turn 11	26*#	11.000	Cooling Turn 10	1.33	-60.7	-51.7
27	10.750	Warming Turn 11	27	11.250	Earth Encounter	1.00	-5.4	3.6
28	11.000	Cooling Turn 11	28	11.500	Pre-Warming Turn 10a	1.07	-9.8	-0.8
29	11.500	Warming Turn 12	29	11.750	Warming Turn 10a	1.07	3.8	12.8
30	12.000	Cooling Turn 12				1.32	-60.7	-51.7
31	12.500	Cooling Turn 12	30	12.000	Cooling Turn 10a	1.40	-14.7	-5.7
			31	12.500	Post-Cooling Turn 10a	1.57	-65.1	-56.1
						1.57	-30.4	-21.4

* - Remove to eliminate turns 8,9,8,10
- Remove to eliminate turn 7,8,9,10

68

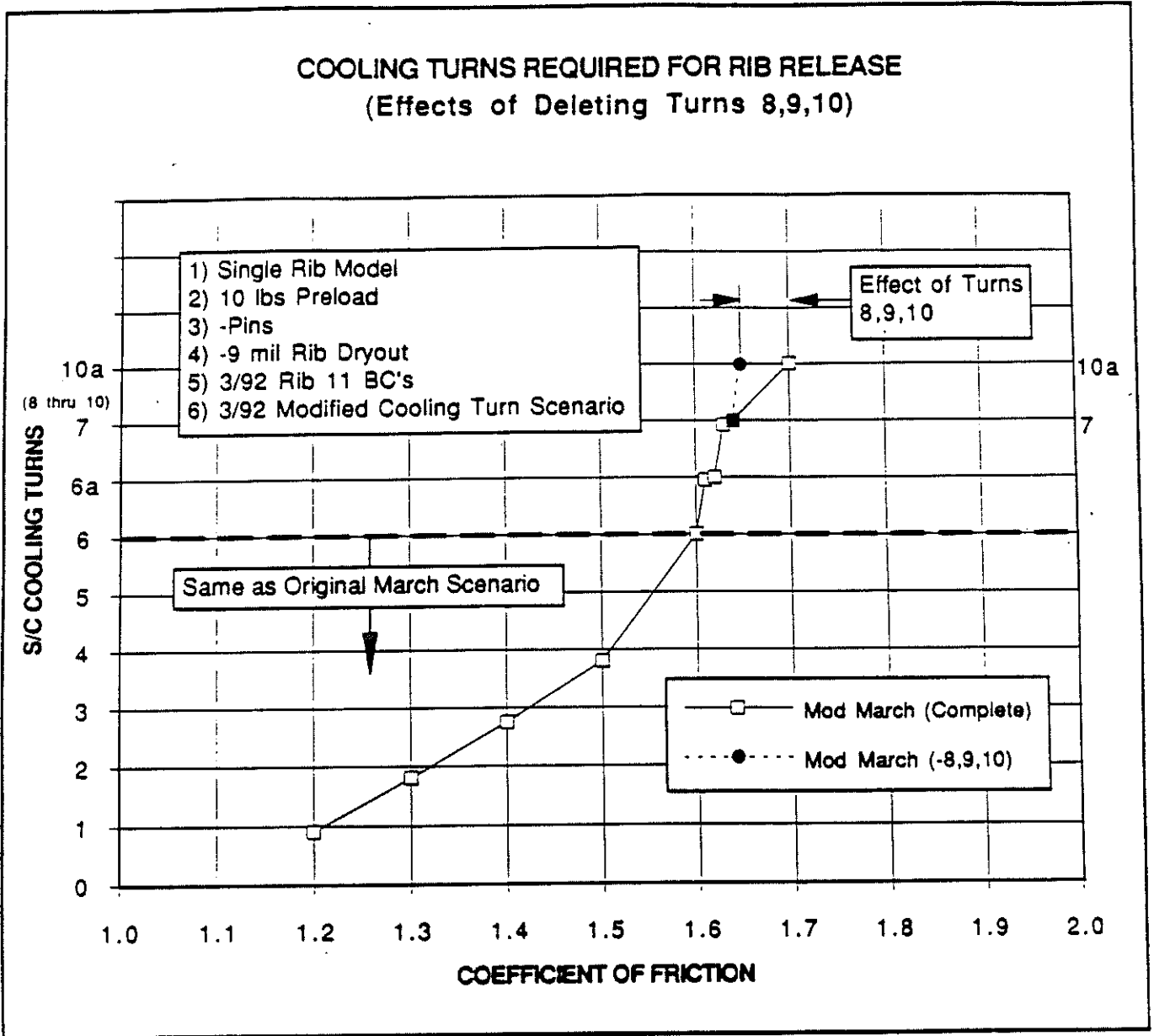


Figure 5.2.3-1: Rib Release Curves - Effects of Deleting Turns 8, 9 & 10

69

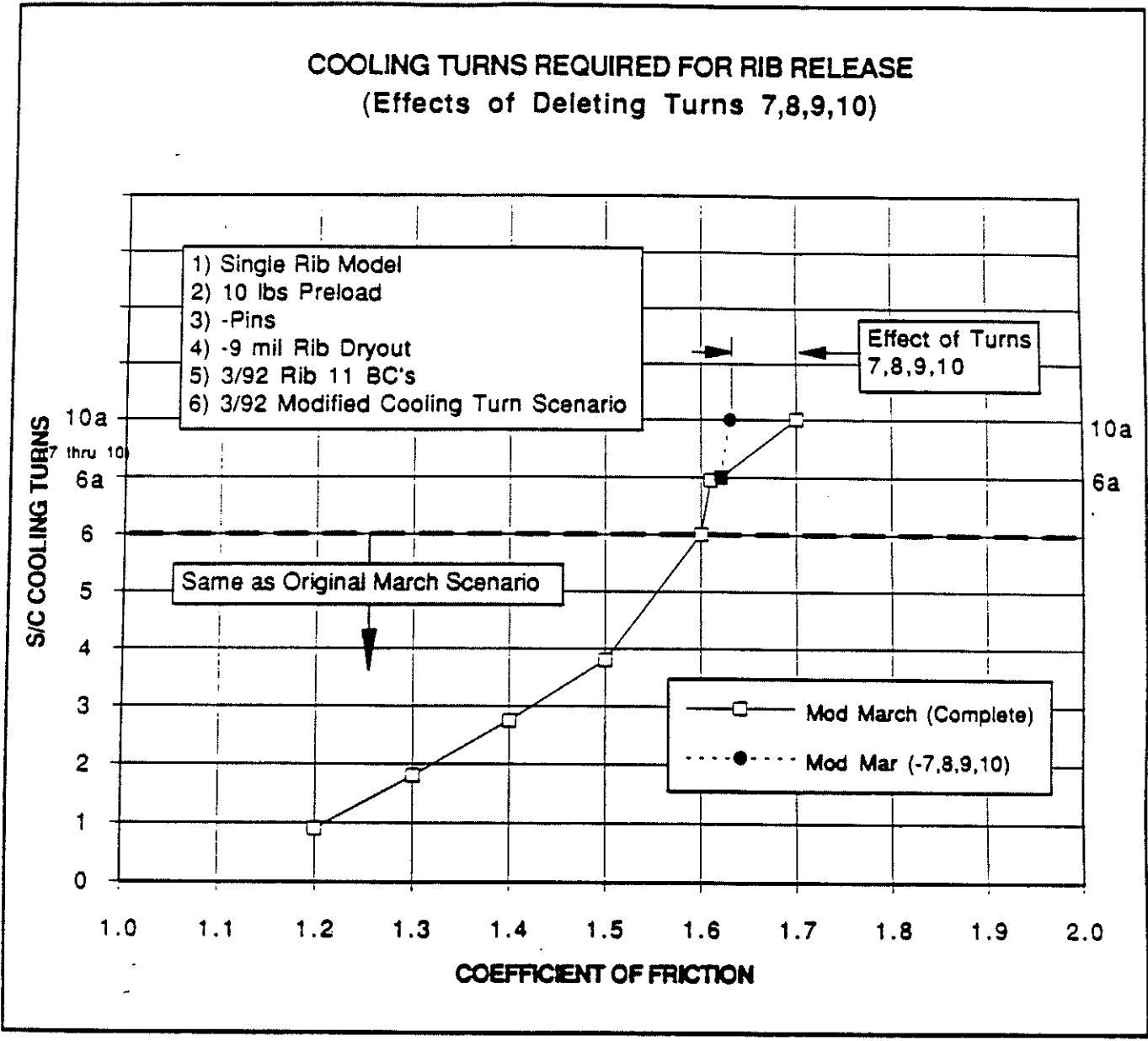


Figure 5.2.3-2: Rib Release Curves - Effects of Deleting Turns 7, 8, 9 & 10

6.0 CONCLUSION

For the partially deployed HGA with three ribs (nos 9, 10 & 11) stuck in the stowed position, ballscrew stalled at 5.1 turns, and pins misaligned opposite to one another and in a direction perpendicular to the pin axis, rib release by pin walking was analytically shown to be possible for the tower motions expected from the thermal cycles. Curves that provide the required number of spacecraft cooling turns to free a stuck rib were presented as a function of pin preload and friction coefficient. These curves showed that for certain combinations of preloads and friction coefficients, rib release by pin walking could be achieved within a reasonable number of cooling turns.

However, with six cooling turns completed and having no indications of rib release, the prospect of releasing the ribs by continued thermal cycling do not appear promising. The first rib release curves presented in Figure 5.1.3-3 showed that preloads greater than 10 lbs are required for the ribs to currently be stuck; otherwise friction coefficients in excess of 1.8 are required. As preload increases, however, rib release efficiency decreases because of the increasing steepness of the rib release curves. Moreover, for a given preload, the rib release efficiency diminishes as more turns are made. In addition, the sequential rib release curves presented in Figure 5.1.4-1 showed that preloads less than 15 lbs but greater than 10 lbs are required to have any chance of releasing all ribs by thermal cycling. More specifically, for a preload of 15 lb, if no ribs had released by cooling turn six, then release of the first rib during a subsequent turn would make it impossible for the remaining ribs to release within the planned 12 cooling turns. On the other hand, if the preload is too low (i.e., 10 lbs or less), release of the last rib would not occur due to disengagement of the upper pin from its contact surface.

Because of the diminishing returns of cooling turns performed after the sixth, alternatives for releasing the ribs were investigated. Contracting the tower a large amount to cause rib release is possible, but no significant benefits are seen for the 85 mil maximum tower contraction estimated for 5 AU. Performing the remaining six turns at 3 AU provides some benefits over performing them in accordance with the March 92 scenario, but the benefits do not appear to warrant the wait. The effectiveness of cooling turns 7 thru 10 was evaluated for a representative case that allows rib release with reasonable combinations of preloads and friction coefficients. The benefits provided by these turns were found to be small, and therefore, a recommendation to delete these turns was made.

7.0 REFERENCES

- 1 "Galileo Antenna Description, S/X Antenna Anomaly Review #1," presented by Gary Coyle, April 26, 1991.
- 2 "HGA Failure Analysis/Test Status, HGA Deploy Anomaly Review #2," presented by Gary Coyle, May 16, 1991.
- 3 GLL-350GC-92-016, "Division 35 HGA Anomaly Investigation Team Meeting Minutes of 5/22/91," G. Coyle/E. Nilsen to Distribution, 23 May 1991.
- 4 "HGA Failure Analysis/Test Status, HGA Deploy Anomaly Review #3," presented by Gary Coyle, June 13, 1991.
- 5 "HGA Failure Analysis/Test Status, HGA Deploy Anomaly Review #4," presented by Gary Coyle, July 16, 1991.
- 6 "HGA Failure Analysis/Test Status, HGA Deploy Anomaly Review #5," presented by Gary Coyle, August 22, 1991.
- 7 IOM 3541-91-267, "Galileo SXA 3 Stuck Rib Analysis Results," P. M. Rapacz to Gun-Shing Chen, November 26, 1991.
- 8 IOM 3541-91-277, "Galileo SXA Estimated Number of Stuck Ribs in Flight Revisited," P. M. Rapacz to Gun-Shing Chen, December 9, 1991.
- 9 GLL-350GC-91-013, "Division 35 HGA Anomaly Investigation Team Meeting Minutes of 4/29/91," G. Coyle/E. Nilsen to Distribution, 30 April 1991.
- 10 IOM 3541-91-070, "Analysis of Galileo High Gain Antenna Deployment with One or More Ribs Restrained," Andy Kissil to Jim Staats, May 1, 1991.
- 11 IOM 3541-91-230, "Galileo SXA Deployment Anomaly Nonlinear Analysis Model Documentation," P. M. Rapacz to Gun-Shing Chen, November 15, 1991.
- 12 IOM 3541-91-273, "Galileo SXA Full Model for Pin Walkout Study," P. M. Rapacz to Gun-Shing Chen, December 3, 1991.
- 13 "HGA Recovery Team Status Report #10, Tower Thermal Analysis/Near Earth Thermal Status," presented by Ron Reeve, March 25, 1992.
- 14 IOM 3522-92-138, "Recommendation to Delete S/C Turn 7," J. Staats/G. Coyle to W. O'Neil/R. Ploszaj, May 28, 1992.

APPENDIX 8.1

Warming Turn Benefits

From the standpoint of pin walkout, maximizing both tower contraction and expansion, and therefore, stroke are desirable goals. In view of this, the Thermal group found that turning the spacecraft to a 45 degree off-sun attitude provides near optimum expansion of the tower; the actual optimum was later found to have an angle slightly greater than this, but was not used since the resulting incremental tower expansion was small. This study investigates the pin walking benefits of adding warming turns to the existing cooling turns in an effort to maximize tower expansion and stroke during each thermal cycle.

In this study, the single rib model with rib 10 boundary condition (assuming three stuck ribs and ballscrew stalled at 5.1 turns) and the pins in the "-Pin" configuration was used. Rib dryout was not included since this effect was not known when the analysis was performed. The cooling scenario used is the December 91 scenario shown in Table 1. In this Table, the first column provides the NASTRAN subcase numbers for the scenario where the warming turns are performed, while the second column provides the subcase numbers for the scenario without the warming turns.

Results from this analysis are summarized in Figure 1. Curves that provide the required number of spacecraft cooling turns to release a rib are shown as functions of assumed pin preloads and friction coefficient. For each preload, two curves are shown, the one on the left results when no warming turns are performed, while the one on the right is obtained when warming turns are performed. The curves show that adding warming turns to the existing cooling turns results in quicker rib release.

Table 1: December 91 Cooling Turn Scenario - With and Without Warming Turns

NASTRAN Loadcase		EVENT	Heliocentric Distance (AU)	Tower Displacement (mils)
With Warming	W/O Warming			
1	1	Pin Preload	1.00	0.0
2	2	Pre-Deploy	1.32	-20.3
3	3	Deploy Attempt	1.32	-20.3
4	4	Pre-Warming Turn 1	1.58	-29.7
5	5	Warming Turn 1	1.58	-20.1
6	6	Post-Warming Turn 1	1.58	-29.7
7	7	Cooling Turn 1	1.84	-68.1
8	8	Post Cooling Turn 1	1.84	-35.8
9	9	Cooling Turn 2	1.98	-70.3
10	10	Post-Cooling Turn 2	1.98	-40.0
11	11	Cooling Turn 3	2.25	-71.7
	12	Post-Cooling Turn 3	2.25	-42.2
12		Warming Turn 4	2.27	-40.1
13	13	Cooling Turn 4	2.27	-71.8
	14	Post-Cooling Turn 4	2.27	-42.4
14		Warming Turn 5	2.24	-39.7
15	15	Cooling Turn 5	2.22	-71.6
	16	Post-Cooling Turn 5	2.22	-42.0
16		Warming Turn 6	2.20	-38.7
17	17	Cooling Turn 6	2.15	-71.2
	18	Post-Cooling Turn 6	2.15	-41.1
18		Warming Turn 7	2.05	-35.4
19	19	Cooling Turn 7	2.00	-70.4
	20	Post-Cooling Turn 7	2.00	-39.1
20		Warming Turn 8	1.80	-28.8
21	21	Cooling Turn 8	1.75	-68.6
	22	Post-Cooling Turn 8	1.75	-34.4
22		Warming Turn 9	1.55	-20.7
23	23	Cooling Turn 9	1.55	-66.8
		Post Cooling Turn 9	1.55	-29.4
24		Warming Turn 10	1.20	-4.2
25		Post-Warming Turn 10	1.20	-16.0
26	24	Earth Encounter	1.00	-4.7
27		Pre-Warming Turn 11	1.20	-16.3
28		Warming Turn 11	1.20	-4.6
		Post-Warming Turn 11	1.20	-16.3
29	25	Cooling Turn 10	1.60	-67.3

GLL HGA DEPLOYMENT ANOMALY ON-SUN & 45 DEG OFF-SUN

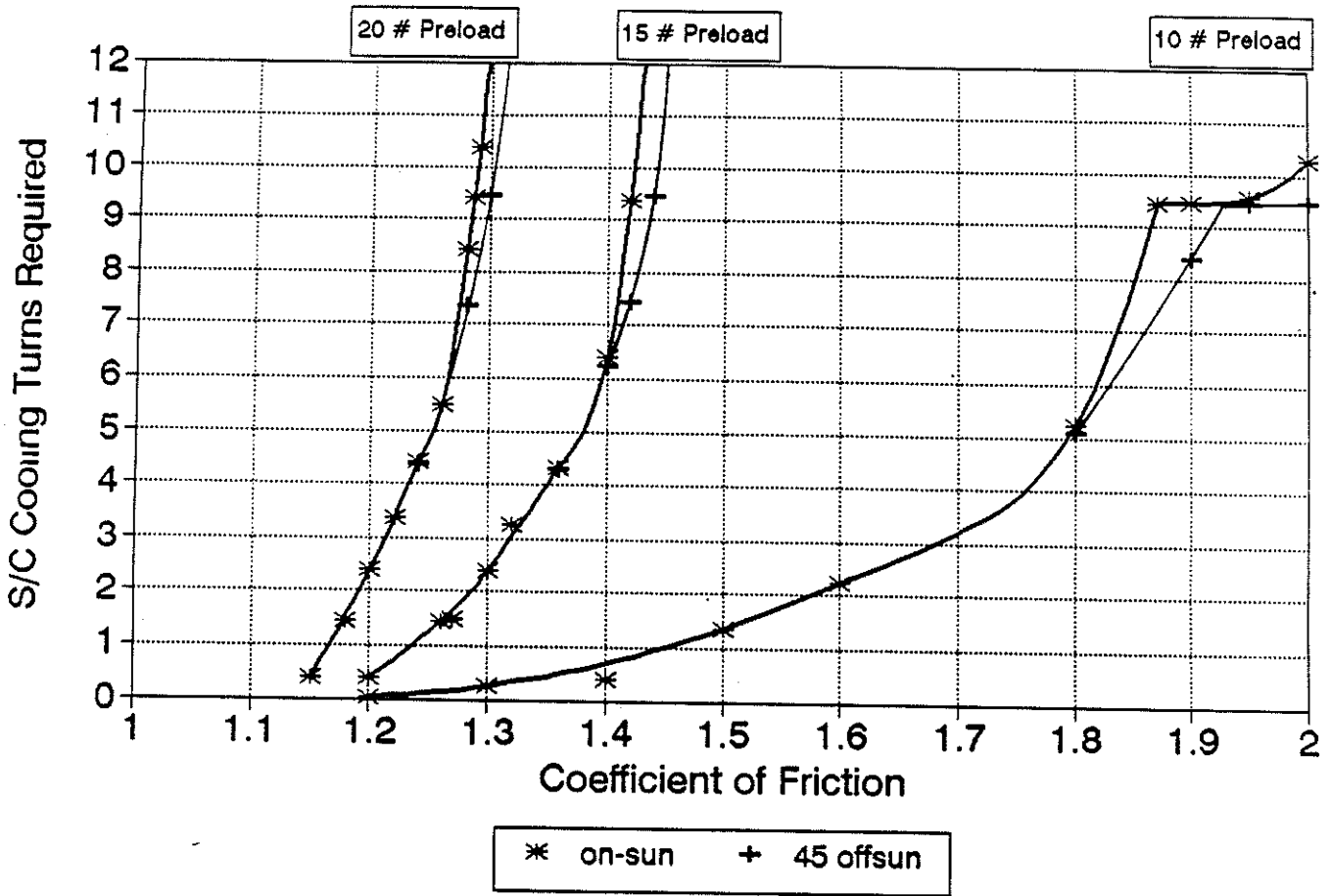
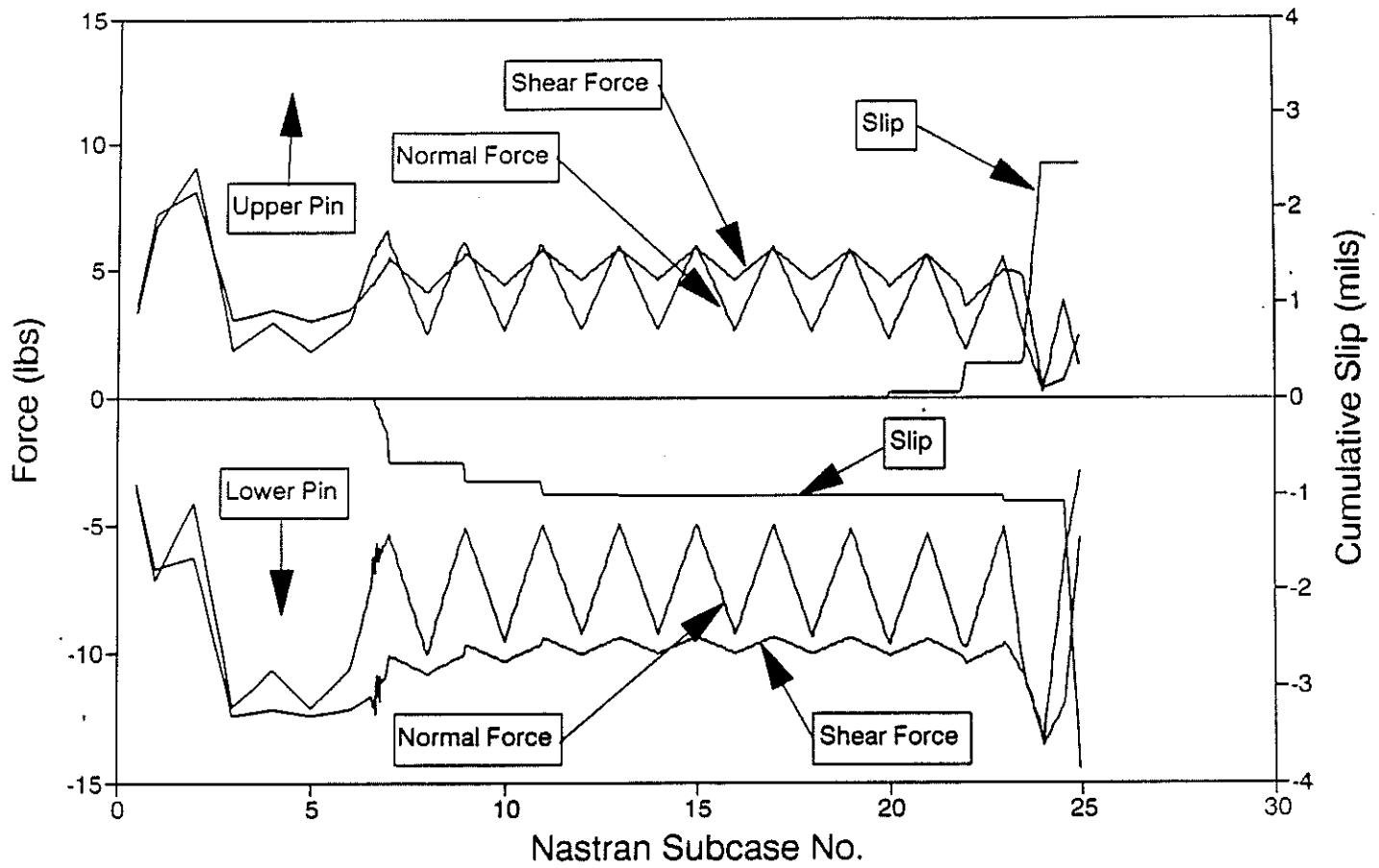
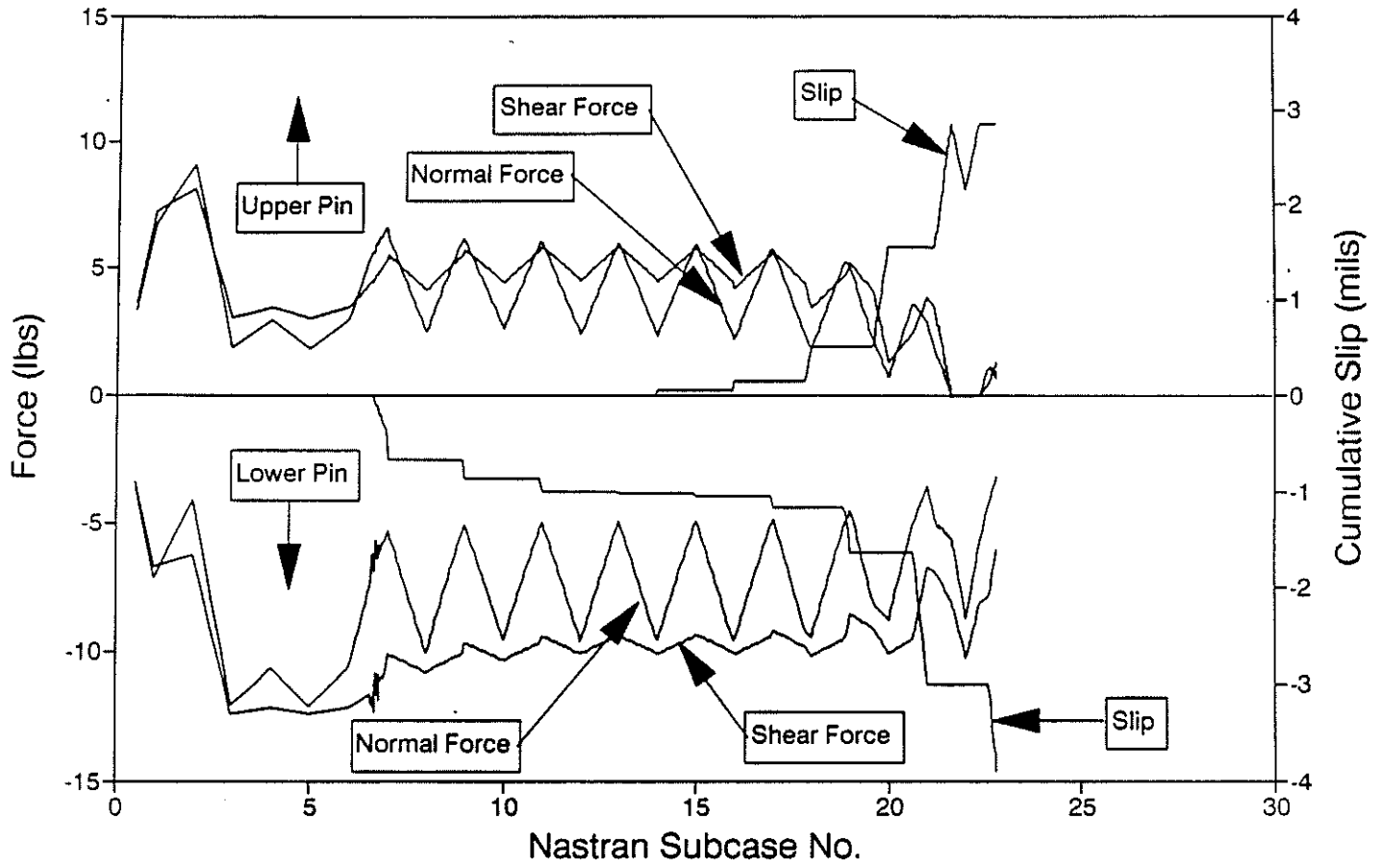


Figure 1: Rib Release Curves - Effects of Warming Turns

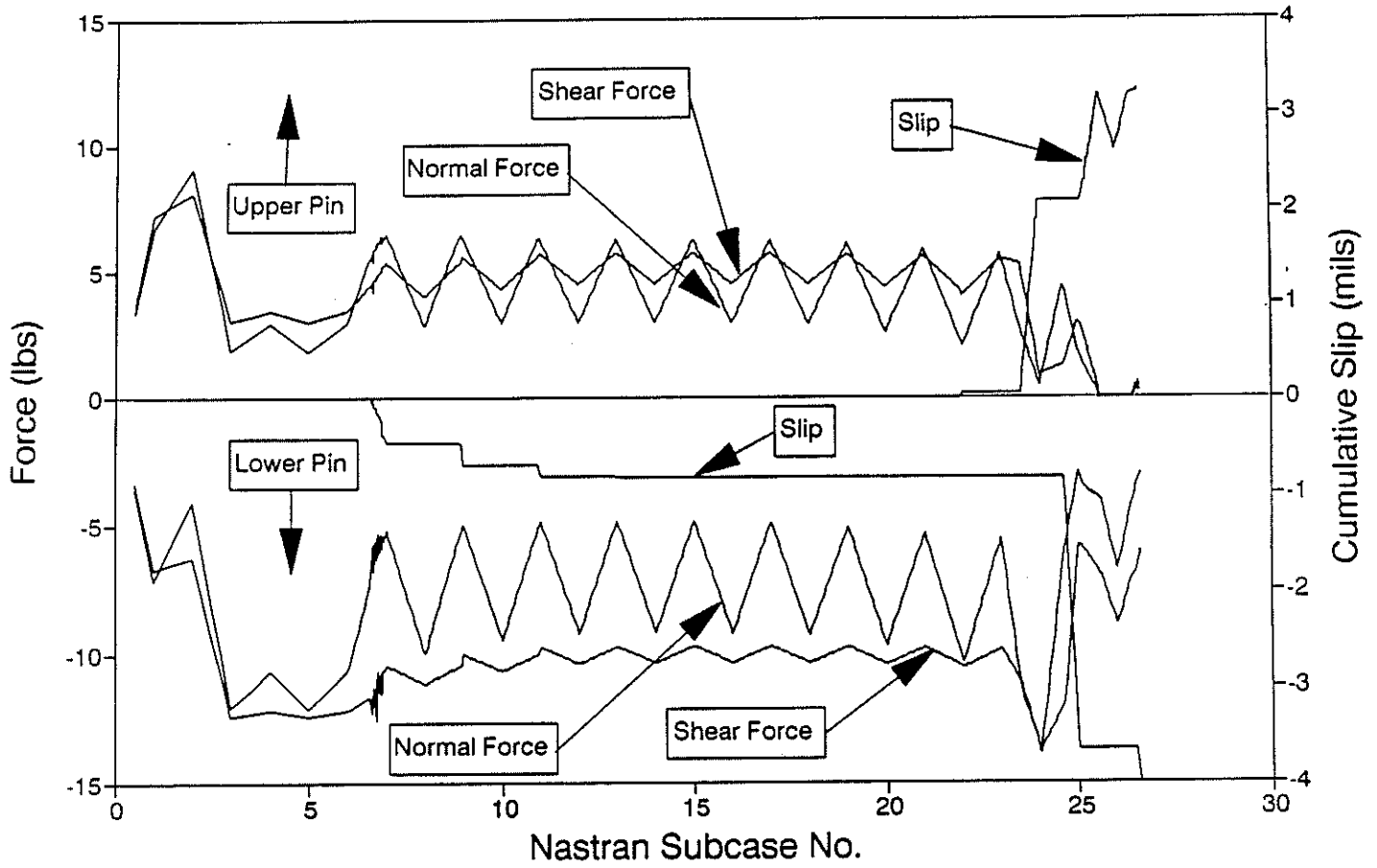
PIN FORCES AND SLIPPAGE On-Sun, 10 lb Preload, $\mu = 1.90$



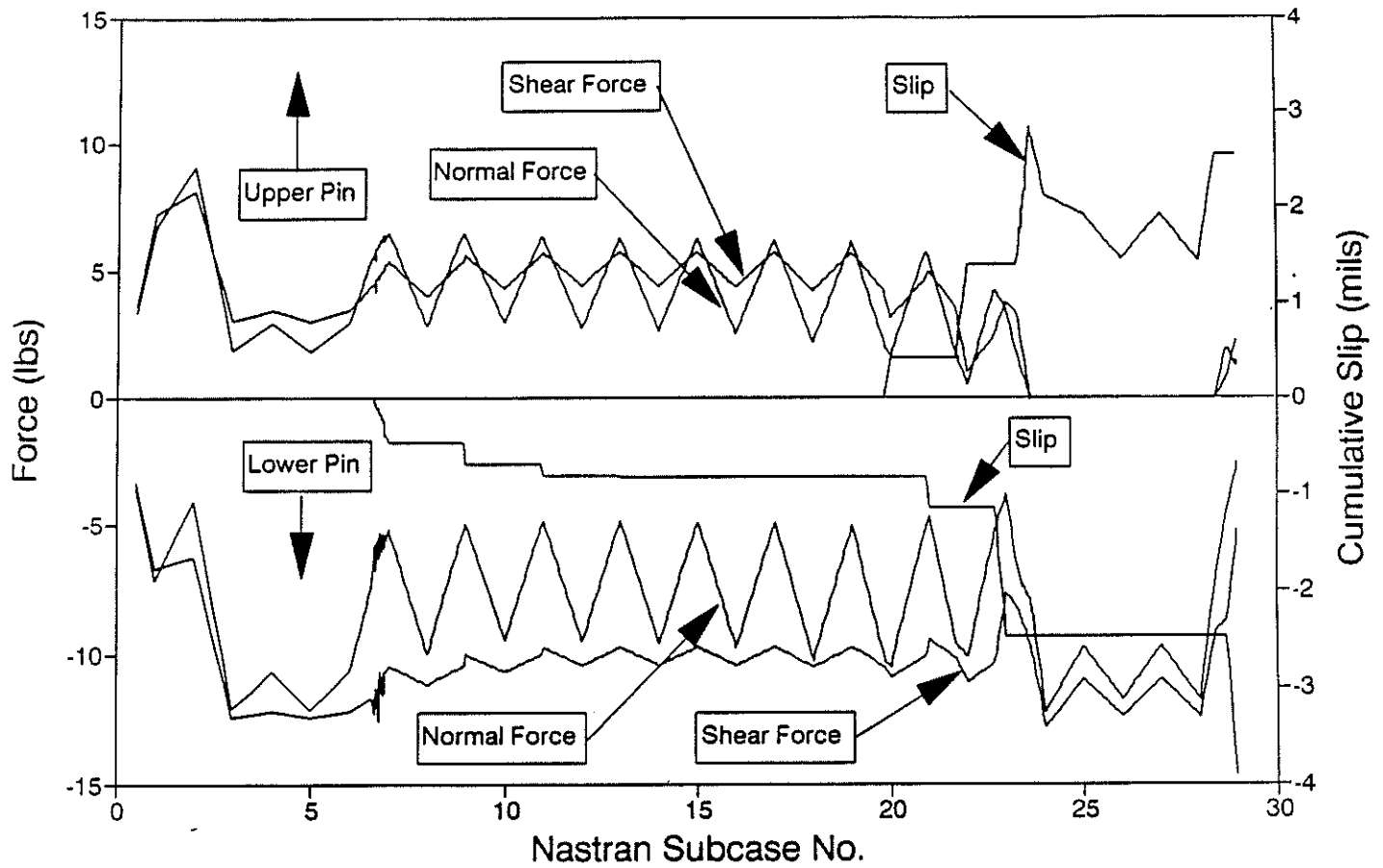
PIN FORCES AND SLIP 45 Off-Sun, 10 lb Preload, $\mu=1.90$



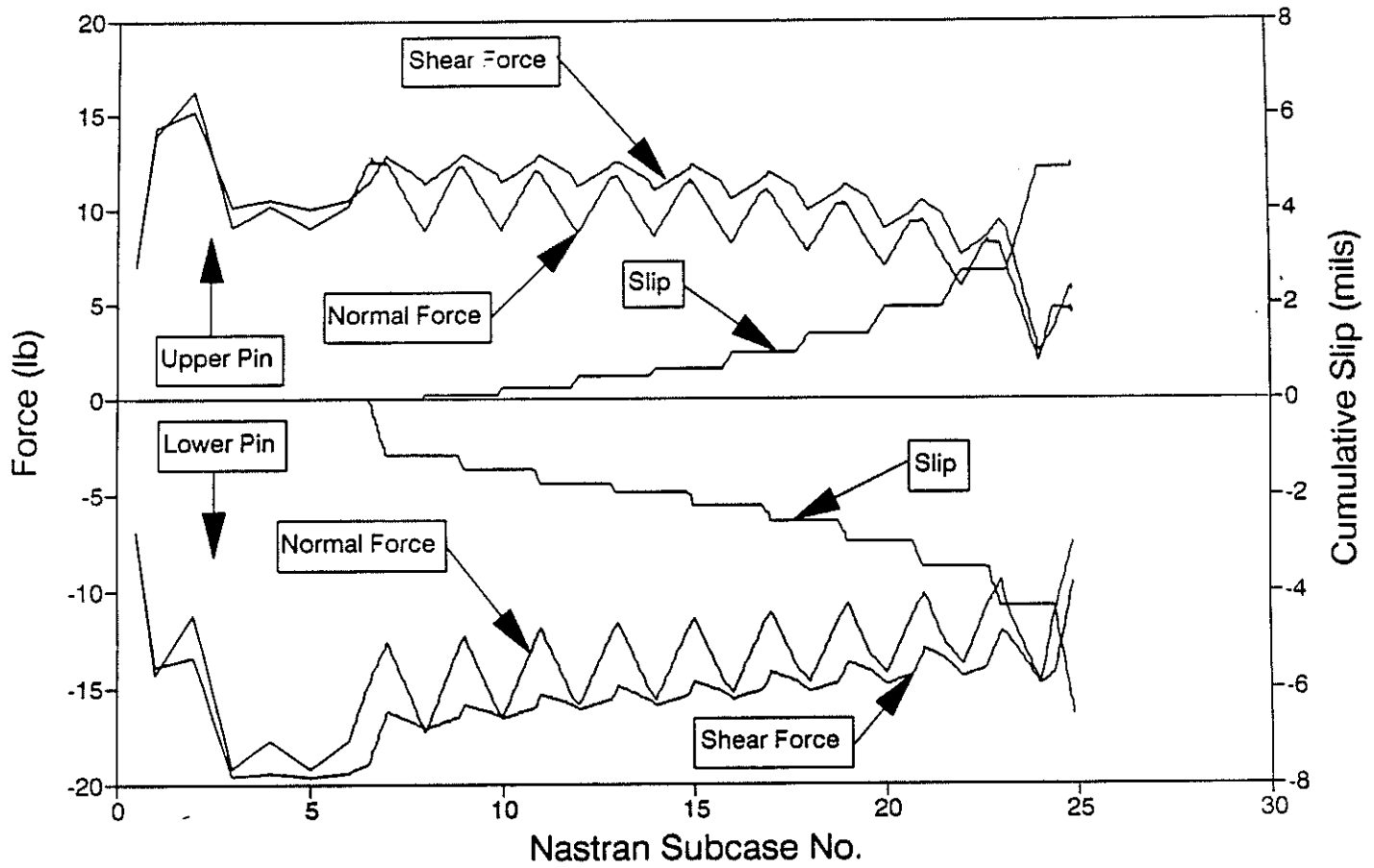
PIN FORCES AND SLIPPAGE On-Sun, 10 lb Preload, $\mu=2.00$



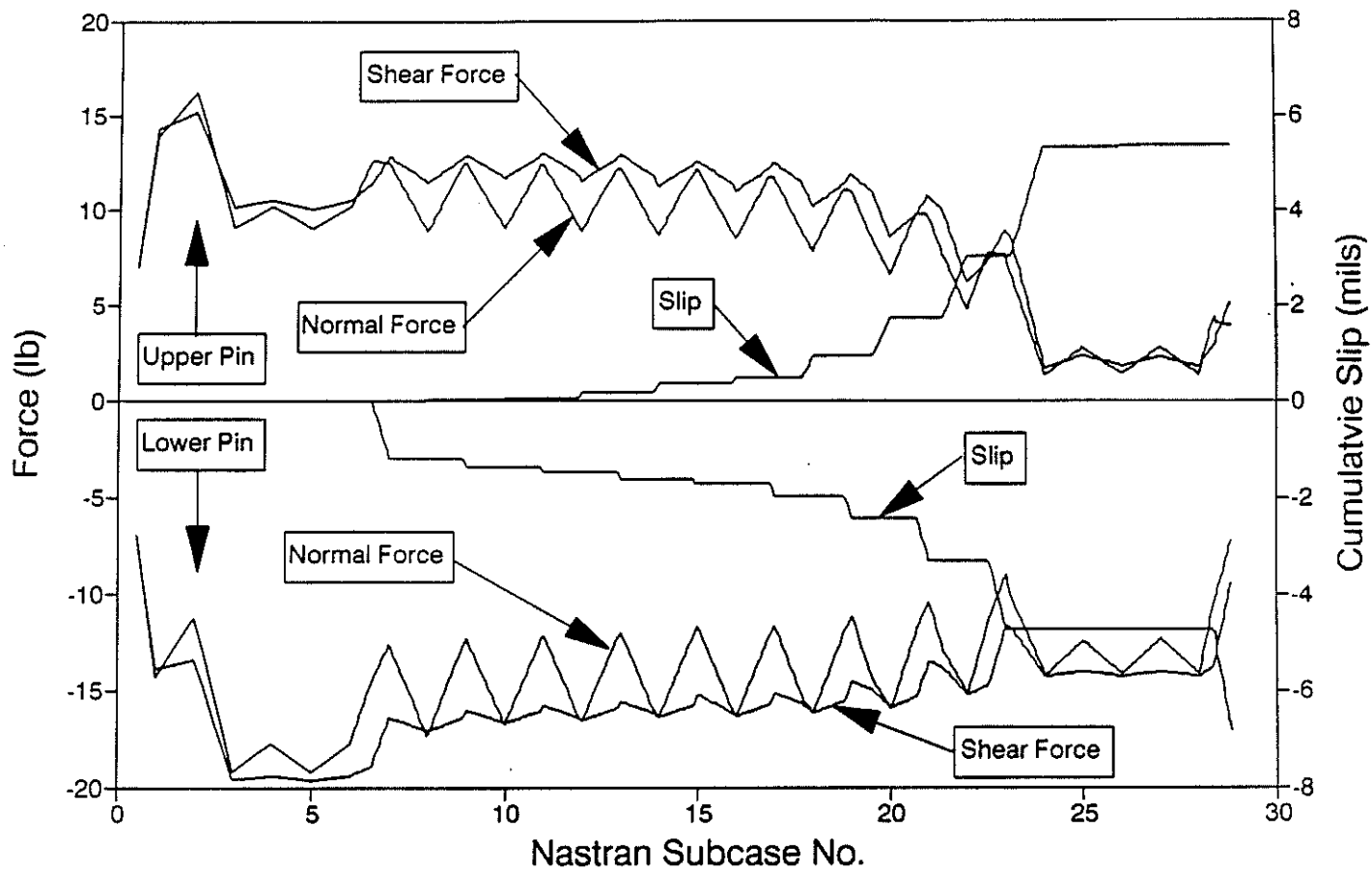
PIN FORCES AND SLIP 45 Off-Sun, 10 lb Preload, $\mu=2.00$



PIN FORCES AND SLIPPAGE On-Sun, 20 lb Preload, $\mu=1.285$



PIN FORCES AND SLIPPAGE Off-Sun, 20 lb Preload, $\mu=1.30$



D-9932

APPENDIX 8.2

Thermal Cycling at Fixed AU

As the spacecraft's position changes relative to the sun, the pin walking efficiency of each spacecraft thermal cycle varies. At large distances from the sun, the tower contraction is large, but its expansion is small. As the spacecraft approaches the sun, tower contraction decreases while its expansion increases. The stroke, another important parameter controlling pin walkout and defined as the difference between the expansion and contraction of the tower, also changes with heliocentric distance. Complicating matters further, spacecraft thermal constraints places limitations on the duration the spacecraft can remain at off-sun attitudes which directly affects the tower expansion and contraction that can be achieved with each turning cycle. Therefore, it is desirable to evaluate the pin walking efficiency of thermal cycles performed at various heliocentric distance.

In addressing this issue, a study was conducted in which the antenna was brought to the state in which the spacecraft has undergone four cooling turns (this was the current state at the time the analysis was performed) with no rib release. Once brought to that state, the spacecraft executed seven additional cooling turns at a fixed heliocentric distance. Based on the present position of the spacecraft and assuming the turns would be executed on the inbound leg of the Earth-2 encounter, the following distances were selected: 1.1, 1.3, 1.6 and 1.9 AUs. The tower contractions, expansions, and strokes are shown in Table 1.

Figure 1 presents the results from this analysis. Based on the trends provided by the unconstrained curves, it appears as though pin walkout improves as the spacecraft approaches Earth and the tower stroke increases. However, thermal constraints placed on the spacecraft for heliocentric distances less than or equal to 1.3 AU significantly affects this trend. With the constraints placed at 1.3 AU, its curve now lies between the 1.6 and 1.9 AU curves. The constraint at 1.1 AU results in only 11.4 mils of contraction and 9.4 mils of stroke making turns at that distance totally ineffective.

This study was performed using the single rib model with the pins in the "-Pin" configuration. Rib 10 boundary conditions, assuming three stuck ribs and ballscrew stalled at 5.1 turns, were used for the analysis. Since rib dryout was not known at the time of the analysis, its effects was not included.

Table 1: Tower Contractions For Fixed AU Study

NASTRAN Loadcase	EVENT	Heliocentric Distance (AU)	Tower Displacement (mils)
1	Pin Preload	1.00	0.0
2	Pre-Deploy	1.32	-20.3
3	Deploy Attempt	1.32	-20.3
4	Pre-Warming Turn 1	1.58	-29.7
5	Warming Turn 1	1.58	-20.1
6	Post-Warming Turn 1	1.58	-29.7
7	Cooling Turn 1	1.84	-68.1
8	Post Cooling Turn 1	1.84	-35.8
9	Cooling Turn 2	1.98	-70.3
10	Post-Cooling Turn 2	1.98	-40.0
11	Cooling Turn 3	2.25	-71.7
12	Warming Turn 4	2.27	-40.1
13	Cooling Turn 4	2.27	-71.8
14	Warming Turn 5	*	*
15	Cooling Turn 5	*	*

* Repeat warming and cooling turns six more times using the tower contractions corresponding to the AU under investigation shown below.

Solar Distance	Tower Displacement (mils)		
	AU	Cold	Warm
Unconstrained Thermal Cycles:			
1.1	-60.2	1.9	62.1
1.3	-63.7	-9.8	53.9
1.6	-67.3	-22.4	44.9
1.9	-69.8	-31.7	38.1
Constrained Thermal Cycles:			
1.1	-11.4	-2.0	9.4
1.3	-58.0	-12.0	46.0

COOLING TURNS REQUIRED FOR RIB RELEASE FIXED AU=1.1,1.3,1.6 & 1.9 STUDY

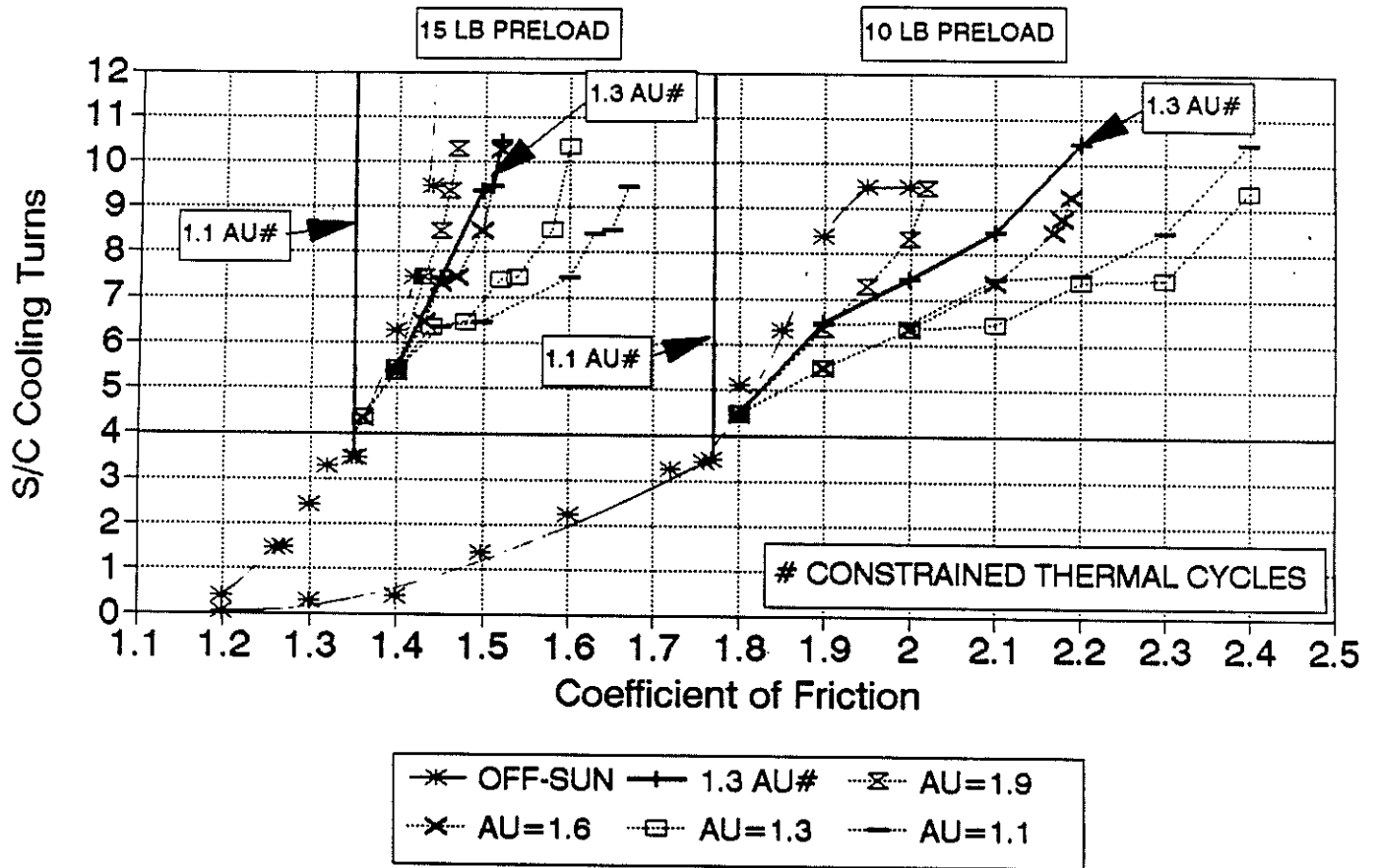
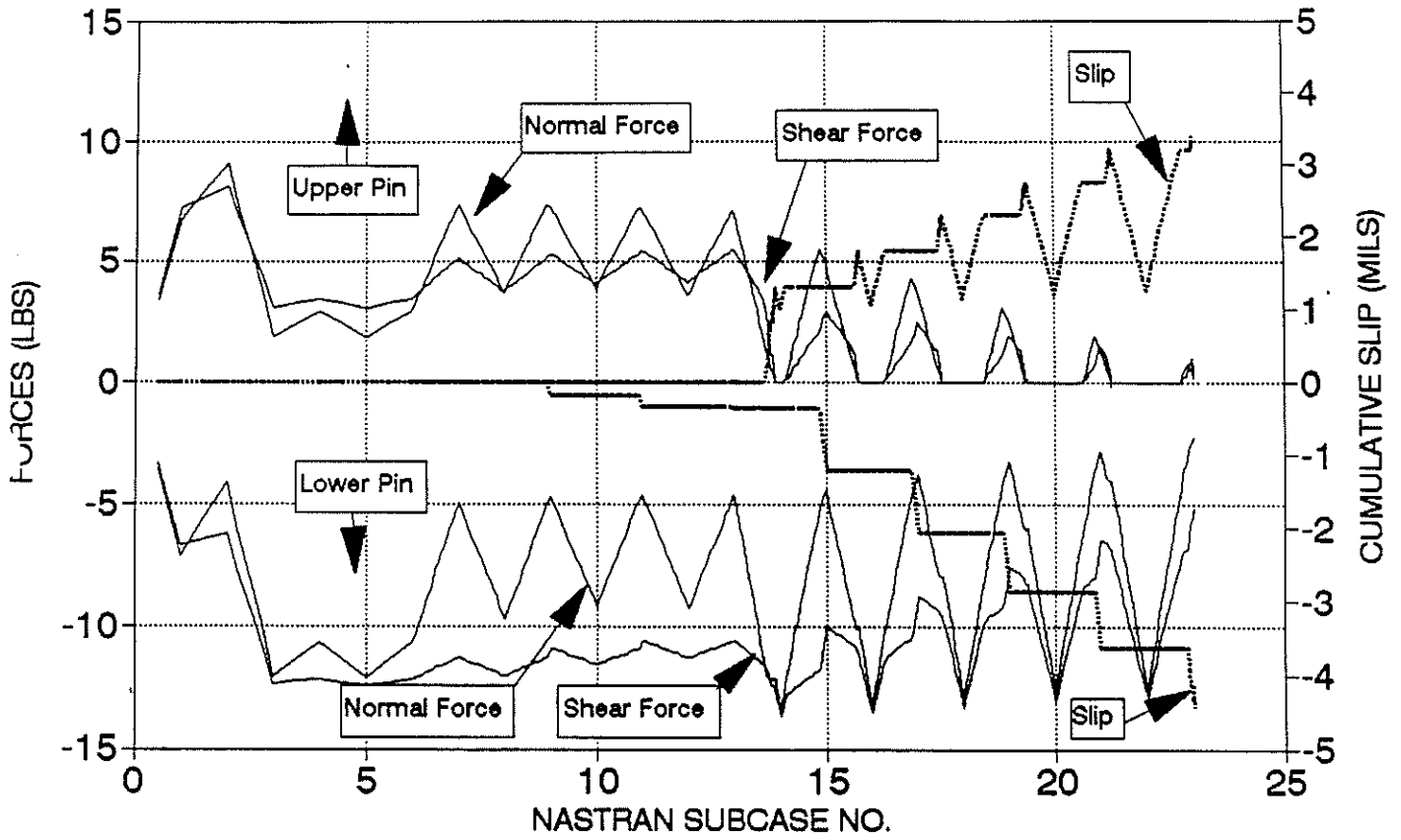
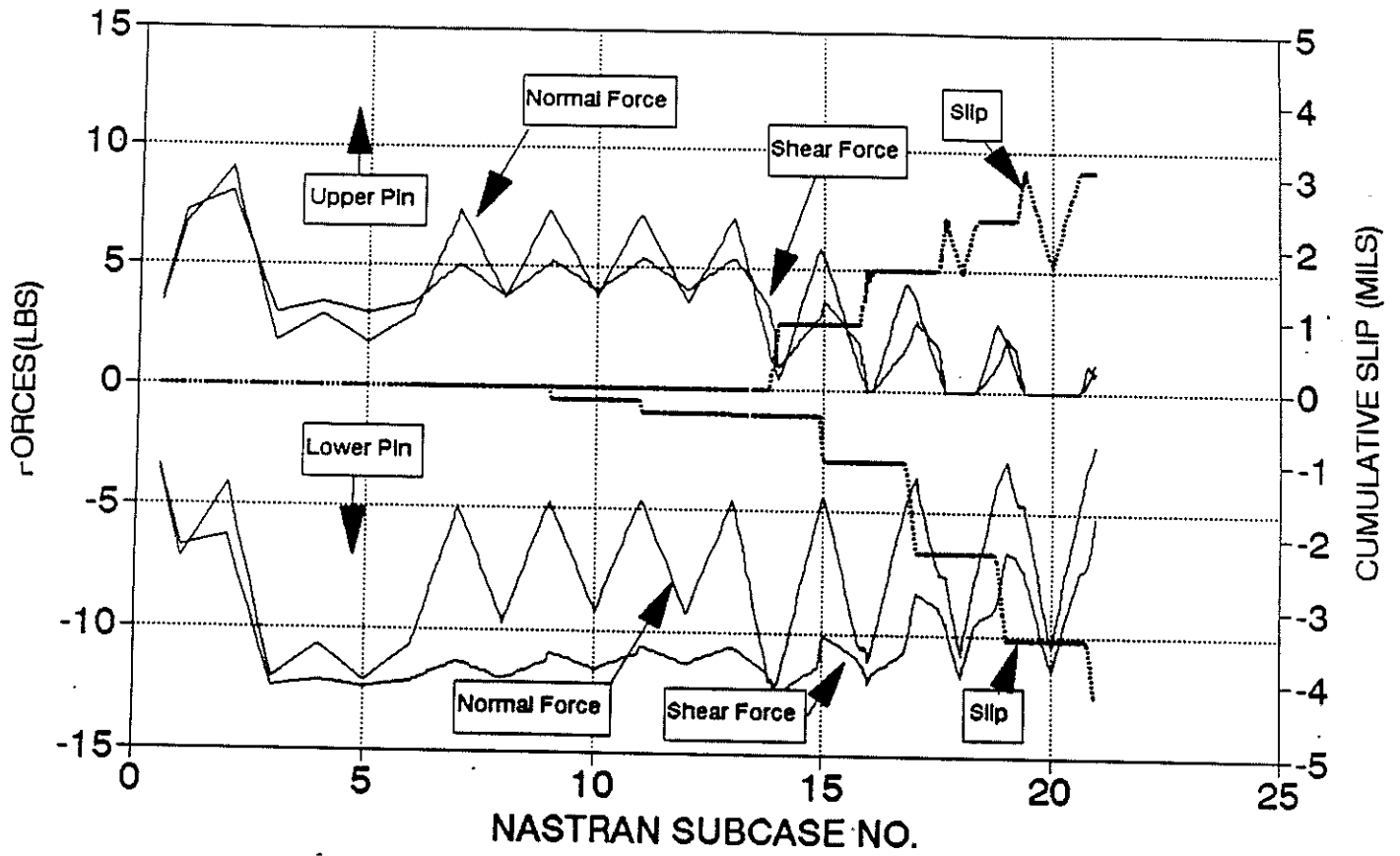


Figure 1: Rib Release Curves - Fixed AU Study

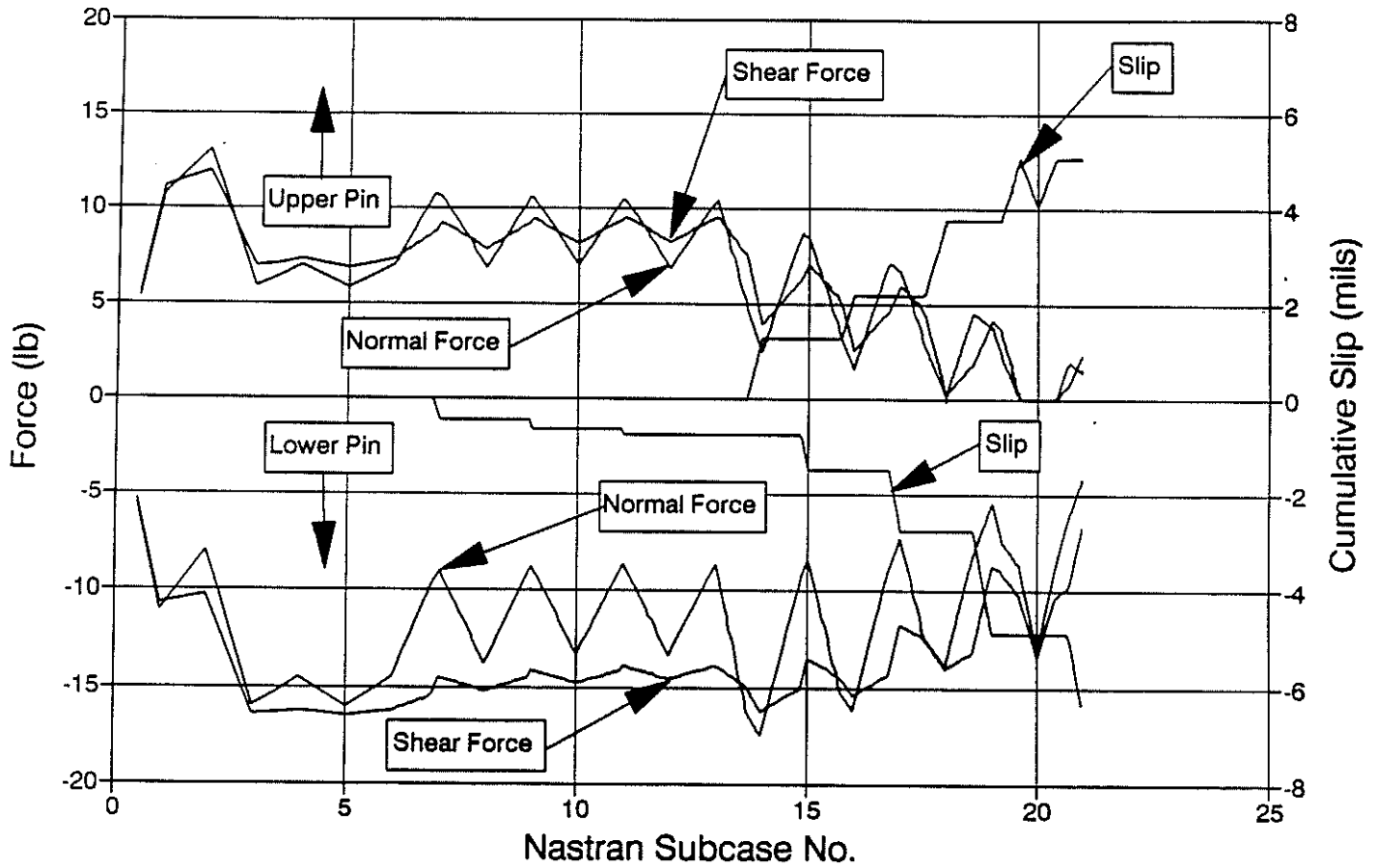
PIN FORCES AND SLIP
AU=1.1, 10LB PRELOAD, MU=2.30



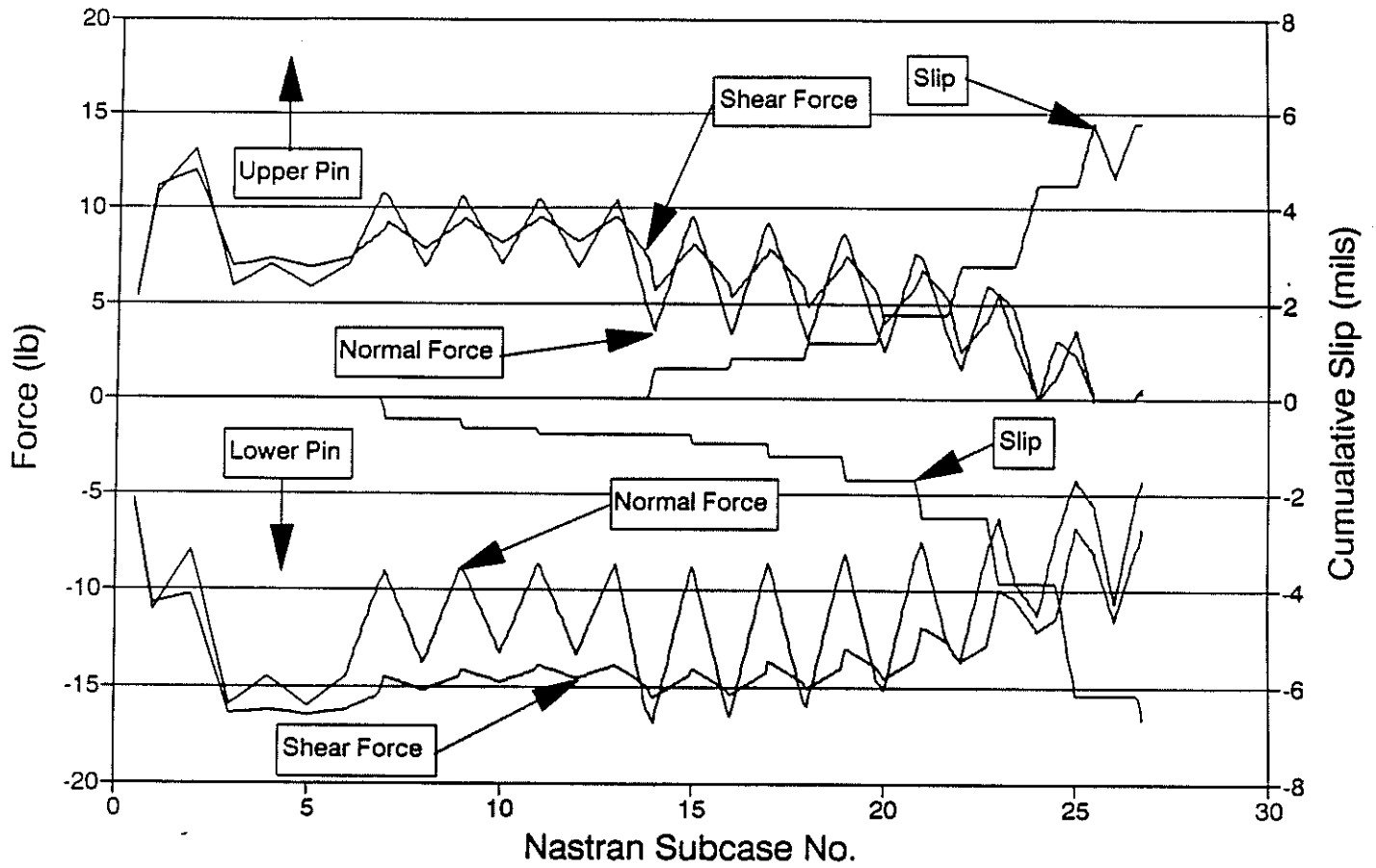
PIN FORCES AND SLIP AU=1.3, 10LB PRELOAD, MU=2.30



PIN FORCES AND SLIPPAGE 1.1 AU, 15 lb Preload, $\mu=1.60$



PIN FORCES AND SLIPPAGE 1.3 AU, 15 lb Preload, $\mu=1.60$



D-9932

APPENDIX 8.3
PWS On/Off Study

D-9932

JET PROPULSION LABORATORY

INTEROFFICE MEMORANDUM
3542/GSC/039-92

January 28, 1992

Revision: February 11, 1992

TO: G. Coyle

FROM: ~~A. Kissil~~ /AK

SUBJECT: PWS On/Off Sensitivity to GLL HGA Pin Walk-Out Analysis

Attached are the results of the subject analysis presented in four different formats, full curves with and without symbols representing the analysis points, and reduced curves (starting from N=3) with and without symbols. For your reference, the tower contraction scenario provided by A. Avila/G. Tsuyuki is also included in the attached Table.

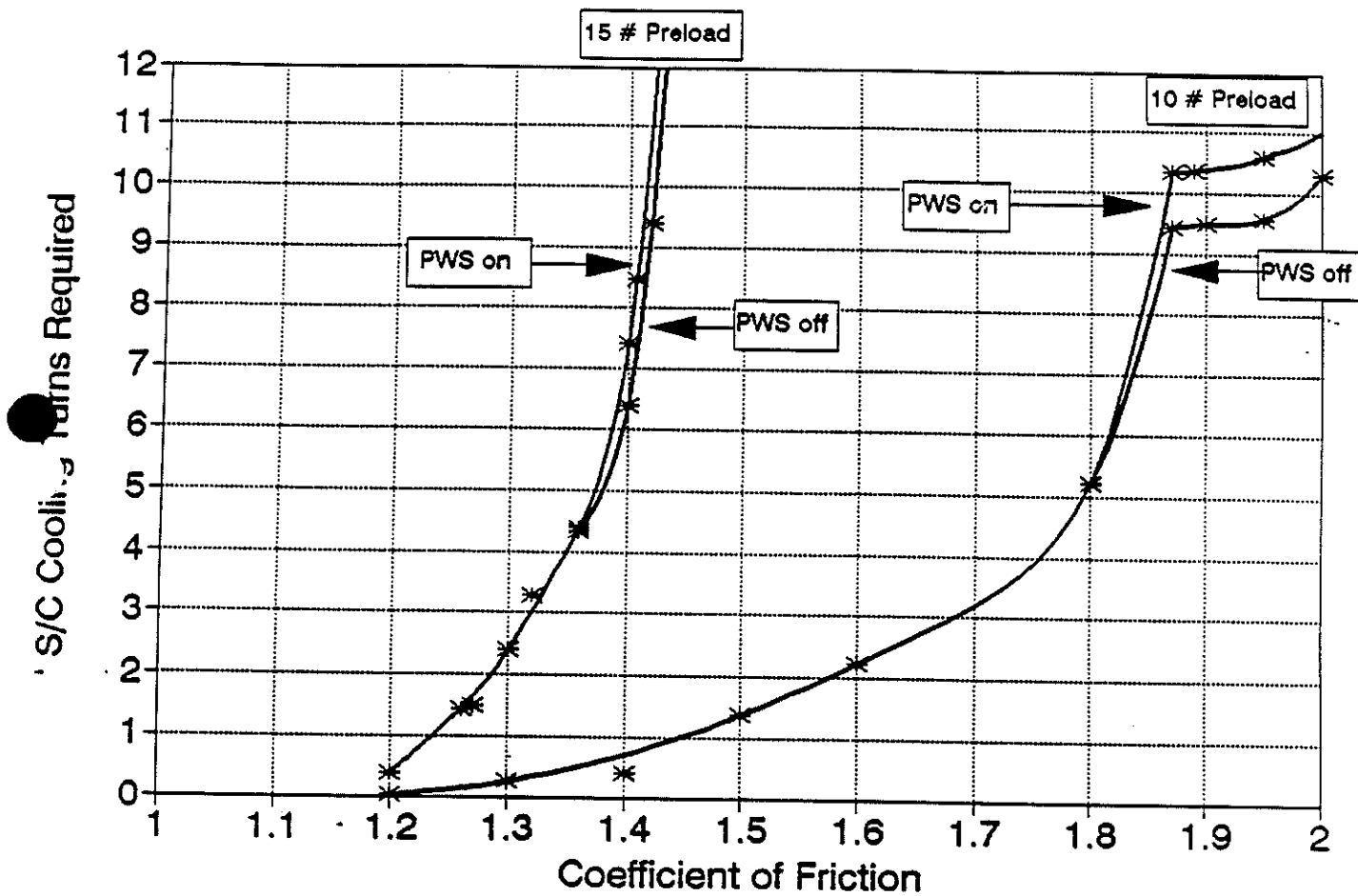
The analysis results indicate that before cooling turn No. 6 there is no noticeable effect from the PWS on pin walk-out analysis. Starting from cooling turn No. 6, the PWS on/off effect becomes profound.

Corrections: Refined analyses show that Earth encounter scenario has significant effect on the pin walk-out analysis with 10 lbs preload. Nevertheless, the effects are similar for both PWS on and PWS off cases.

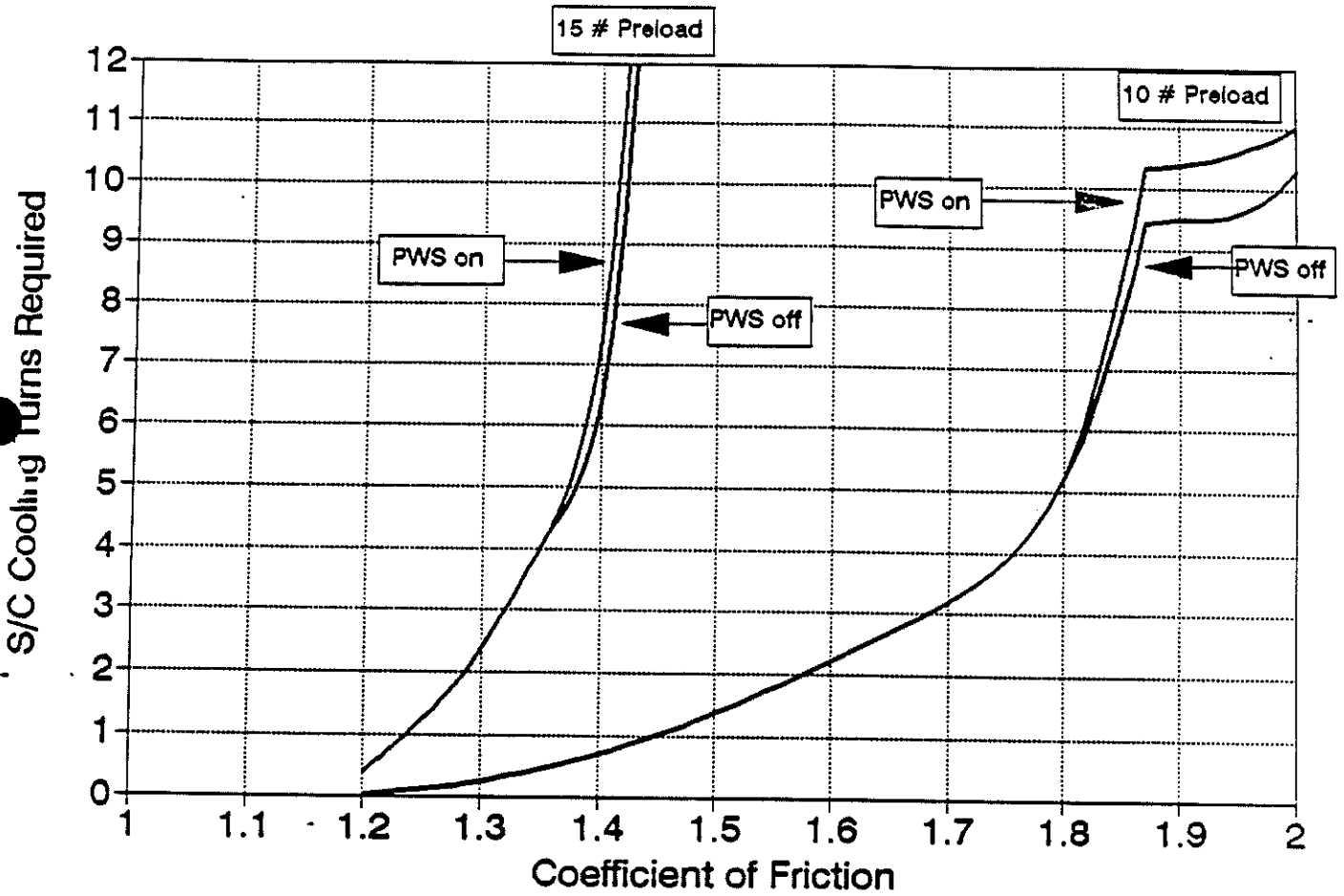
cc:

A. Avila
G-S. Chen
C. Lifer/B. Wada
R. Ploszaj
R. Reeve
J. Staats
R.F. Tillman
G. Tsuyuki

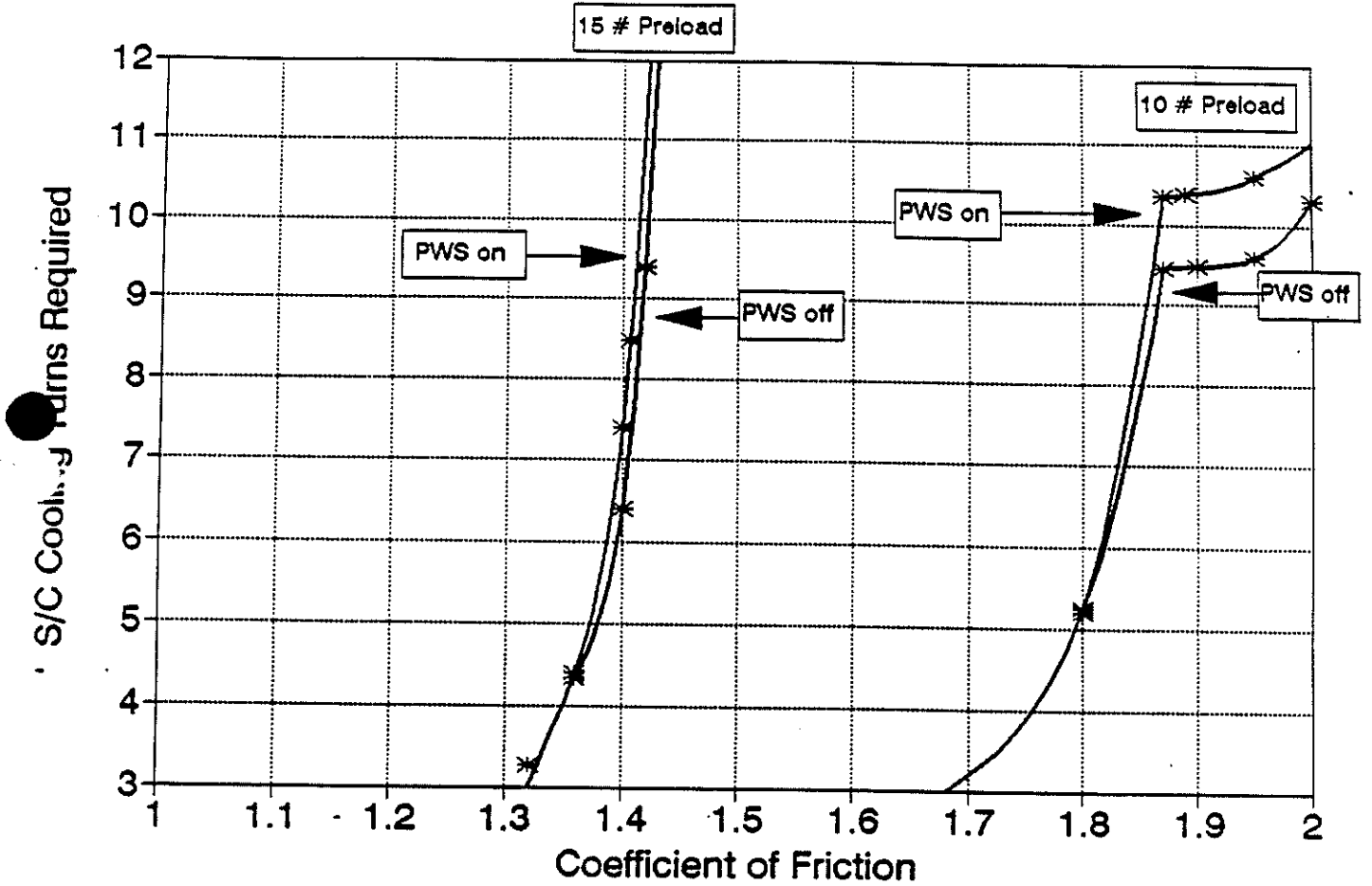
GLL HGA DEPLOYMENT ANOMALY EFFECTS OF PWS ON/OFF



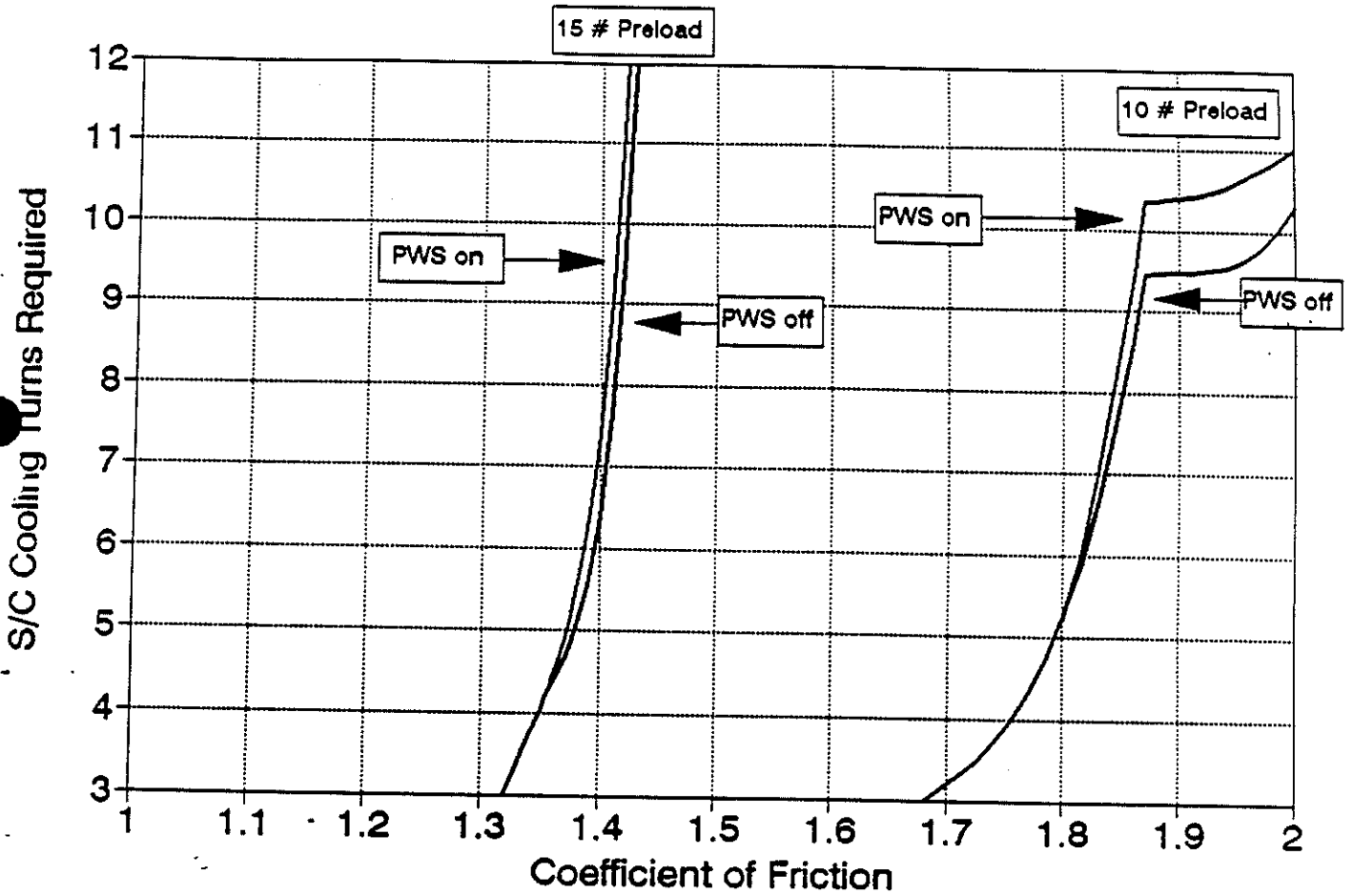
GLL HGA DEPLOYMENT ANOMALY EFFECTS OF PWS ON/OFF



GLL HGA DEPLOYMENT ANOMALY EFFECTS OF PWS ON/OFF



GLL HGA DEPLOYMENT ANOMALY EFFECTS OF PWS ON/OFF



GLL HGA FRICTION ANALYSIS LOADING CONDITIONS 0-9932

NASTRAN JBCASE	HISTORY OF GLL EVENTS	SOLAR AU	TOWER DISPL. (MILS) 12/11/91
1	PRELOAD PIN (20, 15 or 10 LB.)		
2	PRE-DEPLOYMENT	1.32	-20.3
3	DEPLOYMENT	1.32	-20.3
4	SUN POINTED	1.58	-29.7
5	WARMING TURN #1 (MAY '91)	1.58	-20.1
6	RETURN TO SUN POINTED	1.58	-29.7
7	COOLING TURN #1; 165° OFF-SUN (JULY '91)	1.84	-68.1
8	RETURN TO SUN POINTED	1.84	-35.8
9	COOLING TURN #2 (AUG. '91)	1.98	-70.3
10	RETURN TO SUN POINTED	1.98	-40.0
(10)	28° OFF-SUN; GASGRA ENCOUNTER (OCT. '91)	2.08	-40.7
(10)	RETURN TO SUN POINTED (NOV. '91)	2.24	-45.0
11	COOLING TURN #3 (DEC. '91)	2.25	-71.7
12	RETURN TO SUN POINTED	2.25	-42.2
(OMITTED)	WARMING TURN #4 (JAN. '92)	2.27	-40.1
(OMITTED)	RETURN TO SUN POINTED	2.27	-42.4

SUBCASE	FUTURE EVENTS	D-9932	SOLAR AU	TOWER DISPL.	
				PWS OFF (12/11)	PWS ON (+2 ml)
13	COOLING TURN #4; PWS ON (JAN. '92)		2.27	-71.8	-69.8
14	RETURN TO SUN POINTED		2.27	-42.4	
15	COOLING TURN #5; PWS ON (MAR '92)		2.22	-71.6	-69.6
16	RETURN TO SUN POINTED		2.22	-42.0	
17	COOLING TURN #6; PWS ON (APR. '92)		2.15	-71.2	-69.2
18	RETURN TO SUN POINTED		2.15	-41.1	
19	COOLING TURN #7; PWS ON (JUNE '92)		2.0	-70.4	-68.4
20	RETURN TO SUN POINTED		2.0	-39.1	
21	COOLING TURN #8; PWS (JULY '92)		1.75	-68.6	-66.6
22	RETURN TO SUN POINTED		1.75	-34.4	
23	COOLING TURN #9; PWS (SEP. '92)		1.55	-66.8	-64.8
(23)	RETURN TO SUN POINTED		1.55	-29.4	
24	EARTH ENCOUNTER; SUN POINTED (DEC. '92)		1.00	-4.7	
25	COOLING TURN #10 (MAR. '93)		1.60	-67.3	-65.3
26	RETURN TO SUN POINTED		1.60	-30.8	
27	COOLING TURN #11 (APR. '93)		1.90	-69.8	-67.8
28	RETURN TO SUN POINTED		1.90	-37.5	

D-9932

APPENDIX 8.4

Effects of Antenna Hub Offsets

JET PROPULSION LABORATORY

INTEROFFICE MEMORANDUM
3541-92-076

February 18, 1992

TO: G. Coyle

FROM: ~~AK Kissel~~ ^{AK} ^{AK} R. K. Eads

SUBJECT: Study of Effects of Initial Vertical Offset of the GLL HGA Pins with Respect to Receptacles

A parametric study was conducted in which the HGA stow pins were given initial vertical mismatch of position with respect to the receptacles. Initial tilt of the carrier could be a significant contributor to this type of distortion. Initial offsets of +0.02 and +0.03 inch were investigated. A positive value of offset indicates that the receptacles were raised above the pins, similar to a tower expansion. The additional effects of preload were also taken into account. For the 0.02 inch vertical offset, misalignment preloads of 0, 5, and 10 lbs were investigated. For the 0.03 inch offset, only the 10 lb preload was investigated. Figure 1 presents the results obtained in terms of the number of S/C cooling turns required in order to obtain stuck rib release as a function of pin/receptacle coefficient of friction. From the figure we observe that adding the vertical offset has the effect of raising the curve for a given preload, which indicates that a larger number of S/C cooling turns would be required to free the pins for a given value of coefficient of friction.

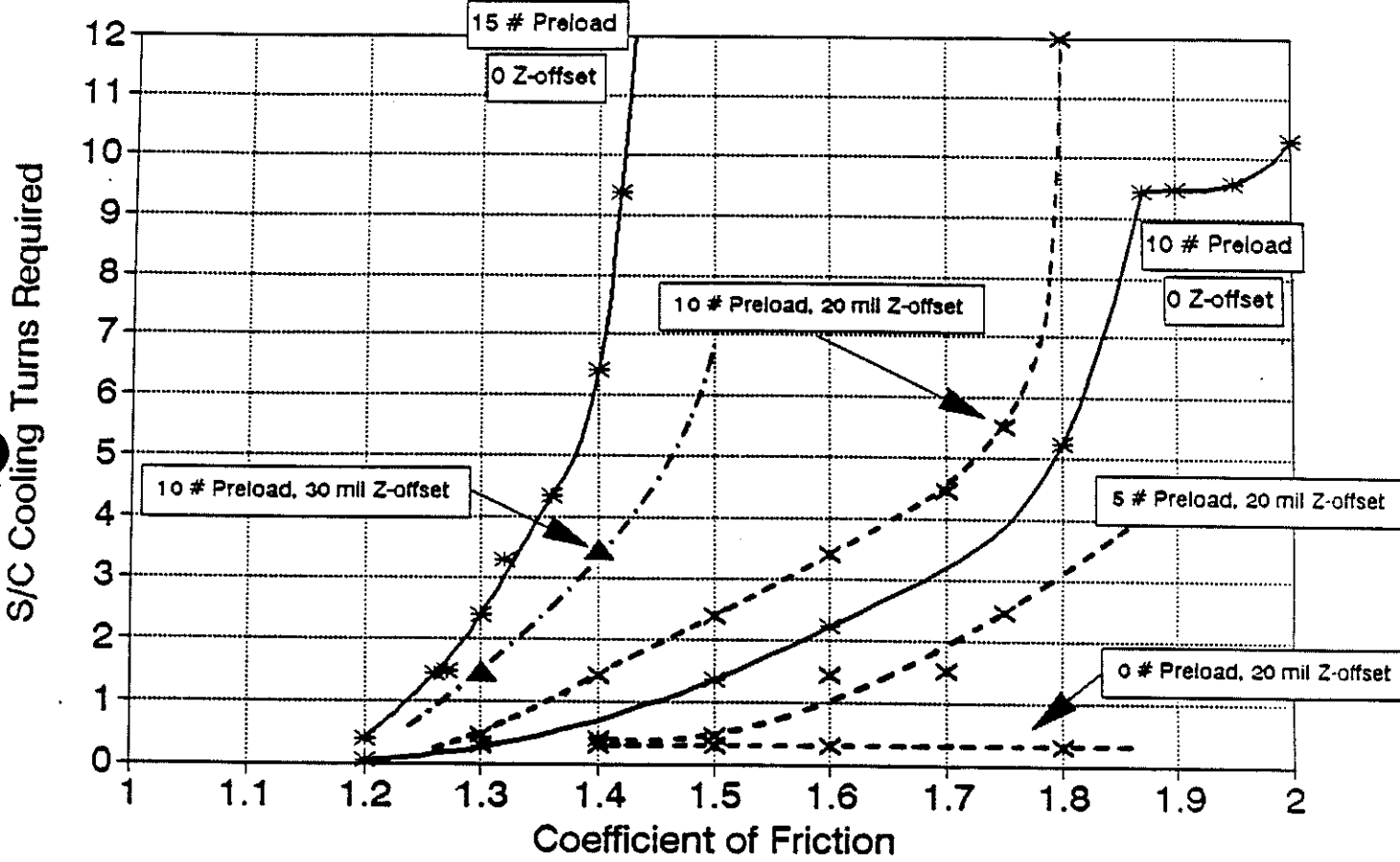
This analysis was conducted using the single rib NASTRAN model, and the boundary conditions obtained from rib #10 of the full model having three ribs stuck. The set of tower contractions used for this analysis was for the nominal on-sun conditions, and is shown in Table 1.

AS/RKE:ipk

cc: A. Avila
G-S. Chen
R. Ploszaj
R. Reeve
J. Staats
R. F. Tillman
G. Tsuyuki
C. Lifer/B. Wada

Figure 1.

GLL HGA DEPLOYMENT ANOMALY EFFECTS OF Z-OFFSET WITH PRELOAD



GLL HGA FRICTION ANALYSIS LOADING CONDITIONS 0-9932

NASTRAN UBCASE	HISTORY OF GLL EVENTS	SOLAR AU	TOWER DISPL. (MILS) 12/11/91
1	PRELOAD PIN (20, 15 or 10 LB.)		
2	PRE-DEPLOYMENT	1.32	-20.3
3	DEPLOYMENT	1.32	-20.3
4	SUN POINTED	1.58	-29.7
5	WARMING TURN #1 (MAY '91)	1.58	-20.1
6	RETURN TO SUN POINTED	1.58	-29.7
7	COOLING TURN #1; 165° OFF-SUN (JULY '91)	1.84	-68.1
8	RETURN TO SUN POINTED	1.84	-35.8
9	COOLING TURN #2 (AUG. '91)	1.98	-70.3
10	RETURN TO SUN POINTED	1.98	-40.0
(10)	28° OFF-SUN; GASRA ENCOUNTER (OCT. '91)	2.08	-40.7
(10)	RETURN TO SUN POINTED (NOV. '91)	2.24	-45.0
11	COOLING TURN #3 (DEC. '91)	2.25	-71.7
12	RETURN TO SUN POINTED	2.25	-42.2
OMITTED)	WARMING TURN #4 (JAN. '92)	2.27	-40.1
OMITTED)	RETURN TO SUN POINTED	2.27	-42.4

U-9452

13	COOLING TURN #4; PWS ON (JAN. '92)	2.27	-71.8	
14	RETURN TO SUN POINTED	2.27	-42.4	
15	COOLING TURN #5; PWS ON (MAR '92)	2.22	-71.6	
16	RETURN TO SUN POINTED	2.22	-42.0	
17	COOLING TURN #6; PWS ON (APR. '92)	2.15	-71.2	
18	RETURN TO SUN POINTED	2.15	-41.1	
19	COOLING TURN #7; PWS ON (JUNE '92)	2.0	-70.4	
20	RETURN TO SUN POINTED	2.0	-39.1	
21	COOLING TURN #8; PWS (JULY '92)	1.75	-68.6	
22	RETURN TO SUN POINTED	1.75	-34.4	
23	COOLING TURN #9; PWS (SEP. '92)	1.55	-66.8	
(23)	RETURN TO SUN POINTED	1.55	-29.4	
24	EARTH ENCOUNTER; SUN POINTED (DEC. '92)	1.00	-4.7	
25	COOLING TURN #10 (MAR. '93)	1.60	-67.3	
26	RETURN TO SUN POINTED	1.60	-30.8	
27	COOLING TURN #11 (APR. '93)	1.90	-69.8	
28	RETURN TO SUN POINTED	1.90	-37.5	

D-9932

APPENDIX 8.5

DDA Motor Pulse

JET PROPULSION LABORATORY

INTEROFFICE MEMORANDUM
3541-92-155

April 28, 1992

TO: G. S. Chen

FROM: ~~RF~~ ^{AK} R. K. Eads/A. Kissil/W. Tsuha ^{TSJ} 410

SUBJECT: Study of the Effects of Motor Turn-on Duration on Second Rib Release for GLL HGA

REFERENCE: 1) IOM 3541-92-130, "GLL HGA Pin Walkout Analysis for March 1992 Cooling Schedule and Model Configuration", April 9, 1992.

Introduction

This study was conducted to evaluate the potential consequences of deployment motor turn-on for the GLL HGA. A motor turn-on was planned to take place near the end of this month, and some concern was expressed whether any detrimental effects regarding subsequent stuck stow pin release would occur as a consequence. If no stuck ribs have been released, and they are not released as a result of motor turn-on, then an attempt to turn on the deployment motor would result in the motor quickly stalling, and any associated rotation of the ballscrew shaft would be negligible. If, however, one rib is released, then the force restraining the rotation of the ballscrew shaft will be reduced. The amount of rotation of the ballscrew shaft that would occur with one rib released would depend upon the duration of motor turn-on.

Model Description and Assumptions

The detailed NASTRAN model and the reduced-single rib models were used for this study. For the sake of expediency, the detailed model analysis used the 12/91 Cooling Scenario with no moisture dryout effects. A coefficient of friction of 1.7 and a pin preload of 10 lbs. were assumed. The additional motor turn-on was imposed after the first rib release. Three different motor turn-on durations were considered: 2, 4 and 10 seconds.

The single rib model analysis used the 3/92 Cooling Scenario and moisture dryout was accounted for. The boundary conditions for the second rib release analysis were taken from an existing output file generated by P. Rapacz (JPL354::USER4:[SXA.RAPACZ.LIFECYCLE]R2FINAL.F-LC.F06). These rib pivot point boundary conditions were extrapolated to account for additional ball screw motion. Motor turn-on durations of 2, 4, and 5 seconds were considered. Pin preloads of 10 and 15 lbs. were used.

Results and Discussion

Figure 1 shows the pin walkout results obtained for this study. The first rib release data are the same as previously presented in Reference 1.

The detailed model results show that 2 seconds of motor turn-on has negligible effect on second rib release. The 4 second motor turn-on requires one additional cooling turn to obtain rib release. The 10 second turn-on results in no rib release being obtained for the whole cooling cycle scenario.

The single rib analysis for 10 lbs. of pin preload shows that the 2 second motor turn-on has negligible effect, in agreement with the detailed model. The 4 second motor turn-on, however is shown to prevent rib release for the whole cooling cycle scenario.

The single rib analysis for 15 lbs of pin preload show that a 4 second motor turn-on requires one additional cooling turn to obtain rib release than the case with no turn-on at all. This result is more consistent with the detailed model results.

The question arises as to why the single rib model with 15 lbs of preload behaves more like the detailed model than does the 10 lb preload. Direct comparison of the detailed model results with the single model results presented in Figure 1 can be misleading, because of the difference in cooling cycle scenarios and rib dryout. However, trends, such as sensitivity to motor turn-on should be similar. Figure 2 shows the pin forces and slippage obtained for the detailed model with a 10 second motor turn-on. Figure 3 shows the pin forces and slippage obtained without additional motor turn-on. Comparing Figures 2 and 3 shows that the motor turn on reduces the loads carried by the upper pin, which has a significant effect on slippage in the lower pin. If the upper pin loses contact all together, then the walking phenomenon no longer can take place. We see that the upper pin loses contact for larger intervals between cooling cycles when the motor turn-on is in effect. These observations shed some light on the behavior of the single rib model. It is probable that the higher preload level keeps the upper pin in better contact with the receptacle surface than the case with the lower preload. The better contact allows the walking phenomenon to proceed more easily.

Conclusion

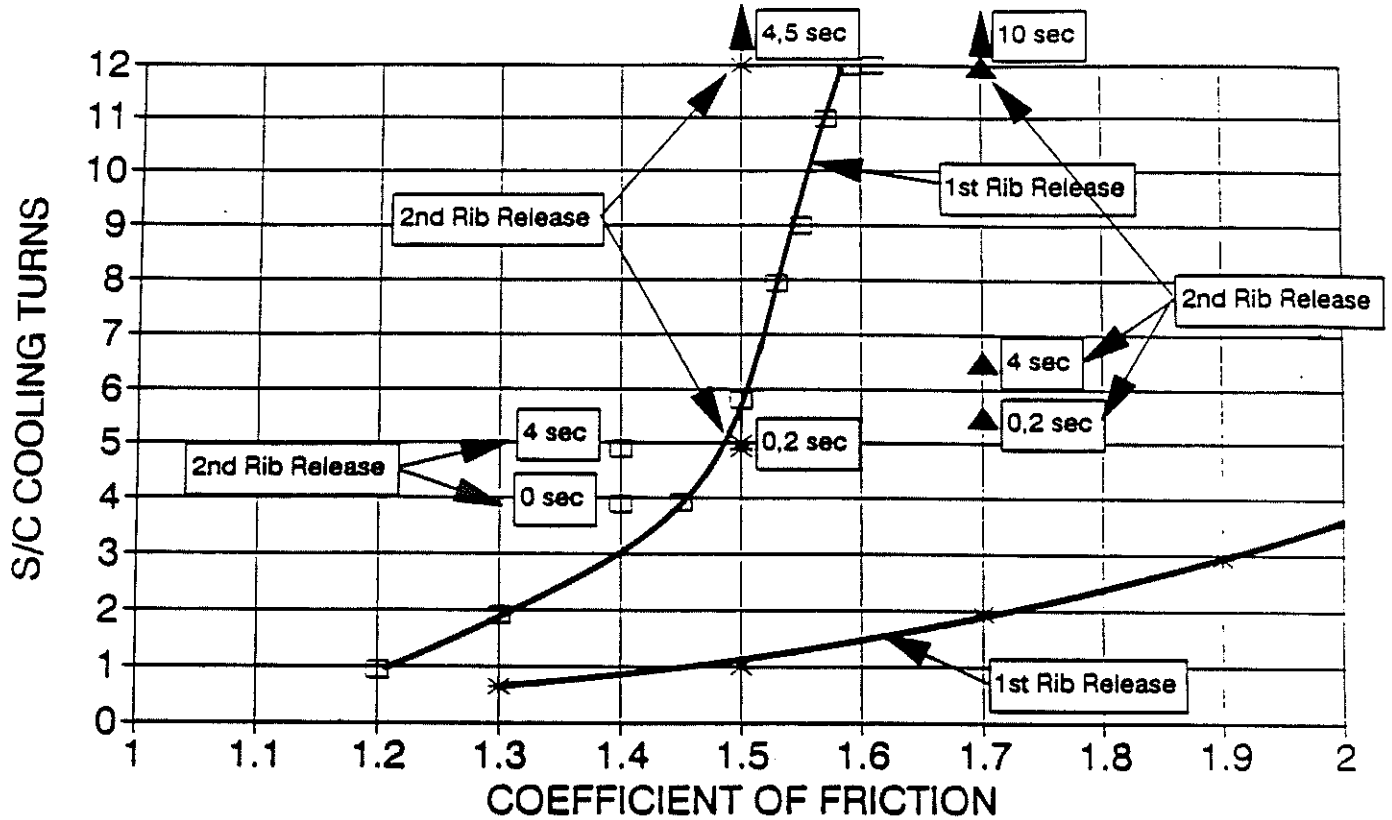
From our analysis it is evident that a 2 second HGA deployment motor turn-on will have no detrimental effects for subsequent rib release. Motor turn-on durations of 4 seconds or longer could potentially make subsequent rib release more difficult, if a rib is released prior to or during motor turn-on.

AK:ipk

cc: A. Avila
G. Coyle
R. Ploszaj
P. Rapacz
R. Reeve

J. Staats
R. F. Tillman
G. Tsuyuki
C. Lifer/B. Wada

COOLING TURNS REQUIRED FOR RIB RELEASE
Study of Motor Turn-on Effects



* 10#-Single Rib □ 15#-Single Rib ▲ 10#-Full Model

- 1.) Single Rib Model- 3/92 Cooling Scenario
- 2.) Full Model- 12/91 Cooling Scenario
- 3.) 12/91- No Dryout / 3/92- 9 mil Dryout
- 4.) +Pin
- 5.) 1st Rib Release- Rib 11, 2nd Rib Release- Rib 10

Figure 1.

RIB 10 PIN FORCES AND SLIPPAGE

Effects of 10 Second Motor Turn-On

Three Rib Model, 10 lb Preload, $\mu=1.70$

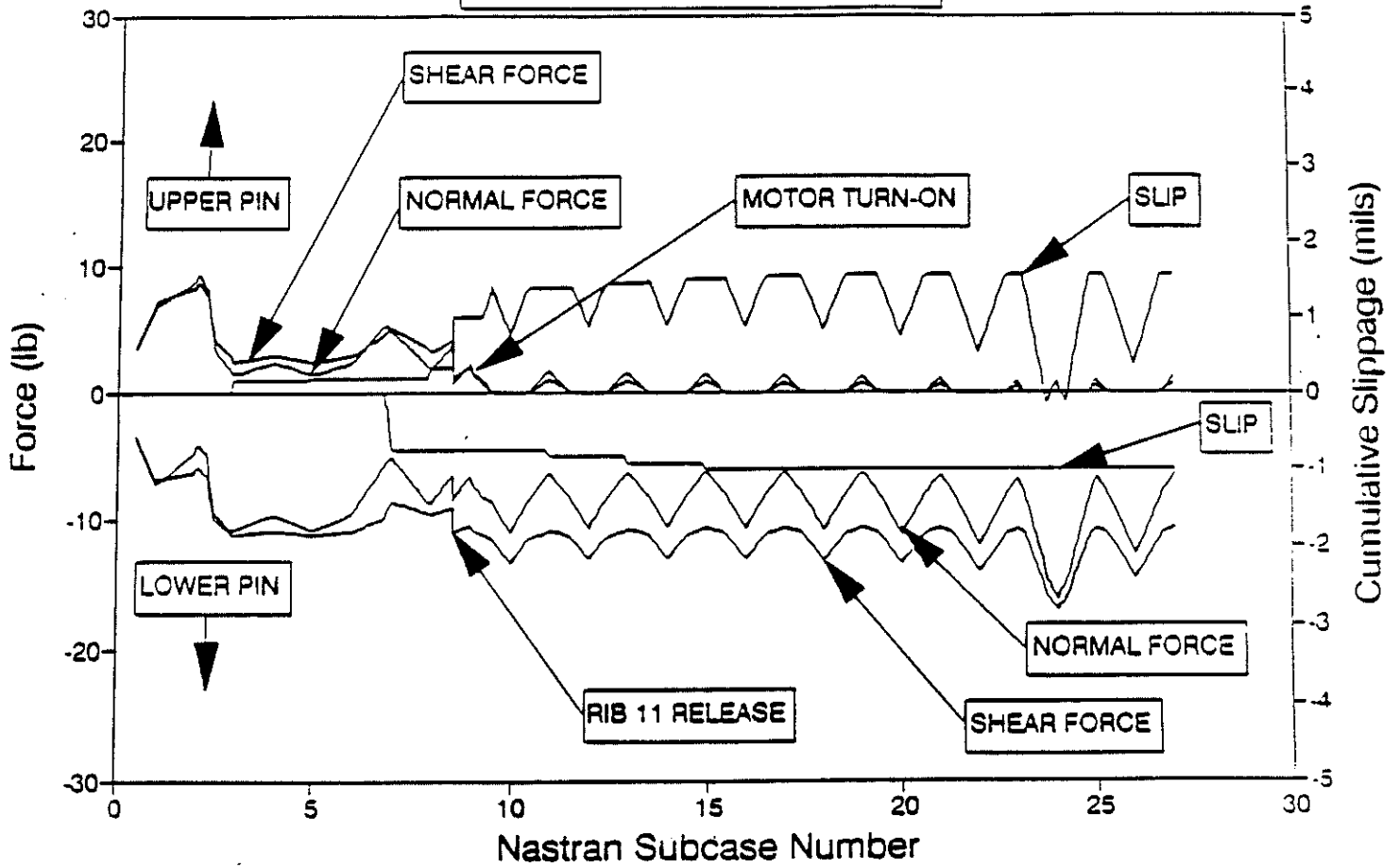


Figure 2.

RIB 10 PIN FORCES AND SLIPPAGE (ON-SUN) Three Rib Model, 10 lb Preload, $\mu = 1.70$

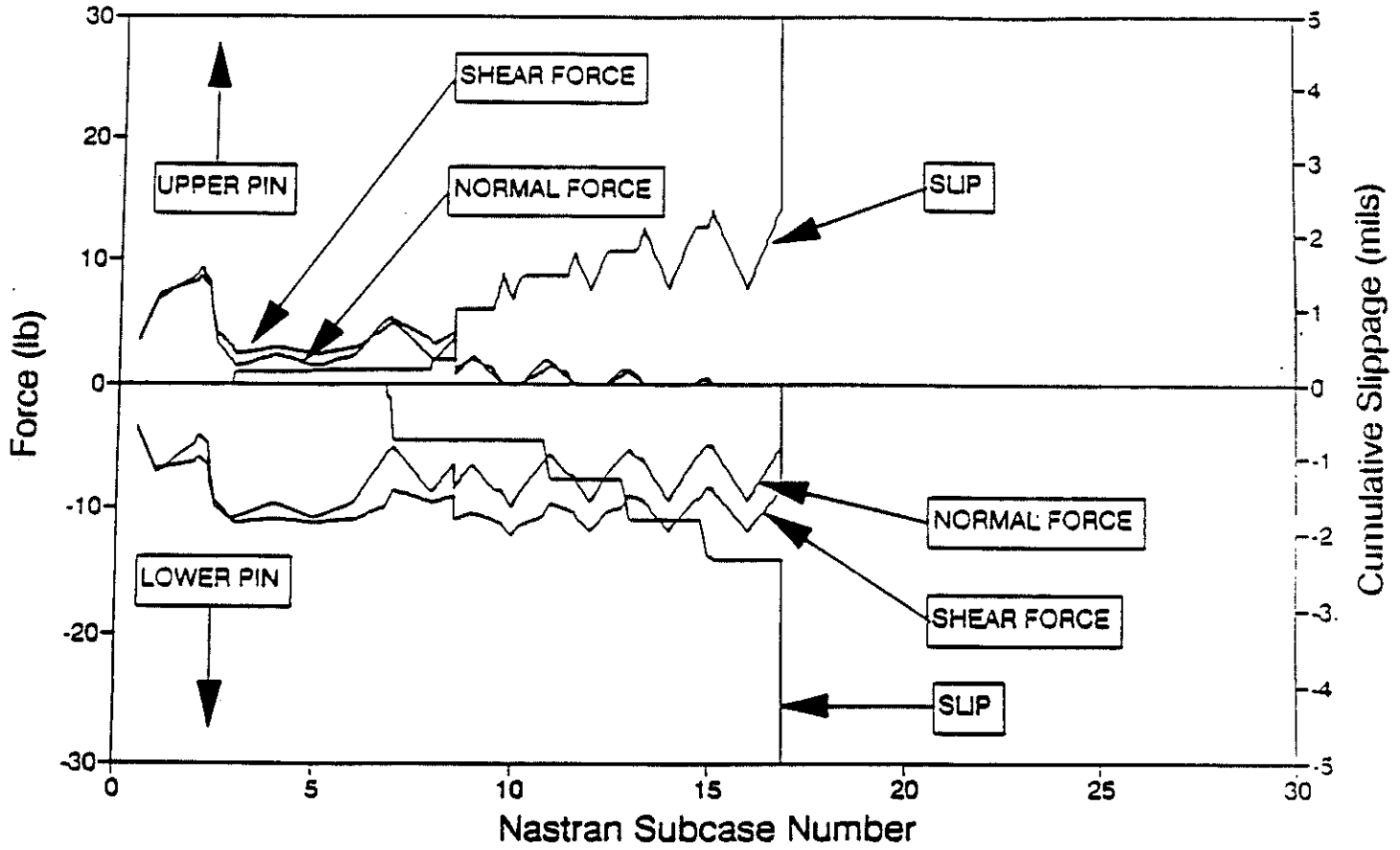


Figure 3.

D-9932

APPENDIX 8.6

Thermal Cycling at 3 AU

JET PROPULSION LABORATORY

INTEROFFICE MEMORANDUM
3541-92-160

May 5, 1992

TO: G-S. Chen

FROM: A. Kissil/R. K. Eads

SUBJECT: GLL HGA Pin Walkout Analysis for the Case of Having 6 Cooling Turns at 3AU After the 6th Cooling Turn

REFERENCE: 1) IOM 3541-92-130 "GLL HGA Pin Walkout Analysis for March 1992 Cooling Schedule and Model Configuration", April 9, 1992.

This analysis addresses the effects of altering the S/C cooling turn scenario from that presented in the March '92 scenario (Reference 1 and Table 1), which will be referred to as the baseline scenario. The 9 mil moisture dryout and "+" pin configuration were incorporated in this analysis. The single rib NASTRAN model and boundary conditions that were used for this analysis are the same as were described in Reference 1. The first alteration that was investigated consisted of modifying the cooling turn history after the sixth cooling turn of the baseline scenario, as presented in Table 2. This new scenario has a much warmer warming turn (@ 1.07 AU) following the sixth cooling turn than did the baseline. Following this very warm warming turn are six very cold cooling turns (@ 3AU). The results of this analysis are presented in Figure 1 in terms of the number of S/C cooling turns required to release the first of three stuck ribs as a function of pin/receptacle coefficient of friction. Only the 15 lb. pin preload case was investigated. It is apparent that this modified cooling turn scenario results in fewer turns being required to obtain rib release, for a given coefficient of friction.

In order to investigate this behavior, the stow pin/receptacle forces and slippage were plotted as a function of cooling turn number for a given coefficient of friction. Figure 2 presents the stow pin forces and slippage for the baseline scenario, and Figure 3 presents those for the modified scenario. Comparison of Figures 2 and 3 shows that for the modified scenario a very large amount of slippage is developed in the upper pin during the Earth encounter, while for the baseline scenario the Earth encounter causes only a small amount of slippage. It is also worth noting from Figure 3 that the 1.07 AU warming turn following the Earth encounter had very little effect because of a loss of contact which occurred in the upper pin near the end of Earth encounter.

The second cooling turn scenario alteration was aimed at confirming the ineffectiveness of the 1.07 AU warming turn. As shown in Table 3, the 1.07 AU warming turn was eliminated along with its associated pre and post sun-pointed turns. Figure 4 shows the effect of eliminating the

The detailed model results show that 2 seconds of motor turn-on has negligible effect on second rib release. The 4 second motor turn-on requires one additional cooling turn to obtain rib release. The 10 second turn-on results in no rib release being obtained for the whole cooling cycle scenario.

The single rib analysis for 10 lbs. of pin preload shows that the 2 second motor turn-on has negligible effect, in agreement with the detailed model. The 4 second motor turn-on, however is shown to prevent rib release for the whole cooling cycle scenario.

The single rib analysis for 15 lbs of pin preload show that a 4 second motor turn-on requires one additional cooling turn to obtain rib release than the case with no turn-on at all. This result is more consistent with the detailed model results.

The question arises as to why the single rib model with 15 lbs of preload behaves more like the detailed model than does the 10 lb preload. Direct comparison of the detailed model results with the single model results presented in Figure 1 can be misleading, because of the difference in cooling cycle scenarios and rib dryout. However, trends, such as sensitivity to motor turn-on should be similar. Figure 2 shows the pin forces and slippage obtained for the detailed model with a 10 second motor turn-on. Figure 3 shows the pin forces and slippage obtained without additional motor turn-on. Comparing Figures 2 and 3 shows that the motor turn on reduces the loads carried by the upper pin, which has a significant effect on slippage in the lower pin. If the upper pin loses contact all together, then the walking phenomenon no longer can take place. We see that the upper pin loses contact for larger intervals between cooling cycles when the motor turn-on is in effect. These observations shed some light on the behavior of the single rib model. It is probable that the higher preload level keeps the upper pin in better contact with the receptacle surface than the case with the lower preload. The better contact allows the walking phenomenon to proceed more easily.

Conclusion

From our analysis it is evident that a 2 second HGA deployment motor turn-on will have no detrimental effects for subsequent rib release. Motor turn-on durations of 4 seconds or longer could potentially make subsequent rib release more difficult, if a rib is released prior to or during motor turn-on.

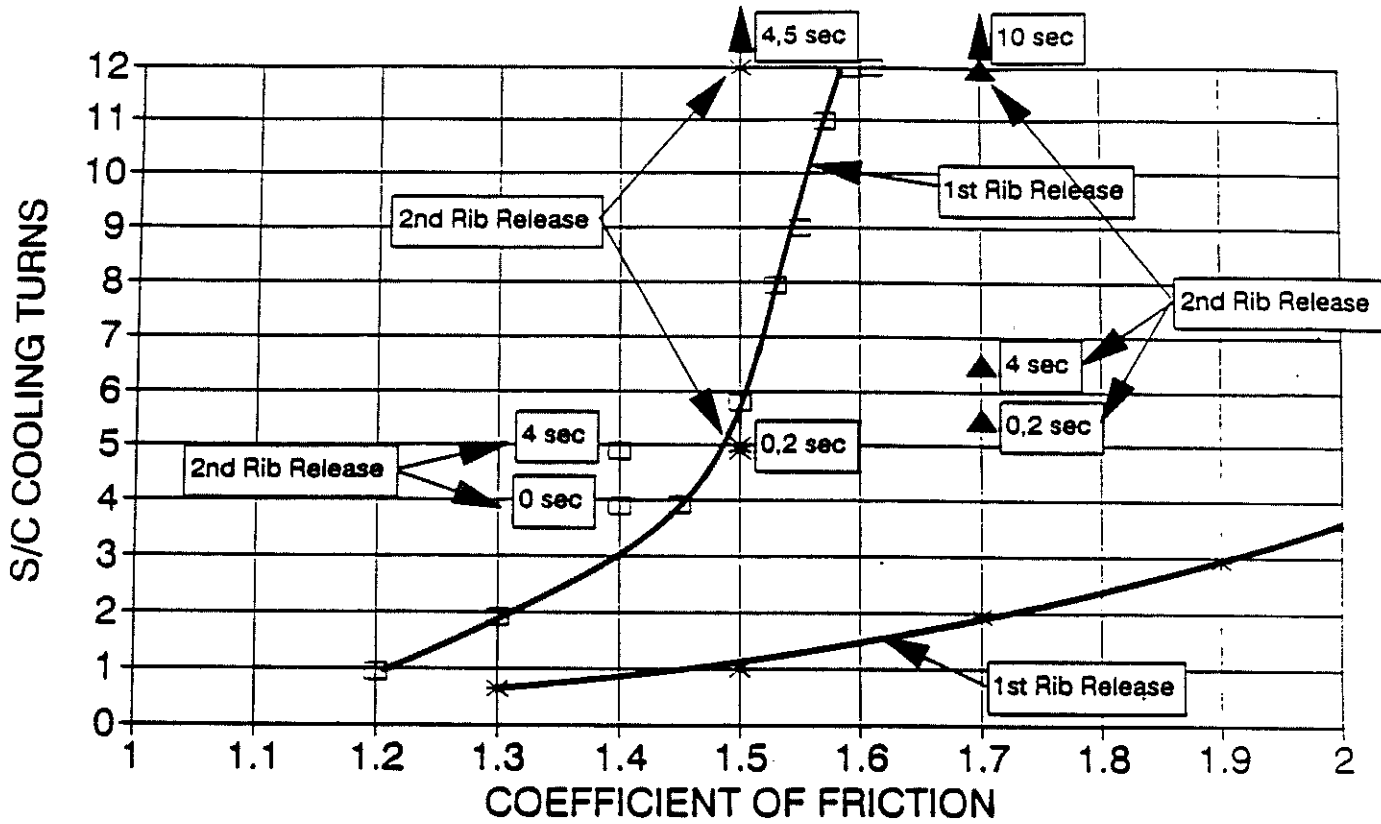
AK:ipk

cc: A. Avila
G. Coyle
R. Ploszaj
P. Rapacz
R. Reeve

J. Staats
R. F. Tillman
G. Tsuyuki
C. Lifer/B. Wada

ink
4/1/92

COOLING TURNS REQUIRED FOR RIB RELEASE
Study of Motor Turn-on Effects



* 10#-Single Rib □ 15#-Single Rib ▲ 10#-Full Model

- 1.) Single Rib Model- 3/92 Cooling Scenario
- 2.) Full Model- 12/91 Cooling Scenario
- 3.) 12/91- No Dryout / 3/92- 9 mil Dryout
- 4.) +Pin
- 5.) 1st Rib Release- Rib 11, 2nd Rib Release- Rib 10

Figure 1.

RIB 10 PIN FORCES AND SLIPPAGE

Effects of 10 Second Motor Turn-On

Three Rib Model, 10 lb Preload, $\mu=1.70$

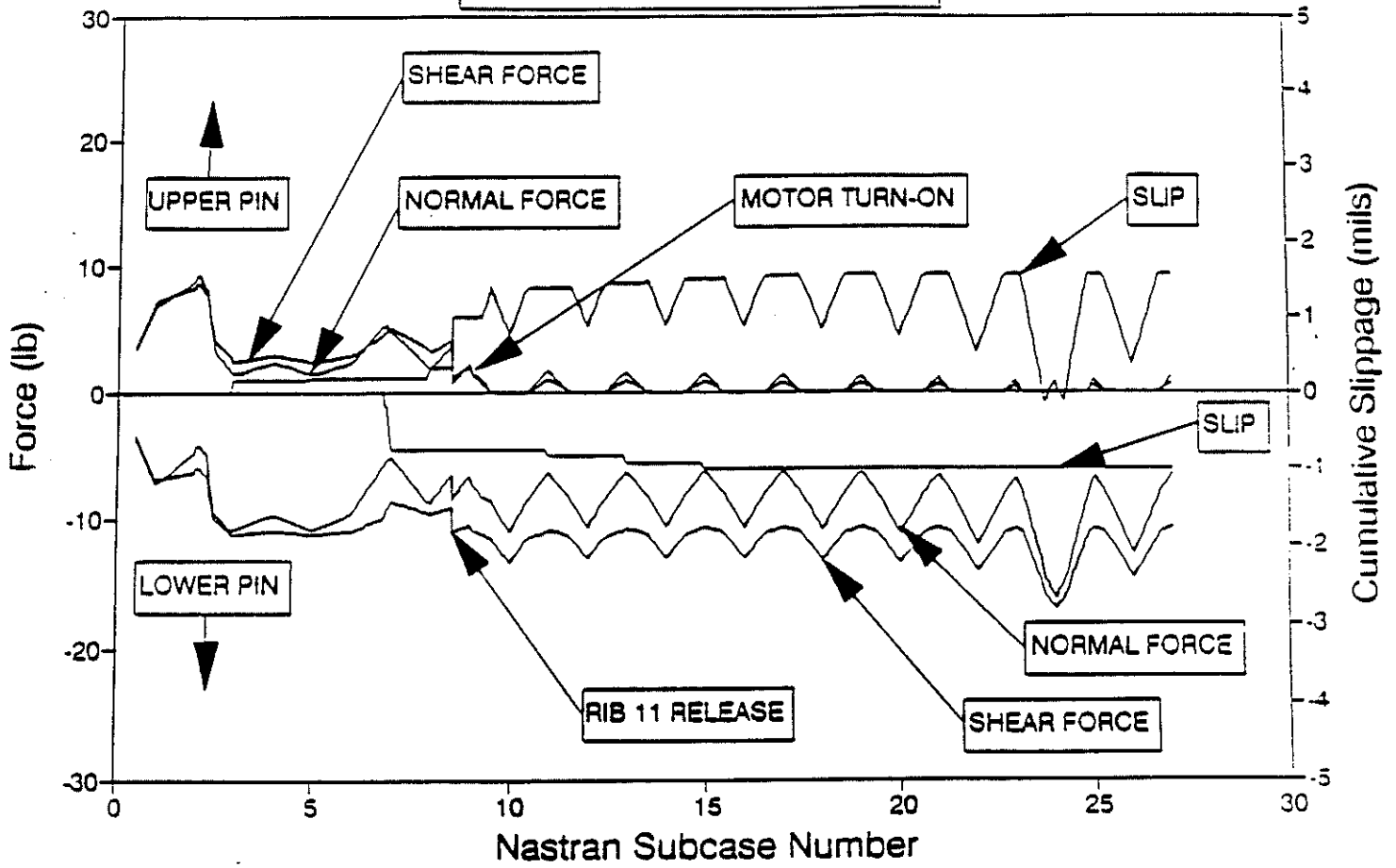


Figure 2.

RIB 10 PIN FORCES AND SLIPPAGE (ON-SUN) Three Rib Model, 10 lb Preload, $\mu=1.70$

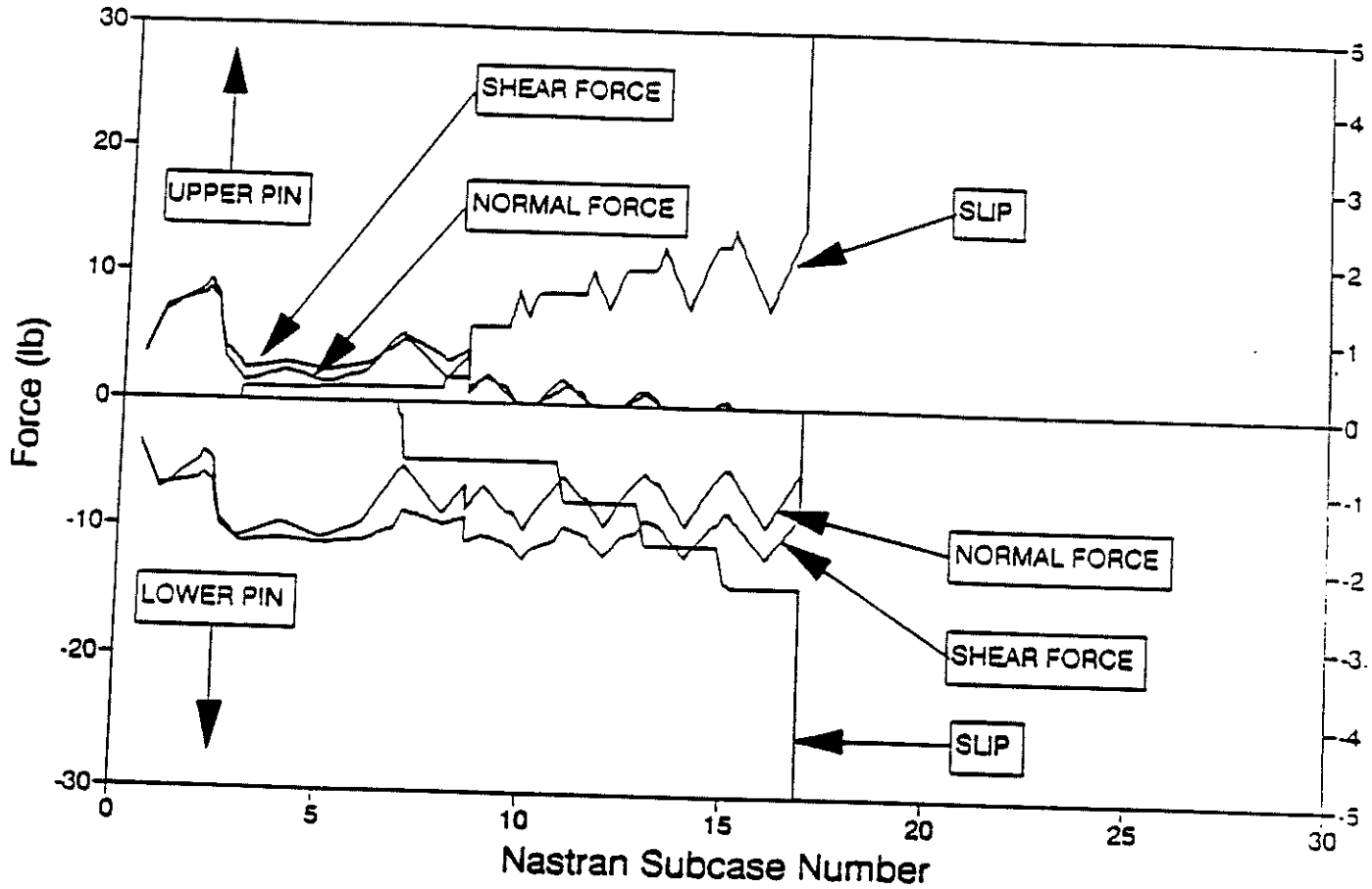


Figure 3.

JET PROPULSION LABORATORY

INTEROFFICE MEMORANDUM
3541-92-160

May 5, 1992

TO: G-S. Chen

FROM: A. Kissil/R. K. Eads

SUBJECT: GLL HGA Pin Walkout Analysis for the Case of Having 6 Cooling Turns at 3AU After the 6th Cooling Turn

REFERENCE: 1) IOM 3541-92-130 "GLL HGA Pin Walkout Analysis for March 1992 Cooling Schedule and Model Configuration", April 9, 1992.

This analysis addresses the effects of altering the S/C cooling turn scenario from that presented in the March '92 scenario (Reference 1 and Table 1), which will be referred to as the baseline scenario. The 9 mil moisture dryout and "+" pin configuration were incorporated in this analysis. The single rib NASTRAN model and boundary conditions that were used for this analysis are the same as were described in Reference 1. The first alteration that was investigated consisted of modifying the cooling turn history after the sixth cooling turn of the baseline scenario, as presented in Table 2. This new scenario has a much warmer warming turn (@ 1.07 AU) following the sixth cooling turn than did the baseline. Following this very warm warming turn are six very cold cooling turns (@ 3AU). The results of this analysis are presented in Figure 1 in terms of the number of S/C cooling turns required to release the first of three stuck ribs as a function of pin/receptacle coefficient of friction. Only the 15 lb. pin preload case was investigated. It is apparent that this modified cooling turn scenario results in fewer turns being required to obtain rib release, for a given coefficient of friction.

In order to investigate this behavior, the stow pin/receptacle forces and slippage were plotted as a function of cooling turn number for a given coefficient of friction. Figure 2 presents the stow pin forces and slippage for the baseline scenario, and Figure 3 presents those for the modified scenario. Comparison of Figures 2 and 3 shows that for the modified scenario a very large amount of slippage is developed in the upper pin during the Earth encounter, while for the baseline scenario the Earth encounter causes only a small amount of slippage. It is also worth noting from Figure 3 that the 1.07 AU warming turn following the Earth encounter had very little effect because of a loss of contact which occurred in the upper pin near the end of Earth encounter.

The second cooling turn scenario alteration was aimed at confirming the ineffectiveness of the 1.07 AU warming turn. As shown in Table 3, the 1.07 AU warming turn was eliminated along with its associated pre and post sun-pointed turns. Figure 4 shows the effect of eliminating the

1.07 AU warming turn. We see that rib release is obtained one cooling turn sooner for the coefficient of friction investigated (1.6). Figure 5 shows the stow pin forces and slippage obtained for this scenario. Comparing Figures 3 and 5 shows that eliminating the 1.07 AU warming turn makes the 3.0 AU pre-warming sun pointed turn to be more effective in causing slippage in the lower pin. We can also see a much smaller interval of pin/receptacle separation when the 1.07 AU warming turn is eliminated.

The last alteration to the cooling turn scenario was to eliminate the Earth encounter as well as the 1.07 AU warming turn. Figure 6 shows the stow pin forces and slippage as a function of cooling turns. It is evident that no slippage is obtained for any of the cooling turns.

Conclusions

- 1) The modification to the baseline cooling turn scenario of having all cooling turns after the sixth occur at 3AU has a beneficial effect of obtaining rib release for fewer spacecraft cooling turns.
- 2) The Earth encounter is very effective in causing slippage in the upper stow pin and promoting the walking phenomenon in subsequent cooling cycles.
- 3) The 1.07 AU warming turn is actually detrimental to pin walking, and should be eliminated.

AK:ipk

cc: A. Avila
G. Coyle
R. Ploszaj
R. Rapacz
R. Reeve
J. Staats
R. F. Tillman
G. Tsuyuki
C. Lifer/B. Wada

Table 1

March 1992 Cooling Turn Scenario		December 1991 Cooling Turn Scenario	
Event	Heliocentric Distance (AU)	Tower Displacement (mils)	Event
Pin Preload	1.00	0.0	Pin Preload
Pre-Deploy	1.32	-21.4	Pre-Deploy
Deploy Attempt	1.32	-21.4	Deploy Attempt
Pre-Warming Turn 1	1.57	-30.4	Pre-Warming Turn 1
Warming Turn 1	1.57	-21.4	Warming Turn 1
Cooling Turn 1	1.84	-67.9	Cooling Turn 1
Post Cooling Turn 1	1.84	-36.1	Post Cooling Turn 1
Cooling Turn 2	1.98	-70.0	Cooling Turn 2
Post-Cooling Turn 2	1.98	-39.1	Post-Cooling Turn 2
Cooling Turn 3	2.25	-72.3	Cooling Turn 3
Warming Turn 4	2.27	-40.1	Warming Turn 4
Cooling Turn 4	2.26	-71.7	Cooling Turn 4
Warming Turn 5	2.25	-39.7	Warming Turn 5
Cooling Turn 5	2.24	-71.6	Cooling Turn 5
Warming Turn 6	2.21	-38.9	Warming Turn 6
Cooling Turn 6	2.16	-71.2	Cooling Turn 6
Warming Turn 7	1.81	-29.1	Warming Turn 7
Cooling Turn 7	1.77	-68.5	Cooling Turn 7
Warming Turn 8	1.58	-21.7	Warming Turn 8
Cooling Turn 8	1.53	-64.4	Cooling Turn 8
Warming Turn 9	1.45	-16.6	Warming Turn 9
Cooling Turn 9	1.41	-62.6	Cooling Turn 9
Pre-Cooling Turn 10	1.33	-22.4	Pre-Cooling Turn 10
Cooling Turn 10	1.33	-60.7	Cooling Turn 10
Earth Encounter	1.00	-5.4	Earth Encounter
Pre-Warming Turn 11	1.07	-9.8	Pre-Warming Turn 11
Warming Turn 11	1.07	3.8	Warming Turn 11
Cooling Turn 11	1.32	-60.7	Cooling Turn 11
Warming Turn 12	1.40	-14.7	Warming Turn 12
Cooling Turn 12	1.57	-65.1	Cooling Turn 12
Post-Cooling Turn 12	1.57	-30.4	Post-Cooling Turn 12

APRIL 10, 1992
JAR 6th THERMAL DATA

D-9932

APRIL 3 JAU SCENARIO

REVISED WARMING AND COOLING TURNS

COOL TURN	EVENT	AJ	NO DRYOUT TOWER CONT. MILLS	WITH DRYOUT TOWER CONT. MILLS	NEW SUBCASE NUMBER
6	C TURN 6	2.16	-71.2	-62.2	16
	P-COOL-SP	2.16	-41.5	-32.8	17
	E.E-SP	1.0	-5.4	3.6	18
	PRE-W-SP	1.07	-9.8	-0.8	19
6.5	WARM	1.07	3.8	12.8	20
	POST-W-SP	1.07	-9.8	-0.8	21
	PRE-W-SP	3.00	-51.5	-42.5	22
	WARM	3.00	-49.7	-40.7	23
7.0	COOL	3.00	-73.6	-66.6	24
7.5	WARM	3.00	-49.7	-40.7	25
8.0	COOL	3.00	-73.6	-66.6	26
8.5	WARM	3.00	-49.7	-40.7	27
9.0	COOL	3.00	-73.6	-66.6	28
9.5	WARM	3.00	-49.7	-40.7	29
10.0	COOL	3.00	-73.6	-66.6	30
10.5	WARM	3.00	-49.7	-40.7	31
11.0	COOL	3.00	-73.6	-66.6	32
11.5	WARM	3.00	-49.7	-40.7	33
12.0	COOL	3.00	-73.6	-66.6	34

1
2
3
4
5
6

APRIL 3 JAU SCENARIO

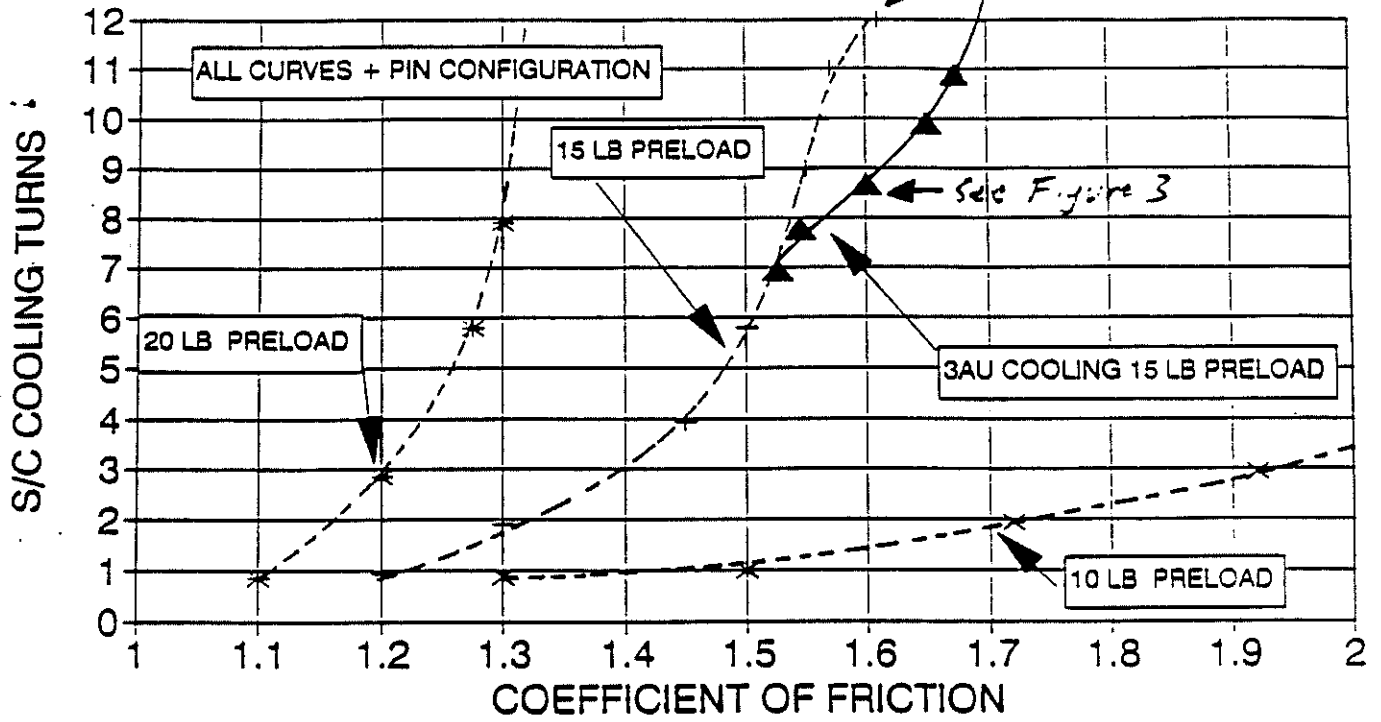
REVISED WARMING AND COOLING TURNS

COOL TURN	EVENT	AU	NO DRYOUT TOWER CONT. MILLS	WITH DRYOUT TOWER CONT. MILLS	NEW SUBCASE NUMBER
6	C TURN 6	2.16	-71.2	-62.2	16
	P-COOL-SP	2.16	-41.5	-32.8	17
	E.E-SP	1.0	-5.4	3.6	18
	PRE-W-SP	1.07	9.8	0.8	19
6.5	WARM	1.07	9.8	12.0	20
	POST-W-SP	1.07	9.8	0.8	21
	PRE-W-SP	3.00	-51.5	-42.5	22
	WARM	3.00	-49.7	-40.7	23
7.0	COOL	3.00	-73.6	-64.6	24
7.5	WARM	3.00	-49.7	-40.7	25
8.0	COOL	3.00	-73.6	-64.6	26
8.5	WARM	3.00	-49.7	-40.7	27
9.0	COOL	3.00	-73.6	-64.6	28
9.5	WARM	3.00	-49.7	-40.7	29
10.0	COOL	3.00	-73.6	-64.6	30
10.5	WARM	3.00	-49.7	-40.7	31
11.0	COOL	3.00	-73.6	-64.6	32
11.5	WARM	3.00	-49.7	-40.7	33
12.0	COOL	3.00	-73.6	-64.6	34

} Eliminated

1
2
3
4
5
6

COOLING TURNS REQUIRED FOR RIB RELEASE 3/92 Truncated & Baseline Cooling Turns



—x— 10# BASELINE + 15# BASELINE * 20# BASELINE ▲ 15# @ 3AU

Figure 1.

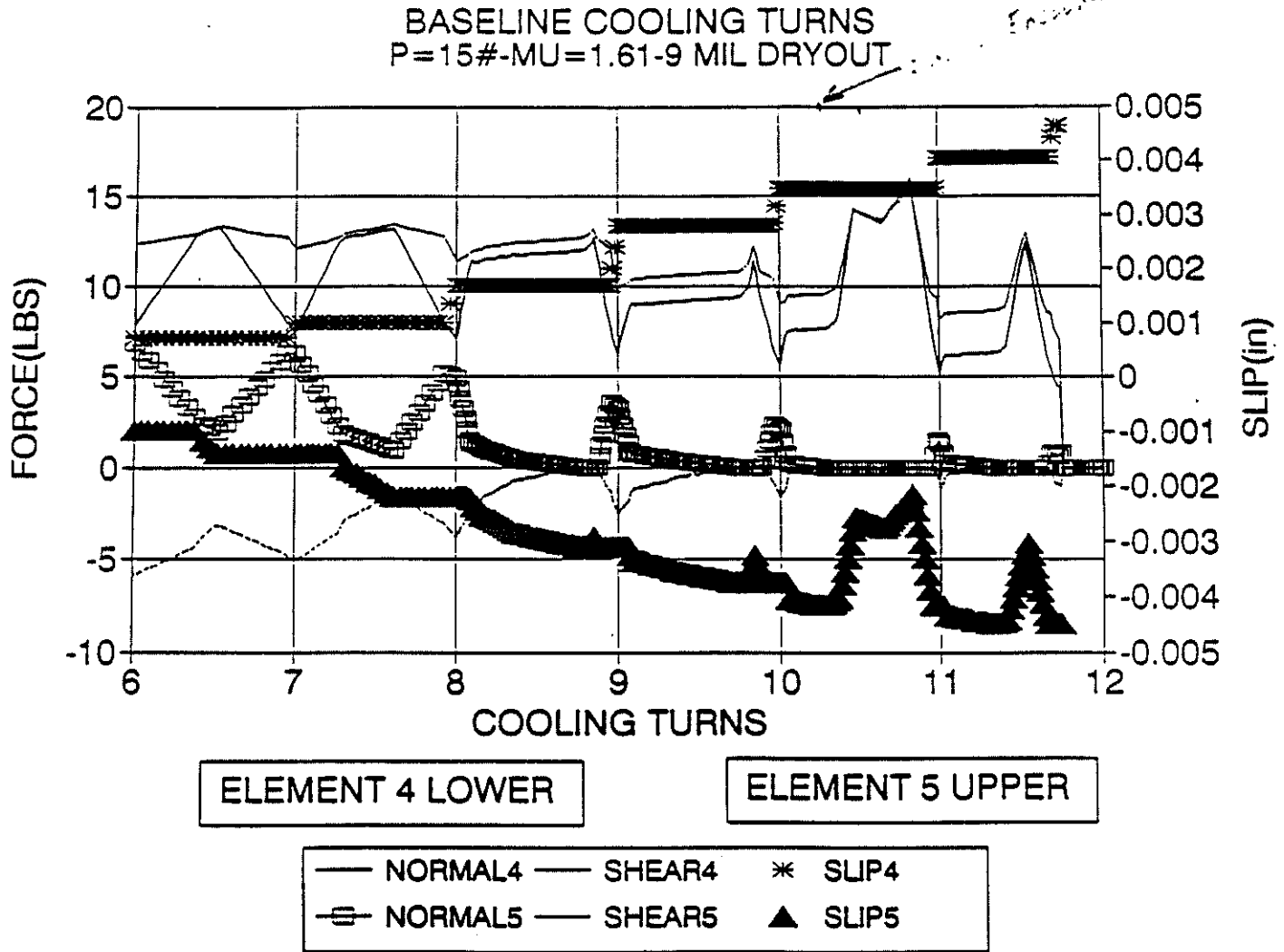


Figure 2.

4/15/92

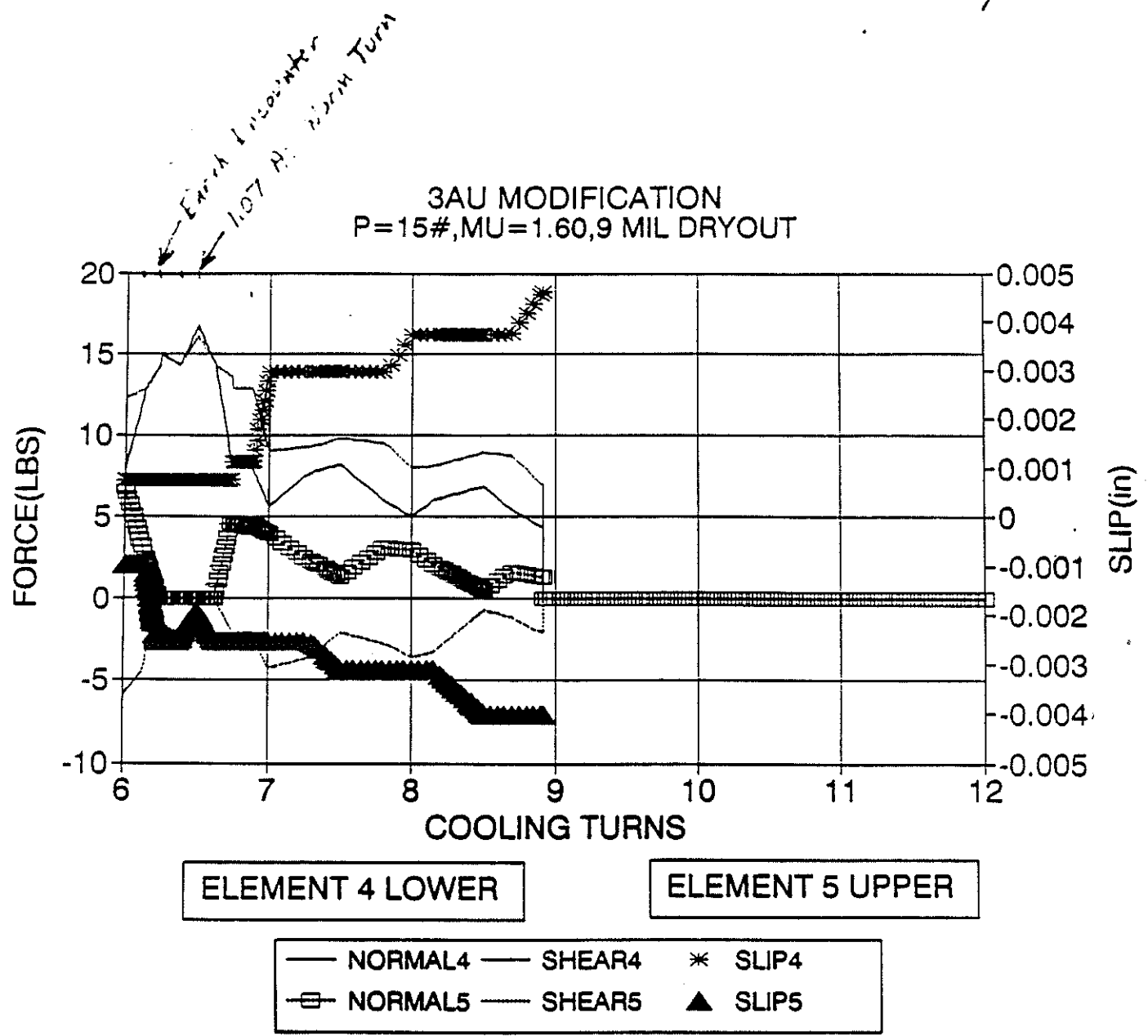
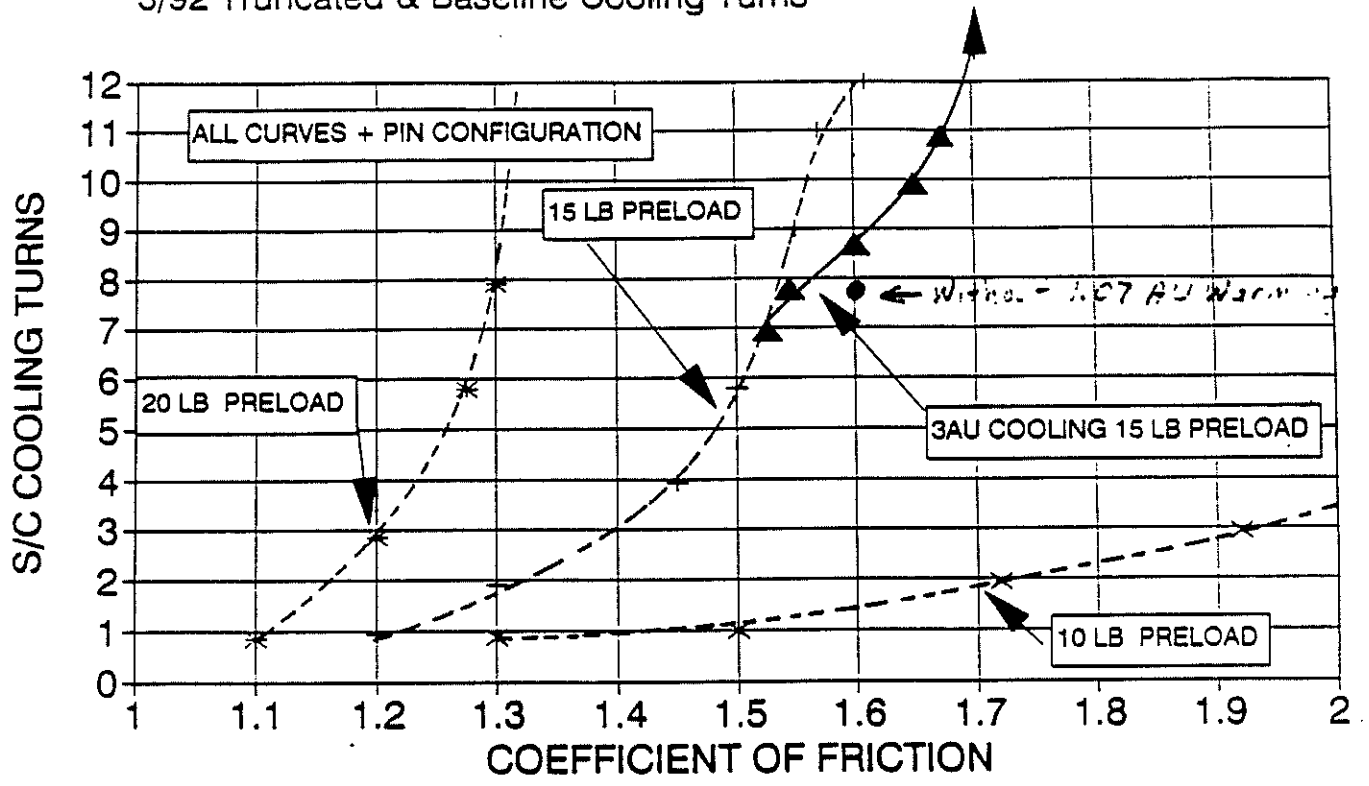


Figure 3.

COOLING TURNS REQUIRED FOR RIB RELEASE
 3/92 Truncated & Baseline Cooling Turns

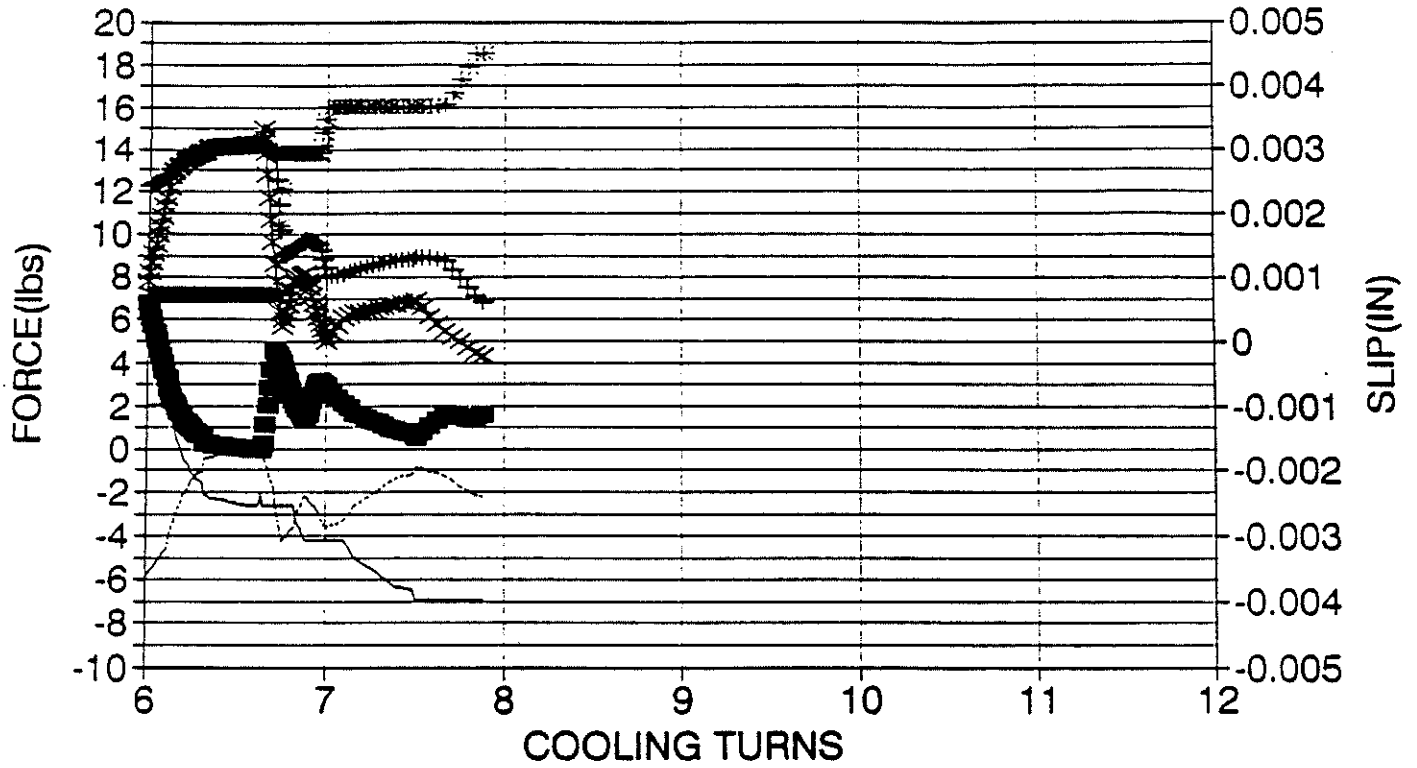


—x— 10# BASELINE + 15# BASELINE * 20# BASELINE ▲ 15# @ 3AU

Figure 4.

MODIFIED EARTH-3AU TURNS
P=15#, MU=1.6, 9 MIL DRYOUT

(1.07 AU Warming Eliminated)



—x—	NORMAL4	+ SHEAR4	* SLIP4
■	NORMAL5	— SHEAR5	— SLIP5

Figure 5.

NOEARTH-3AU MODIFICATION
P=15#, MU=1.60, 9 MIL DRYOUT

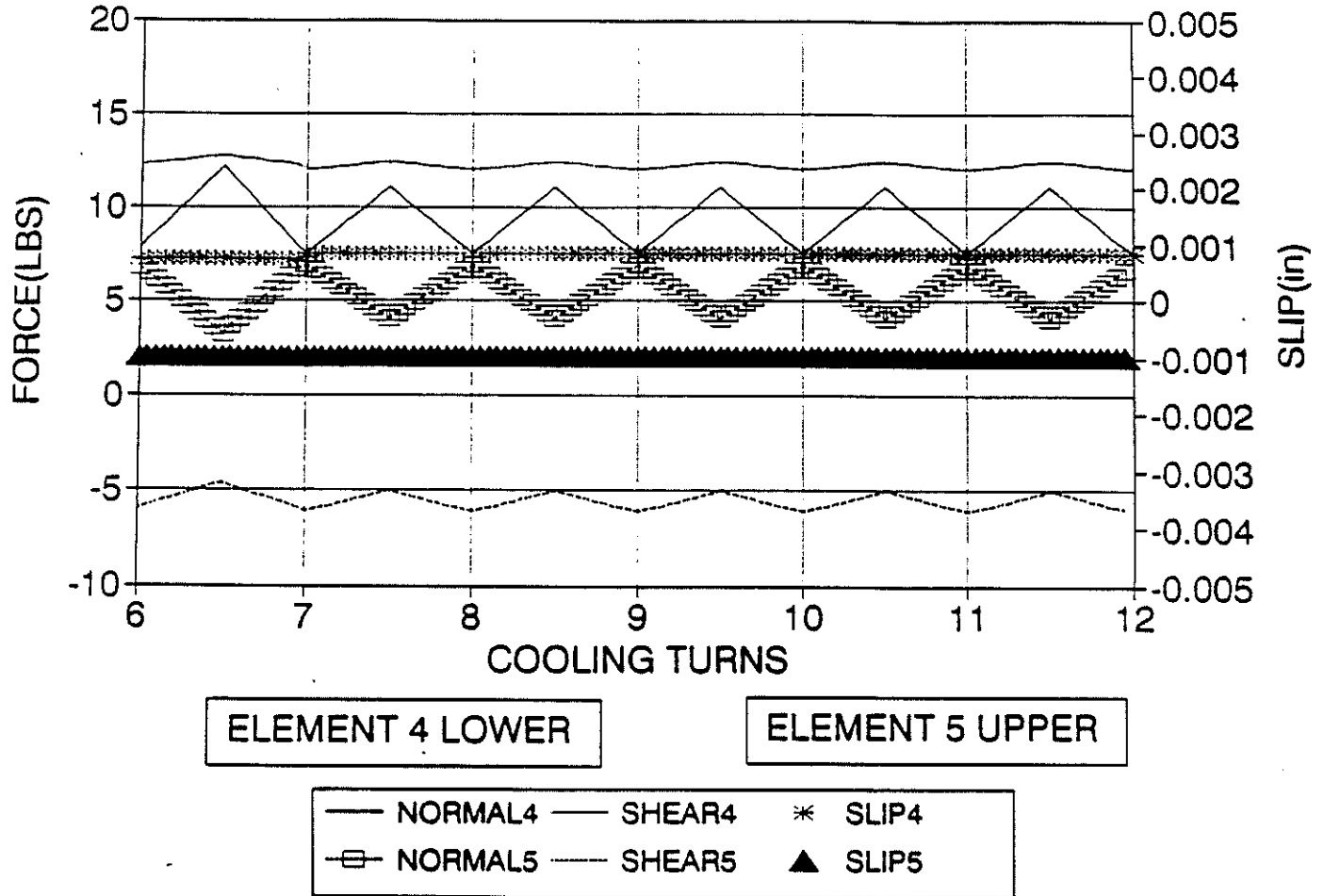


Figure 6.

D-9932

APPENDIX 8.7

Effectiveness of Turns 7, 8, 9 & 10

JET PROPULSION LABORATORY

INTEROFFICE MEMORANDUM
3541-92-167

MAY 8, 1992

TO: Gun-Shing Chen
FROM: P. M. Rapacz
SUBJECT: Study of the Effects of Turns 7 Thru 10 on First Rib Release of the GLL HGA

INTRODUCTION

Recent concerns have been raised with respect to attempting spacecraft (S/C) cooling turns at solar distances less than 1.6 AU. This is because possible damage could result due to excessive heating of the normally shaded S/C components. Since S/C resources such as thruster propellant are limited, the question has been raised as to the effectiveness of these turns on pin walk-out and the consequence of delaying them until after earth encounter. This memo tries to address these concerns by examining a single antenna condition to gain some insight into the effectiveness of cooling turns 7 thru 10.

ANALYSIS ASSUMPTIONS

The cooling turn scenario used in this study is the modified version of the original March 92 scenario shown in Table 1. While it remains similar to the unmodified March 92 scenario, it differs by the addition of cooling turn 6a between turns 6 and 7 and the combination of turns 11 and 12 into a new turn 10a. It also differs slightly from the latest HGA activities schedule, see Figure 1, in that cooling turn 10a occurs at 1.57 AU instead of the schedule's 1.7 AU.

First rib release results were obtained using this modified cooling turn scenario and a single analysis configuration (using the single rib walk-out model) in which the following conditions were assumed:

- 1) 3 Stuck Ribs (#9,10,11)
- 2) Rib 11 Boundary Conditions
- 3) 10 lbs Stow Pin Preload
- 4) - Pin Orientation
- 5) 9 mil Rib Dryout
- 6) Modified March 1992 Cooling Turn Scenario

The effects of inbound cooling turns were then assessed by comparing a baseline analysis, included all turns thru 10a, with two case in which turns 8 thru 10 and turns 7 thru 10 were eliminated.

RESULTS AND DISCUSSION

Figure 2 shows that cooling turns 8,9,&10 by themselves increase the required minimum coefficient of friction (μ) by only 0.02. The effect of turn 10a, however, depends on the previous number of turns. When cooling turn 10a is not preceded by turns 8,9,&10, it is no more effective than the originally scheduled turn 8 and increases μ by only 0.01. When cooling turn 10a follows turns 8,9,&10, μ increases by 0.04. Figure 3 shows the cumulative effect of turns 8,9,&10, however, increase the required minimum coefficient of friction (μ) by approximately 0.05.

Figures 4 and 5 show the corresponding stow pin tip forces and cumulative slip for this last cooling turn cycle after turn 7 both with and without turns 8,9,&10 respectively and $\mu = 1.6475$. The reason for the apparent equal effectiveness of turn 8 and turn 10a can now be seen. Both turns 8 and 10a produce sufficient warming (tower expansion) to cause the upper pin to loose contact with the upper surface. Since pin walk-out can not occur without both pins in contact, no pin slip occurs during the higher heating associated with the earth encounter portion of turn 10a in this particular example. The final pin slip which precipitates rib release is then seen not to occur until near the point of maximum cooling (tower contraction). Since both turn 8 and 10a end with a cooling turn occurring at about the same solar distance, they both result in rib release.

Figures 6-9 present similar results for the case where turns 7,8,9,&10 are eliminated. Again turn 10a appears as effective as turn 7 for the same reasons as above and there appears to be no benefit from earth encounter. The change in μ due to these turns, both by themselves and cumulatively, was slightly larger since more turns were deleted.

CONCLUSIONS

In general, the effect of turns 7/8 thru 10a produce a small, but finite increase (0.06 to 0.08) in the required coefficient of friction required to prevent first rib release.

Because of the nonlinear path dependent nature of the pin walk-out phenomena, the effect of cooling turns 7/8 thru 10 can have a significant effect on subsequent turns. Since most of the benefit is gained by completing turn 10a after turns 7/8 thru 10, as shown in Figure 10, it does not appear useful to attempt turns 7/8 thru 10 without also performing turn 10a.

The warming produced by the 1.07 AU warming turn portion of turn 10a is no more effective than the warming produced by earth encounter. It could, in fact, have been eliminated without affecting pin walkout results since the upper pin loses contact with the upper surface for both these conditions.

Because earth encounter warming is only effective while the upper pin remains in contact, it will be more beneficial in producing pin slip when pin contact loads are high, i.e., higher pin preloads. Since the residual pin preload decreases as walk-out progresses, one could assume the same or better results would be achieved by performing turn 10a sooner in the cooling turn sequence, i.e., delaying turns 7/8 thru 10 until after earth encounter.

While the above conclusions directly apply to only the specific analysis configuration considered here, the limited remaining range of reasonable pin preloads and coefficient of friction still make them applicable to determining the appropriate cooling turn scenario options.

Distribution:

G. Coyle
R. Eads
A. Kissil
C. Lifer/B. Wada
R. Ploszaj
R. Reeve
J. Staats
R. F. Tillman
Y. Tsou
W. Tsuha
G. Tsuyuki

TABLE 1. March 4, 1992 Cooling Turn Scenario

UNMODIFIED			MODIFIED			HELICENTRIC DISTANCE (AU)	NO DRYOUT TOWER CONTRACTION (mils)	WITH 9 MIL DRYOUT TOWER CONTRACTION (mils)
NASTRAN SUBCASE NO.	COOLING TURN CYCLE NO.	EVENT	NASTRAN SUBCASE NO.	COOLING TURN CYCLE NO.	EVENT			
1	N/A	Pin Preload	1	N/A	Pin Preload	1.00	0.0	0.0
2	N/A	Pre-Deploy	2	N/A	Pre-Deploy	1.32	-21.4	-12.4
3	0.000	Deploy Attempt	3	0.000	Deploy Attempt	1.32	-21.4	-12.4
4	0.333	Pre-Warming Turn 1	4	0.333	Pre-Warming Turn 1	1.57	-30.4	-21.4
5	0.667	Warming Turn 1	5	0.667	Warming Turn 1	1.57	-21.4	-12.4
6	1.000	Cooling Turn 1	6	1.000	Cooling Turn 1	1.84	-67.9	-58.9
7	1.500	Post Cooling Turn 1	7	1.500	Post Cooling Turn 1	1.84	-36.1	-27.1
8	2.000	Cooling Turn 2	8	2.000	Cooling Turn 2	1.98	-70.0	-61.0
9	2.500	Post-Cooling Turn 2	9	2.500	Post-Cooling Turn 2	1.98	-39.1	-30.1
10	3.000	Cooling Turn 3	10	3.000	Cooling Turn 3	2.25	-72.3	-63.3
11	3.500	Warming Turn 4	11	3.500	Warming Turn 4	2.27	-40.1	-31.1
12	4.000	Cooling Turn 4	12	4.000	Cooling Turn 4	2.26	-71.7	-62.7
13	4.500	Warming Turn 5	13	4.500	Warming Turn 5	2.25	-39.7	-30.7
14	5.000	Cooling Turn 5	14	5.000	Cooling Turn 5	2.24	-71.6	-62.6
15	5.500	Warming Turn 6	15	5.500	Warming Turn 6	2.21	-38.9	-29.9
16	6.000	Cooling Turn 6	16	6.000	Cooling Turn 6	2.16	-71.2	-62.2
			17	6.500	Warming Turn 6a	1.90	-31.7	-22.7
			18	7.000	Cooling Turn 6a	1.90	-69.2	-60.2
			19*	7.500	Warming Turn 7	1.81	-29.1	-20.1
			20*	8.000	Cooling Turn 7	1.77	-68.5	-59.5
			21*#	8.500	Warming Turn 8	1.58	-21.7	-12.7
			22*#	9.000	Cooling Turn 8	1.53	-64.4	-55.4
			23*#	9.500	Warming Turn 9	1.45	-16.6	-7.6
			24*#	10.000	Cooling Turn 9	1.41	-62.6	-53.6
			25*#	10.500	Pre-Cooling Turn 10	1.33	-22.4	-13.4
			26*#	11.000	Cooling Turn 10	1.33	-60.7	-51.7
			27	11.250	Earth Encounter	1.00	-5.4	3.6
			28	11.500	Pre-Warming Turn 10a	1.07	-9.8	-0.8
			29	11.750	Warming Turn 10a	1.07	3.8	12.8
			30	12.000	Cooling Turn 10a	1.32	-60.7	-51.7
			31	12.500	Post-Cooling Turn 10a	1.40	-14.7	-5.7
						1.57	-65.1	-56.1
						1.57	-30.4	-21.4

* - Remove to eliminate turns 8,9,&10

- Remove to eliminate turn 7,8,9,10

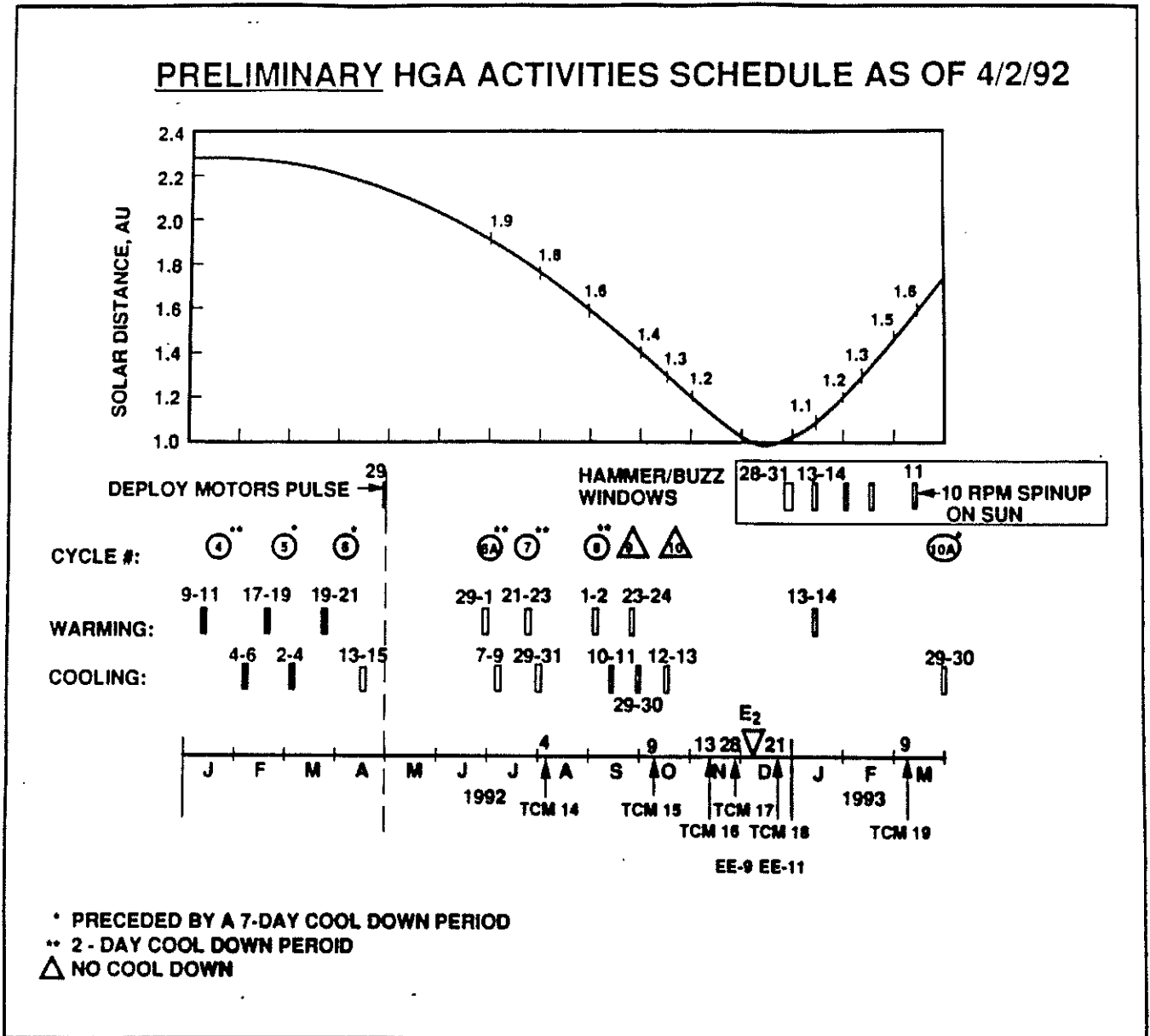


Figure 1. HGA Activities Schedule

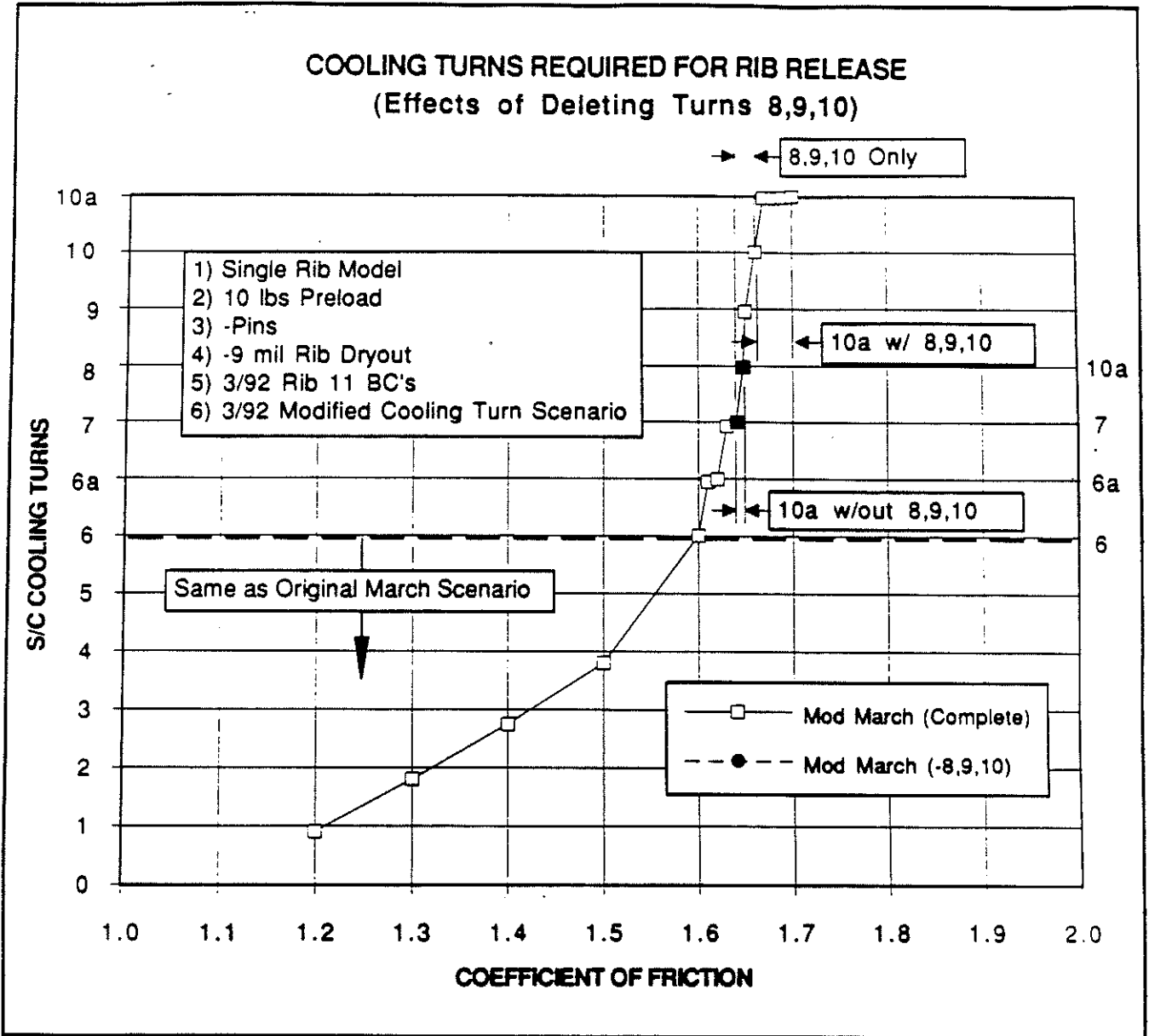


Figure 2. Incremental Effect of Turns 8,9,10 on Pin Walk-Out

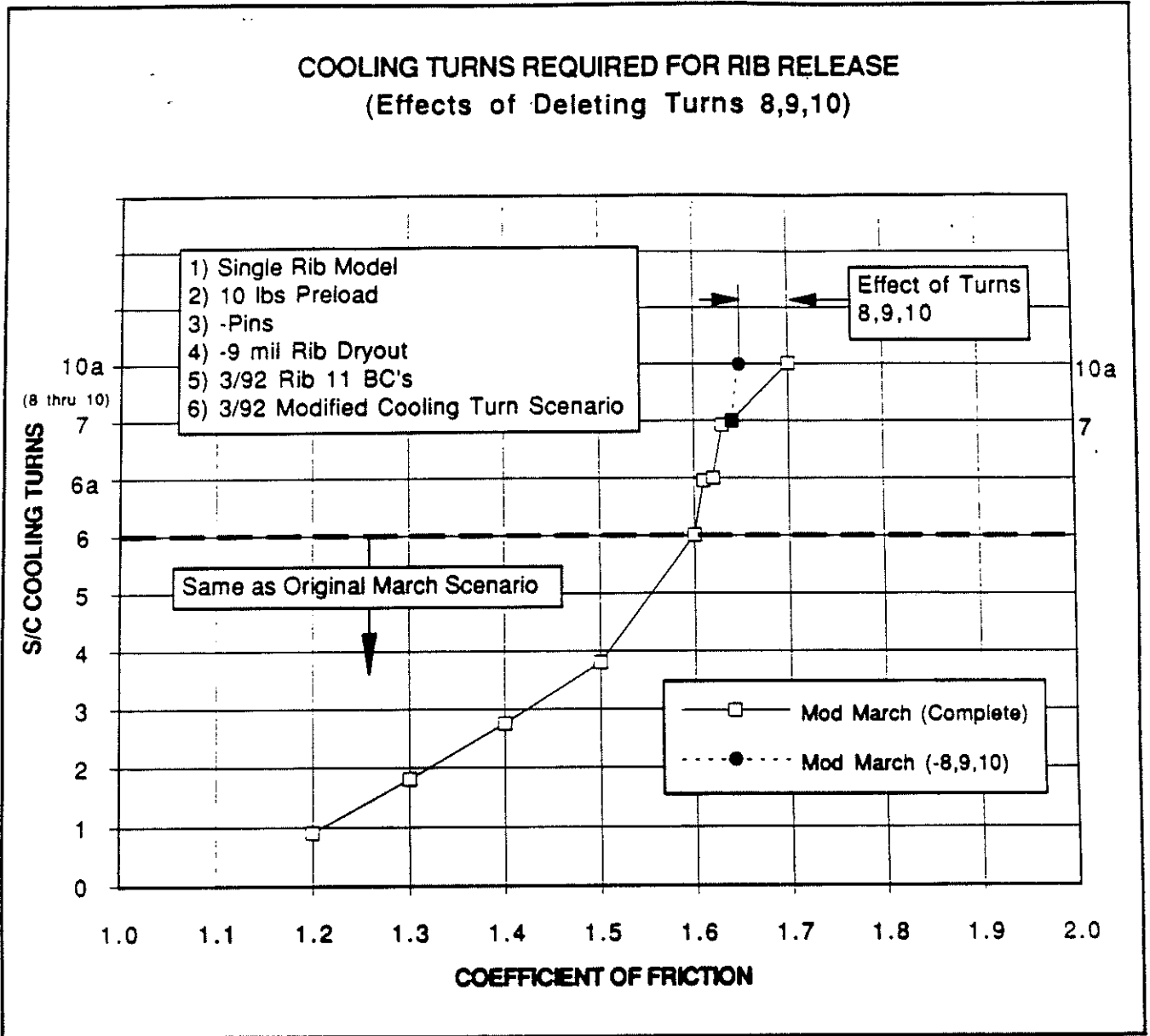


Figure 3. Cumulative Effect of Turns 8,9,10 on Pin Walk-Out

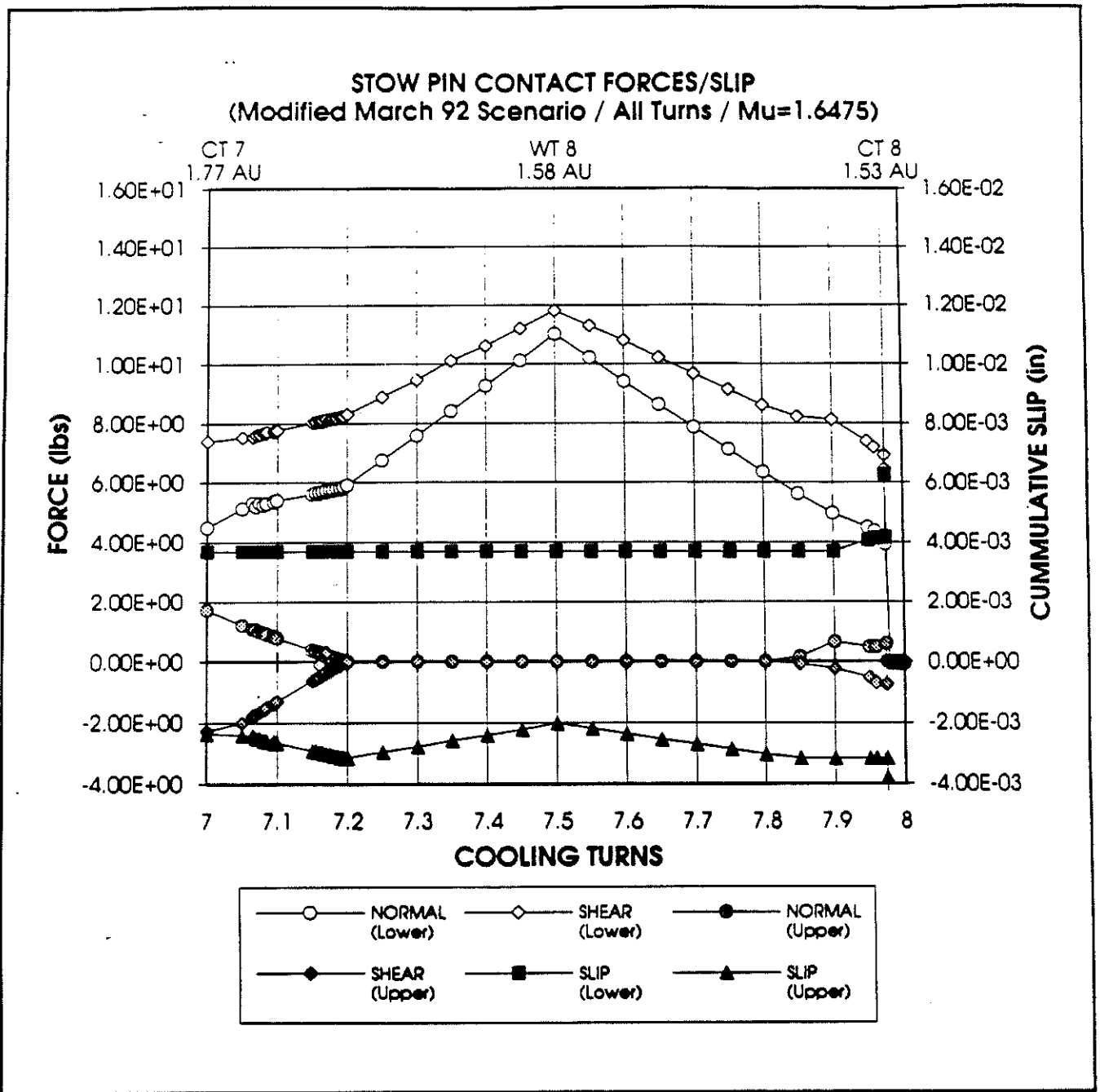


Figure 4. Nomimal Pin Walk-Out - Turn 7 to 8

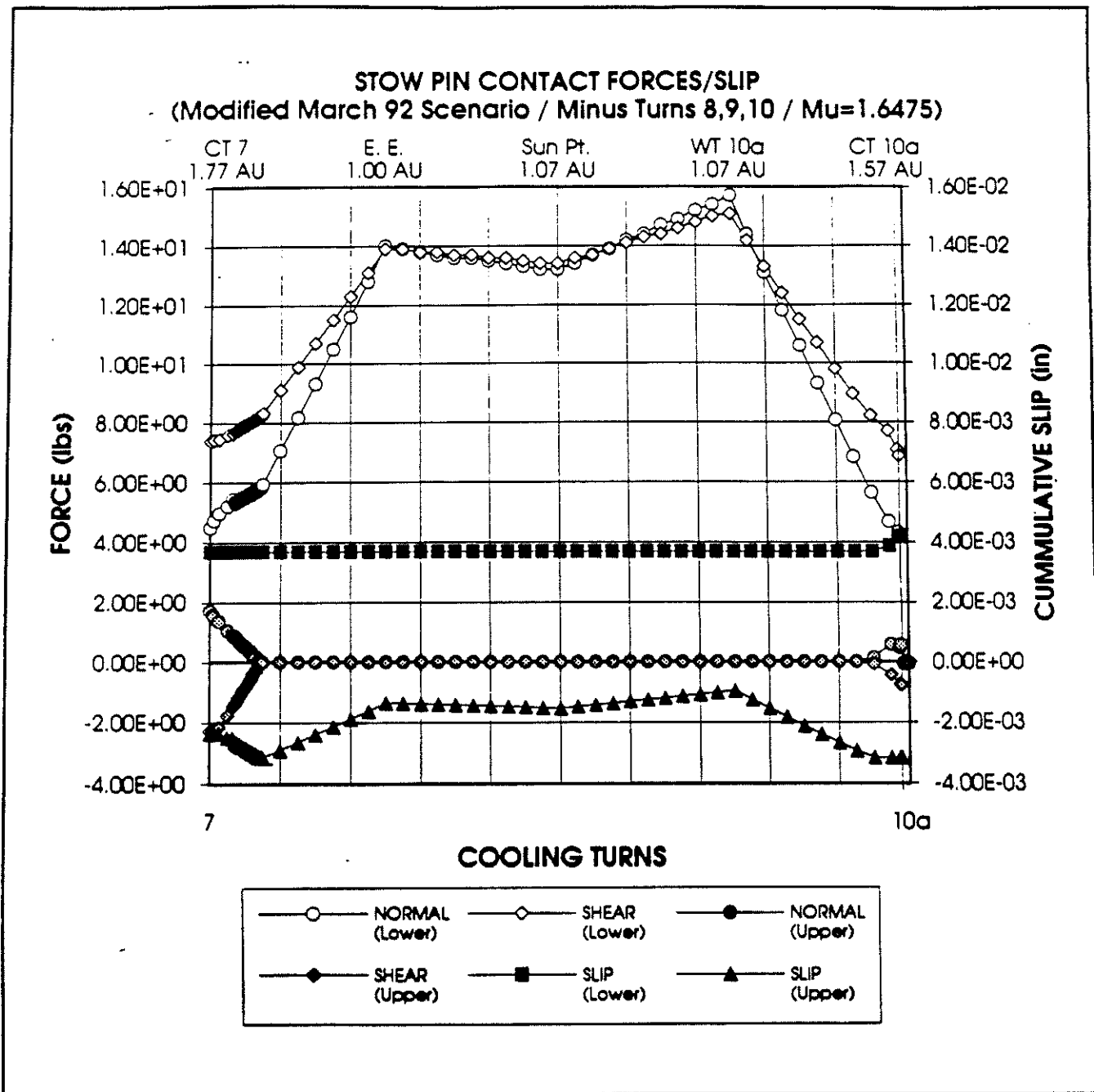


Figure 5. Modified Pin Walk-Out - Turn 7 to 10a

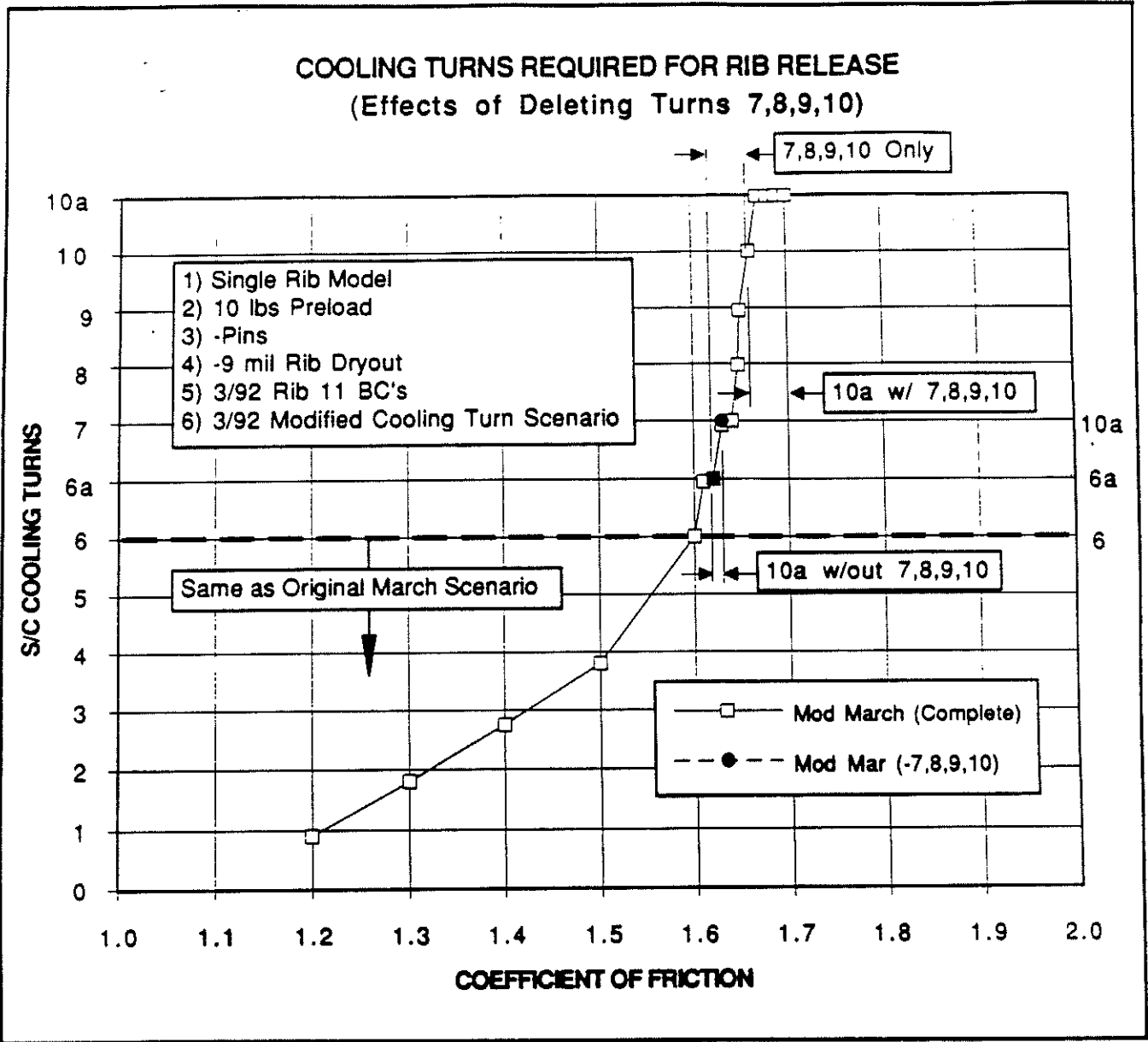


Figure 6. Incremental Effect of Turns 7,8,9,10 on Pin Walk-Out

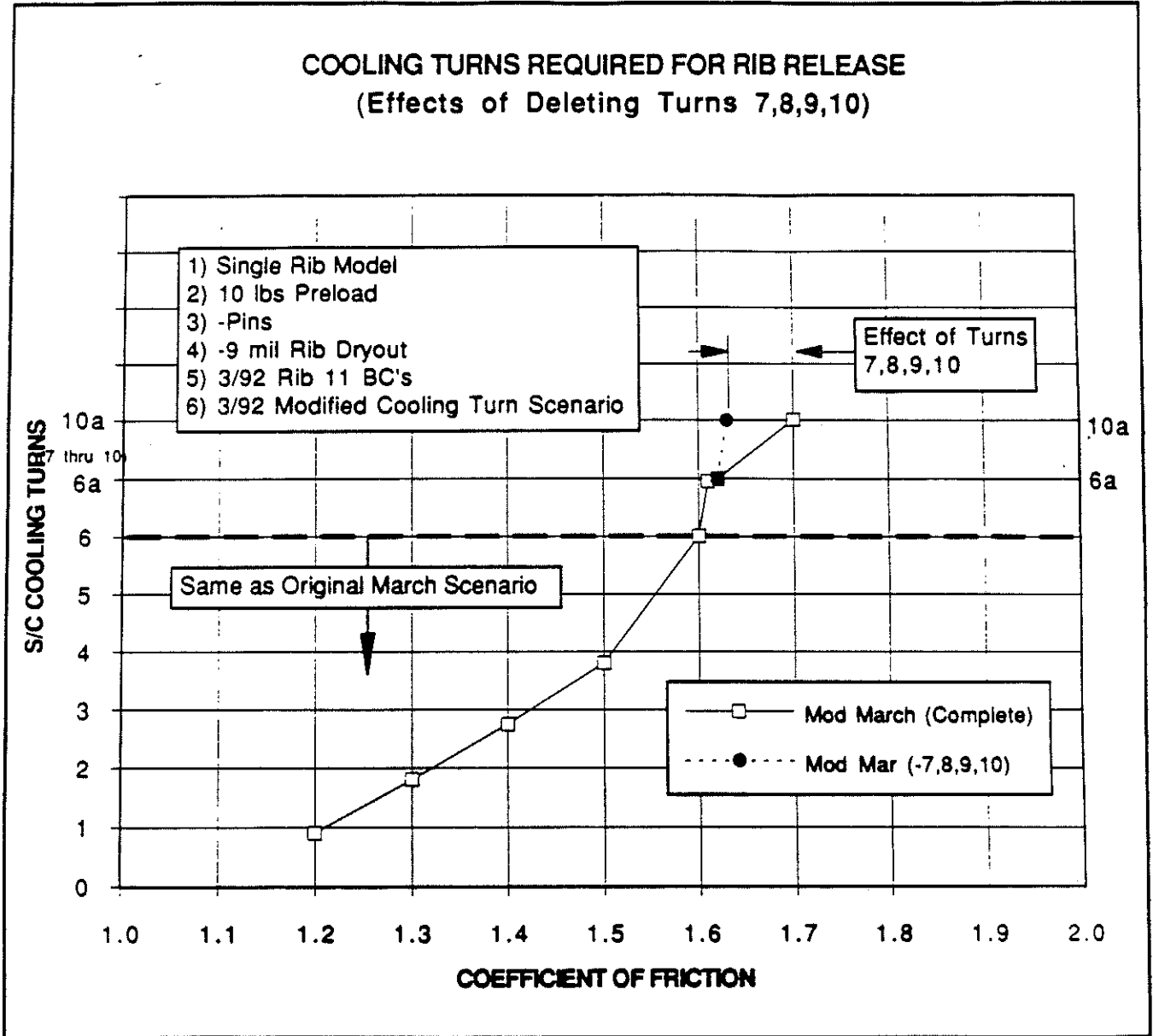


Figure 7. Cumulative Effect of Turns 7,8,9,10 on Pin Walk-Out

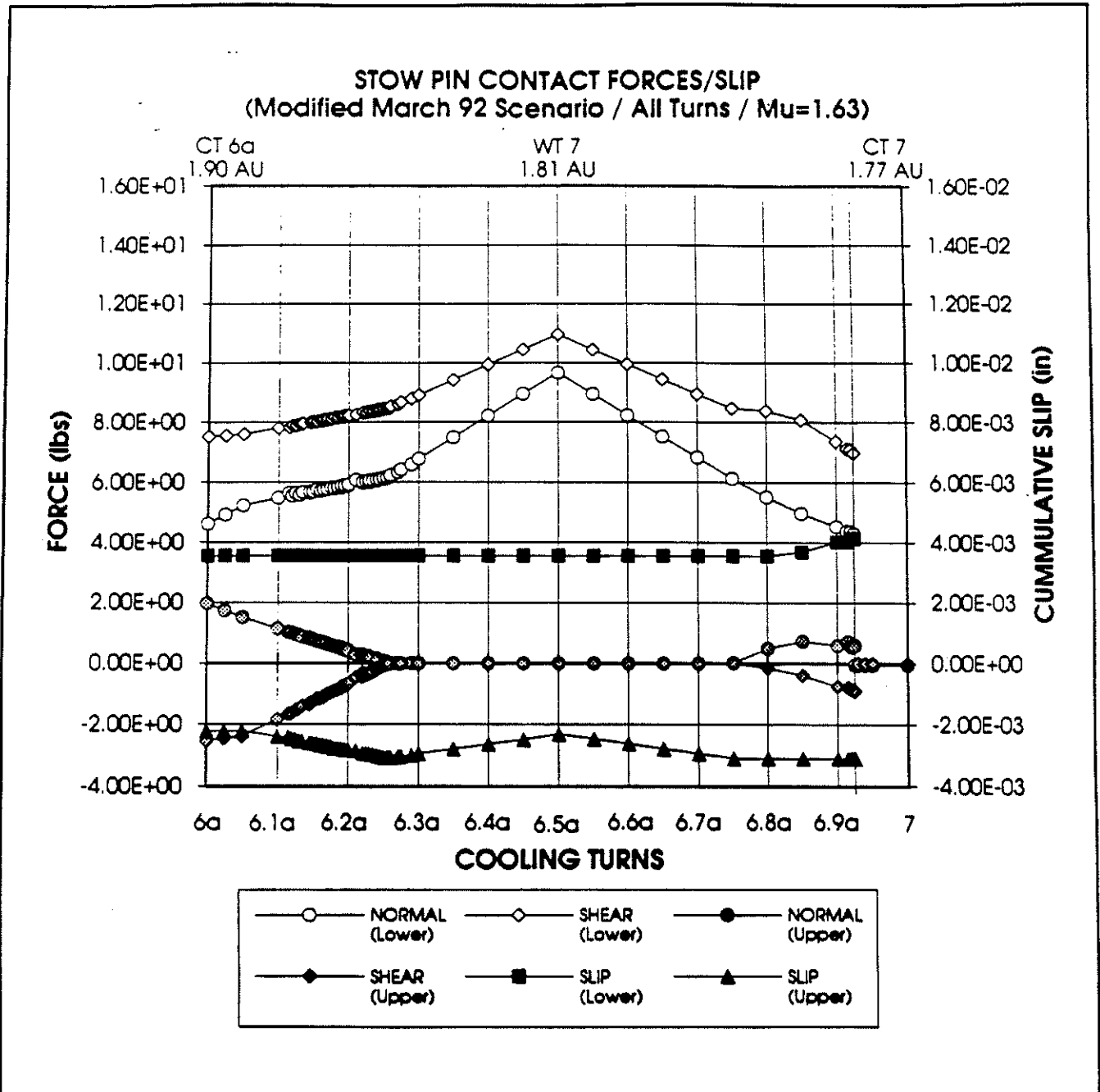


Figure 8. Nominal Pin Walk-Out - Turn 6a to 7

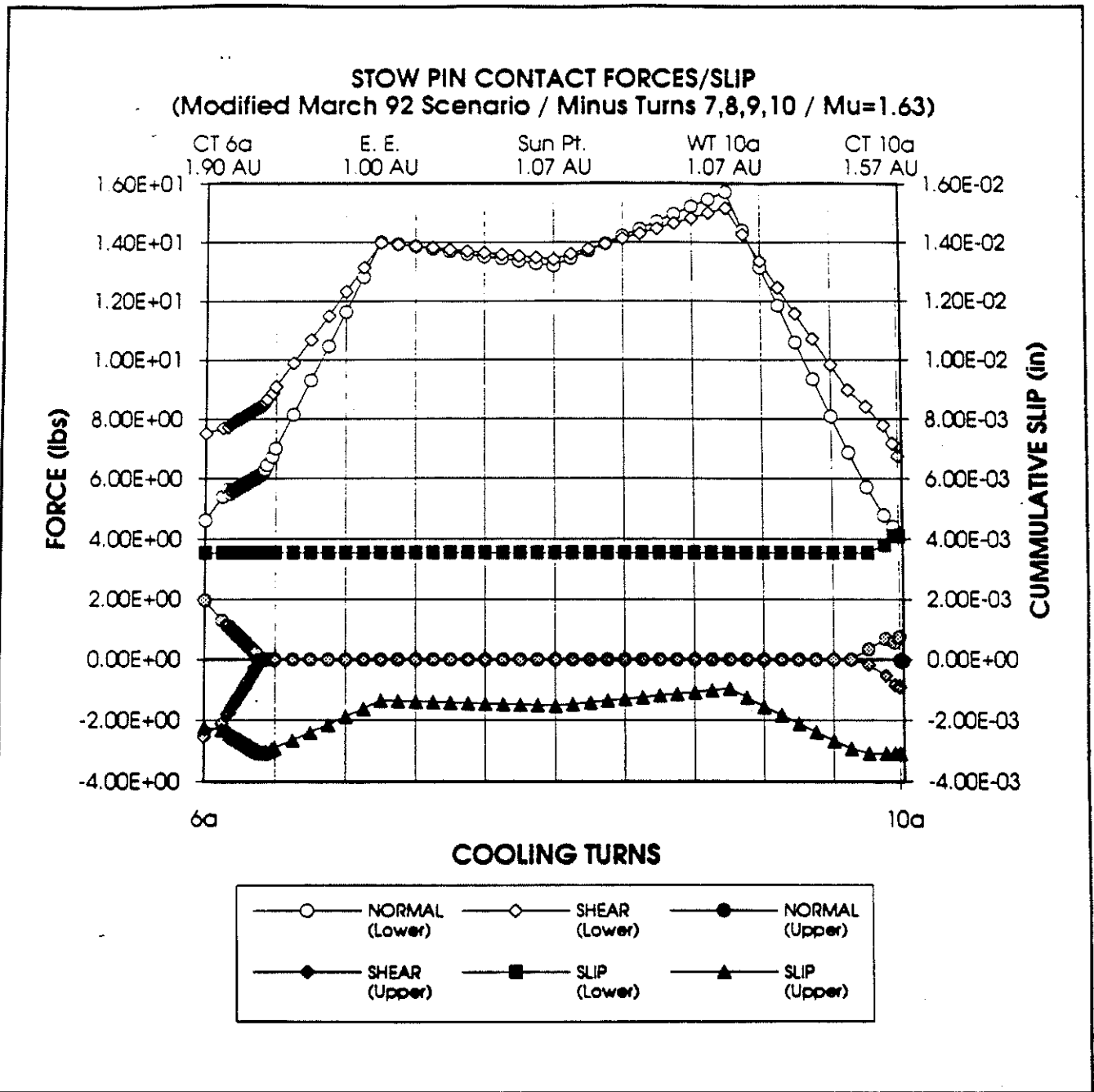


Figure 9. Modified Pin Walk-Out - Turn 6a to 10a

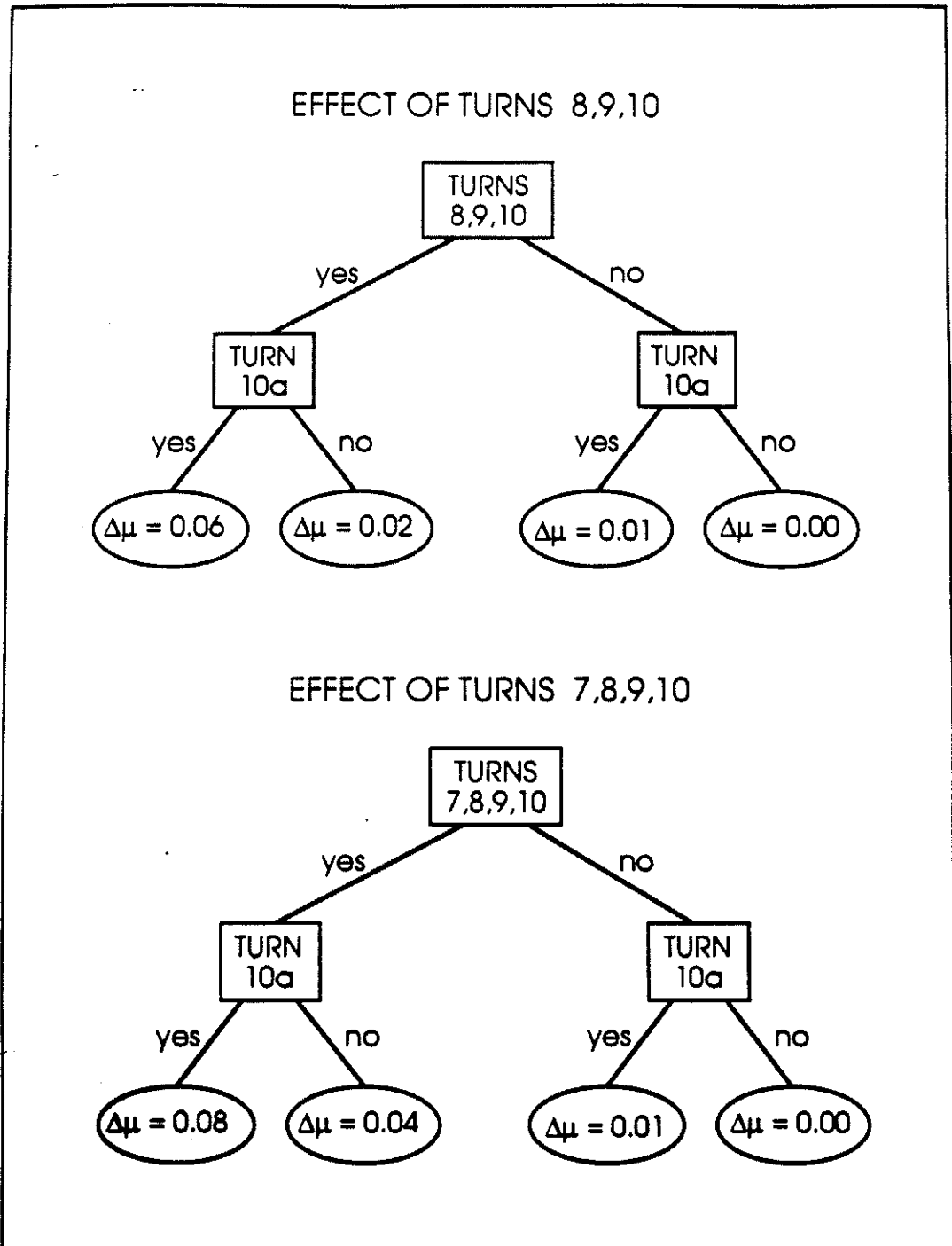


Figure 10. Cooling Turn Effectiveness Logic Tree

D-9932

APPENDIX 8.8

Full Model - NASTRAN Data Deck